Aus der

Medizinischen Klinik und Poliklinik IV

der Ludwig-Maximilians-Universität München

Arbeitsgruppe Klinische Biochemie

Direktor: Prof. Dr. med. M. Reincke

The potential impact of Wnt5a on differentiation and phenotype of dendritic cells found in renal cell carcinoma

Dissertation

zum Erwerb des Doktorgrades der Medizin

an der Medizinischen Fakultät der

Ludwig-Maximilians-Universität zu München

vorgelegt von

Sabine Diepenbruck

aus Köln

2017

Mit Genehmigung der Medizinischen Fakultät

der Universität München

Berichterstatter:	Prof. Dr. Peter J. Nelson, PhD
Mitberichterstatter:	Priv. Doz. Dr. Alexander Buchner
	Priv. Doz. Dr. Jens Neumann
Dekan:	Prof. Dr. med. dent. Reinhard Hickel

Tag der mündlichen Prüfung: 12.10.2017

Table of contents

Abstract

Renal cell carcinoma (RCC) is an immunogenic tumour infiltrated by a high number of leucocytes. However, this infiltrate is not able to induce an efficient anti-tumoural response. Recent studies have attempted to further identify the composition of the immune-infiltrate in order to gain a deeper understanding of how RCC escapes from immune surveillance. Recently, a new dendritic cell (DC) subtype was discovered, co-expressing DC (CD209/DC-SIGN) and Mϕ (CD14, CD163) markers. As this subtype was found to be enriched in RCC tissue it was called "enriched in renal cell carcinoma DC" (ercDC).

Functional tests investigating cytokine expressions and the migration ability of this subtype revealed impaired functioning of ercDC compared to conventional DC (cDC). While being able to migrate towards fMLP, a chemoattractant for immature DC, maturated ercDC do not show directed migration towards CCL19, which is involved in the recirculation and homing of maturated DC. Furthermore, ercDC secrete higher levels of IL-10 and TNF-α, but lower levels of IL-12 upon LPS stimulation. In order to identify possible pathways responsible for differences between myeloid subtypes, transcriptomic profiling of monocytes, cDC, ercDC and Mϕ was performed. Amongst others, regulation was found especially for the canonical as well as non-canonical Wnt-pathways. Following these findings, we investigated the role of Wnt-signalling in the differentiation and functioning of myeloid and especially dendritic cells. Striking was the high expression of Wnt5a, a typical non-canonical Wnt-ligand, in cDC in comparison to all other myeloid subtypes. Furthermore, we could show that Wnt5a is highly expressed in RCC and microarray analysis of RCC tissue samples revealed that Wnt-signalling, especially non-canonical Wnt-signalling, changes with tumour progression.

Functional tests of DC showed, that the addition of Wnt5a during differentiation significantly increases IL-10 and IL-12, but decreases TNF-α secretion. Surprisingly, Wnt5a also inhibited the migratory capacity of cDC, resulting in reduced motility and less directed migration towards CCL19. These results suggest a possible role of Wnt-signalling in the differentiation and functioning of myeloid cells. Through its autocrine, paracrine and juxtacrine effect, Wnt5a present in the tumour milieu may influence the

anti-tumoural immune response. Gaining further insight into the role of myeloid cells and Wnt-signalling in RCC could hence reveal new possible therapeutic targets.

Zusammenfassung

Das Nierenzellkarzinom (RCC, renal cell carcinoma) wird als immunogener Tumor von einer Vielzahl an Immunzellen infiltriert. Trotz dieses Immunzellinfiltrats, kommt es jedoch nicht zu einer effektiven Kontrolle des Tumorwachstums durch das Immunsystem. Um die Mechanismen der Immunevasion des Nierenzellkarzinoms besser zu verstehen, ist das Ziel neuerer Studien, dieses Immuninfiltrat besser zu charakterisieren. Kürzlich wurde hierbei ein neuer myeloischer Zelltyp entdeckt, welcher sowohl dendritische Zell (DC)- (CD209/DC-SIGN), als auch Makrophagen (Mϕ)-Marker (CD14, CD163) exprimiert. Da dieser Zelltyp im RCC im Vergleich zu tumorfreien Nierenparenchym besonders angereichert ist, wurde er „enriched in renal cell carcinoma DC“ (ercDC) genannt.

Bei unserer Untersuchung dieses Zelltyps zeigte sich interessanterweise, dass maturierte ercDC zwar zu fMLP, einem Chemoattractant unreifer DC, gerichtet migrieren, allerdings keine gerichtete Migration zu CCL19 aufweisen. Im Vergleich zu konventionellen Dendritischen Zellen (cDC) sezernierten ercDC nach Stimulation mit LPS höhere Mengen IL-10 und TNF-α, aber geringere Mengen IL-12. Um mögliche relevante Unterschiede in den Signalwegen von Monozyten, cDC, ercDC und Mϕ zu identifizieren, führten wir Transkriptomanalysen an Microarray-Daten dieser Zelltypen durch. Hierbei zeigte sich unter anderem eine differenzielle Expression in dem „canonical“ und den „non-canonical“ Wnt-Signalwegen. Auffallend war die, im Vergleich zu den anderen myeloischen Zelltypen, starke Expression von Wnt5a, einem typischen „non-canonical“ Wnt-Liganden, in cDC. Darüber hinaus konnten wir immunhistochemisch eine hohe Wnt5a Expression im Gewebe des Nierenzellkarzinoms nachweisen. Auch in der Microarray-Analyse von Nierenzellkarzinomproben zeigte sich eine starke differenzielle Expression der Wnt-Signalwege, mit evidenten Unterschieden abhängig vom Tumorstadium.

Durch die Zugabe von Wnt5a während der Differenzierung von cDC konnte eine vermehrte Sekretion von IL-10 und IL-12, sowie eine Reduktion der TNF-α Sekretion erreicht werden. Interessanterweise führte Wnt5a Zugabe auch zu einer geringeren Mobilität und Direktionalität von cDC bei der Migration zu CCL19. Zusammenfassend weisen diese Ergebnisse auf eine Rolle der Wnt-Signalwege in der Differenzierung und

Funktionalität von myeloischen Zellen hin. Wnt5a im Tumormilieu kann so durch autokirne, parakrine und juxtakrine Mechanismen die Immunantwort gegen den Tumor modulieren. Ein weitergehendes Verständnis über die Bedeutung des Wnt-Signalweges in den myeloischen Zellen des Nierenzellkarzinoms könnte so sogar mögliche neue Therapieansätze aufdecken.

1 Introduction

1.1 Renal cell carcinoma

Originating from the renal cortex, Renal Cell Carcinoma (RCC) is the most common renal malignancy accounting for 90% of all renal neoplasms with an incidence of over 3% of all cancers in Europe [1]. Despite ongoing research and a number of different therapeutic approaches, there exists no satisfying therapy for RCC. While nephrectomy is the most effective treatment for non-metastatic RCC, the therapy of metastatic RCC remains difficult with poor survival rates. Similar to certain other solid cancers, such as melanoma, RCC is an immunogenic cancer showing infiltration by a multitude of immune cells [2]. These include mainly $CD3^-$ Natural killer cells (NK) and $CD3^+$ lymphocytes of CD4 and CD8 type [3]. In addition, rare cases of spontaneous remission of metastatic lesions have been observed, and there is evidence that IL-2 and IFN-α can induce this remission. Contrarily to other immunogenic cancers, for example colorectal cancer, RCC shows a negative correlation of lymphocyte infiltration with survival rate [4].

Because of this, and the fact that RCC is highly resistant to chemotherapy and radiation, the application of immuno- and antiangiogenic therapies are currently of high interest in the treatment of RCC [5]. While the treatment with IFN-α and IL-2 have shown consistent results in remission of metastatic lesions, they have only modest overall benefits for patients. Hence high dose IL-2 remains the only supportable cytokine therapy for carefully selected patients [6]. Antiangiogenic-therapy, such as vascular epithelial growth factor (VEGF)-targeted therapy with Sunitinib and Bevacizumab, have improved outcomes, but could not assure a sustained remission or complete response when therapy was discontinued. The results of combining cytokine and antiangiogenic therapy suggest enhanced efficacy and an additive, albeit not a synergistic effect of this therapeutic approach [5].

As RCC is able to avoid immune surveillance, and develops resistance to immunotherapies, it is important to understand the molecular mechanisms at work. Some of the mechanisms involved in therapy resistance include the production of

specific cytokines, the presence of regulatory (CD4+CD25+) T-cells (T-regs), myeloid-derived suppressor cells (MDSC), and increased levels of VEGF [6].

To address these phenomena, a number of novel approaches, such as vaccinations and allogeneic bone marrow transplantation are currently under investigation. The programmed cell death 1 receptor (PD-1) and its ligand PD-L1 have been suggested to be one of the possible pathways responsible for RCC resistance to immunotherapeutic and antiangiogenic therapies [4]. A blockade of the immune checkpoint PD1, reducing the tumour-mediated T-cell-inhibition and self-tolerance, seems a promising therapeutic strategy.

The application of dendritic-cell based vaccinations has also been suggested to launch an anti-tumour immune response [7]. Although this approach is promising, it has so far only shown clinical benefits in a minority of patients. This rather new approach takes into account that while RCC is commonly infiltrated by a number of immune cells, the tumour milieu can inhibit their effector function. While the anti-tumour activity of T-cells in RCC has been widely investigated, only little is known about the potential role of myeloid cells. It has been shown that RCC is infiltrated with tumour-associated macrophages (TAM), NK cells [8] and dendritic cells (DC), which exhibit impaired or differing functions compared to non-cancerous renal tissue. TAM, for example, are thought to contribute to immunosuppression and T-cell tolerance in RCC by their production of the immunosuppressive cytokine IL-10, proinflammatory chemokine CCL2 and induction of factor forkhead box P3 (FOXP3) and cytotoxic T-lymphocyte antigen 4 (CTLA-4) [9].

1.2 Immune system

The immune system comprises the complex interaction of different cells and molecules for effective protection against disease. Its function is to identify and eliminate potential pathogens, such as viruses, bacteria and abnormal cells. It does this in part, by differentiating between self and foreign antigens. However, disorders of the immune system, such as deficiency to identify pathogens or misidentification of healthy cells as pathogens, can result in the development of infectious diseases, autoimmune diseases and also cancer.

The immune response is subdivided in an innate and an adaptive immune response. The innate immune system is an immediate, non-specific response to a pathogen. It comprises a humoral as well as a cellular response. This includes a physical and chemical barrier, activation of the complement cascade, cytokine production and the recruitment of immune cells to the site of infection. Leukocytes involved are NKs, mast cells, eosinophils, basophils, neutrophils, macrophages (MΦ) and DC. These cells recognize the pathogen associated molecular patterns (PAMP) of a pathogen mainly through pathogen recognition receptors (PRC), which activate the cell and result in cytokine and chemokine production. While the innate immune response allows a first elimination of the pathogen, it is not able to develop a long lasting immunity. Hence the activation of an adaptive immune response is an important continuation of immunity.

The adaptive immune system allows a specific and stronger response as well as the development of an immunological memory. It is the interplay of two types of lymphocytes, the B- and the T-cells, which originate from hematopoietic stem cells in the bone marrow. While B-cell activation results in a humoral response via antibody production, T-cells initiate a cell-mediate immune reaction. There are different subsets of T-cells, including T-helper cells (T_H1, T_H2, T_H3, T_H9 and T_H17), regulatory T-cells (T_{Reg}), cytotoxic T-cells and T-follicular cells (T_{FH}). T-cells are activated upon the recognition of antigens presented on major histocompatibility complexes (MHC) either by host cells or by antigen presenting cells (APC), e.g. DC. It is the T-cell receptor (TCR) in combination with a co-receptor, either CD4 or CD8, that recognizes the Antigen-MHC complex. Hence T-cells can be distinguished by their co-receptor in either $CD4^+$ T-helper cells, or $CD8^+$ cytotoxic T-cells. Similar, to B-cells, $CD8^+$ cytotoxic T-cells are specific for the recognition of one particular antigen presented by the host cell on the MHC I receptor. Upon binding, the cytotoxic T-cell is activated and releases perforin, granzymes and granulysin in order to induce apoptosis of the host cell and thereby prevents for example the replication of a virus or cancer development.

$CD4^+$ T-helper cells generally do not have cytotoxic activity, but regulate and potentiate the immune response of the adaptive as well as the innate immune system. Activated upon binding to an Antigen-MHC II complex, they produce cytokines, which guide, influence and reinforce the activity of e.g. MΦ and cytotoxic T-cells. Furthermore, $CD4^+$

T-cells can also develop into T_{reg}-cells. These cells are critical in the maintenance of immune cell homeostasis, the balance between immunity and self-tolerance, by preventing overshooting immune reactions.

1.3 Myeloid cells in cancer:

The tumour microenvironment is a complex system of epithelial and endothelial cells, lymphatic and vascular vessels, cytokines and chemokines as well as myeloid and lymphatic cells [10]. Within this milieu, the tumour develops, is influenced, and influences the milieu itself. Like other tissues, a tumour is continuously infiltrated by immune cells, which affect its progression, prognosis and differ depending on the type of cancer [11]. While being important for the cancers' characterisation, these immune infiltrates are also an interesting approach for cancer therapy. Though the function of immune cells is the protection against diseases and the elimination of abnormal cells, cancers are often able to prevent this and create an immunosuppressive milieu with impaired immune cell functioning. Immune infiltrates associated with this include myeloid-derived suppressor cells (MDSC), TAM, DC and T-cells.

MDSC are immune suppressive immature myeloid cells, which are, depending on their expression of plasma membrane markers and the content of immune suppressive molecules, subdivided into monocytic or granulocytic MDSC. They are able to inhibit innate as well adaptive immune responses and promote angiogenesis within the tumour. By impeding cytotoxic T-cell activation and function and on the other hand promoting T_{reg} cells, they contribute to an immunosuppressive tumour milieu [12].

1.3.1 Macrophages

Macrophages are key regulators of the adaptive and innate immune response by acting as APCs or by phagocytosis of infectious agents. Furthermore, they promote wound healing and have a homeostatic role, by for example eliminating apoptotic cells and cellular debris [13]. The original idea that macrophages develop from peripheral-blood mononuclear cells, which migrate into the tissue in steady state or during inflammation, has been revised and a more complex spectrum of differentiation is now thought to be a more appropriate way of looking at these cells [14]. As a simplified overview, MΦ have been grouped into M1 and in M2. Recent research, however, suggest that these only

represent extreme states of macrophage differentiation and that MΦ form rather a continuous linear scale than only two distinct subtypes. Their differentiation within this scale depends on the tissue milieu and soluble factors, such as granulocyte-macrophage colony-stimulating factor (GM-CSF) and macrophage colony-stimulating factor (M-CSF) [15].

The combination of IFN-γ and TLR signalling results in the differentiation of M1, also referred to as classically activated macrophages. This type of MΦ is part of the cell-mediated immunity and has microbicidal and tumourdicidal activity. Distinctive is the secretion of high levels of pro-inflammatory cytokines, e.g. IL-1, -6, -12 and -23, superoxide anions and oxygen as well nitrogen radicals [12] and the expression of MHCII. Hence, they are able to induce a Th1 and Th17 response [16].

M2 alternatively activated macrophages were originally thought to be activated upon IL-4 and IL-13 signalling. However, as the M2 phenotype is represented by a heterogeneous group of subtypes, it is more accurate to describe their differentiation as dominated by the STAT6-transcription factor, and incorporating signalling from different mediators, such as M-CSF, TGF-β, glucocorticoids, IL-1β, IL-4, IL-10 and IL-13 [17]. The result is a continuum of possible phenotypes and functions, depending on the combination of mediators. At least four different subtypes, M2a-, M2b-, M2c- and M2d-MΦ, have been suggested, which differ in expression of receptors and cytokine, as well as chemokine production. The general phenotype is characterized by up-regulation of mannose and scavenger receptors, as well as Toll-like receptors (TLR) and high expression of IL-10, TNF-α, but not IL-12. Their functions include the promotion of tissue remodelling, e.g. wound healing, angiogenesis, parasite encapsulation and regulation of immune response by recruiting immune cells and T_H2-cell promotion [18]. M2d- MΦ, have only recently been associated with M2, and are also referred to as TAM. They promote tumour growth by moderating angiogenesis, immune suppression and are linked to the induction of metastasis. They also produce high levels of IL-1β, IL-10, TGF-β and MMP and low levels of IL-12 [18].

1.3.2 Dendritic cells

Similar to MΦ and B-cells, Dendritic cells are professional APC with the capacity to induce a primary adaptive immune response by antigen-specific activation of $CD4^+$ and

$CD8^+$ T-cells. They differentiate from bone-marrow derived progenitor cells that migrate via the blood into lymphoid and non-lymphoid organs. Immature DC constantly sample antigens from their surroundings, but only undergo maturation upon pathogenic antigen uptake and stimulation. The complex process of maturation includes antigen presentation on MHC molecules on their surface, the down regulation of pro-inflammatory chemokine receptors, and the expression of CCR7 which facilities migration towards lymph nodes, cytokine production and finally T-cell activation [19]. While acting as a link between innate and adaptive immune system, DC also induce tolerance towards self-antigens and maintain tissue homeostasis. Simplified there are two broad subtypes of DC, plasmacytoid DC (pDC) and myeloid or conventional DC (mDC/cDC). Phenotypically all DC express high levels of MHC II (HLA-DR), but no hematopoietic lineage markers CD3, 14, 15, 19, 20, and 56 [20]. pDC are $CD11c^-CD123^+$ DC, which are able to produce high amounts INF-α upon virus recognition via TLR7 and TLR9, and can induce T_H1 and T_H2, and cross-present antigens to CTL [21]. Furthermore, they express BDCA2/CD303 (blood dendritic cell antigen 2), BDCA4/CD304 und IL-3R/CD123, which distinguishes them from cDC [22].

While summarized into one subgroup, cDC present a heterogeneous spectrum of phenotypes with at least two general subtypes $CD1c^+CD209^{+/-}$ DC and $CD141^+$ DC. They respond to microbial and other pathogens, produce high amounts of IL-12 and can induce T_H1. $CD1c^+$ cDC represent the major population of cDC in blood, tissue and lymphoid organs. When found in tissues, $CD1c^+$ cDC appear more activated as compared to their blood counterparts, and up regulate a series of surface markers such as CD80, CD83, CD86, CD40 and the chemokine receptor CCR7 [20]. They express a number of lectins and toll-like receptors (TLR 1-8), and are activators of naïve $CD4^+$ T-cells, with only moderate capacity to cross-present antigens and activate $CD8^+$ T-cells. Furthermore, they produce a number of cytokines such as TNF-α, IL-8, IL-10 and IL-12 when stimulated [20]. $CD141^+$ DC are infrequent, as they only represent 10% of cDC. They express less CD11b and CD11c than do $CD1c^+$ cDC, but co-express CADM1, CLEC9A, TLR3 und XCR1 [20]. Additionally, they are more competent in phagocytosis of dead or necrotic cells, detection of viruses with TLR3 and TLR8, and in antigen cross-presentation to $CD8^+$ T-cells. They also secrete TNF-α, CXCL10 and IFN-λ, but produce less IL12p70.

1.3.3 Enriched in renal cell carcinoma dendritic cells

In order to launch an effective anti-tumoural immune response, the recognition and phagocytosis of tumour-specific antigens by DC, with consequent maturation and migration towards lymph nodes to activate T-cells, is required. However, various studies have shown that DC found in RCC tissue samples present with impaired function and reduced ability to mature and activate T-cells [23]. While the percentage of DC, cDC as well as pDC, in peripheral blood of RCC patients was significantly lower than of healthy donors, the number of infiltrating DC in RCC tissue was found to be higher than seen in healthy kidney (unaffected pole of kidneys from tumour patients) [24]. These DC in RCC do not express the maturation marker DC-LAMP, which is considered to be a prognostic marker for functioning DC [25]. These RCC-DC also failed to up regulate CD80 and CD86 – an additional sign of impaired functionality [23]. Furthermore, ex vivo cultured DC obtained from patients with RCC exhibited a fully-matured surface with maturation-associated markers CD54, CD80, CD40, CD86, CD83 and CCR7, and were able to induce RCC-specific, IFN-γ producing T cells in vitro [24]. This suggests that the impaired functioning of DC in RCC might be due to the surrounding tumour milieu, e.g. IL-6, IL-10, VEGF or PGE_2.

In another study by A. Figel et. al., triple positive $CD209^+CD14^+CD163^+$ DC, which are considered to represent interstitial immature DC, where found to be predominant within the RCC and hence named “enriched in RCC dendritic cells” (ercDC) [26]. These $CD209^+$ DC unusually co-express the MΦ markers CD14 and CD163, which results in a difficult demarcation between DC and MΦ. Functionally, ercDC show weak allostimulation and T_H1 polarisation, due to the absence of specific cytokine production. Unlike TAM and MDSC, however, they do not compromise T-effector lymphocyte function, as they show no down-regulation of CD3ε or CD3ζ, FOXP3 induction, T-cell apoptosis, inhibition of cognate CTL cytotoxicity or CTL cytokine secretion. They are shown to secrete high levels of MMP-9 and CTL/tumour-cell co-cultures result in increased levels of TNF-α, and a reduction in CXCL10/IP-10 and CCL5/RANTES levels. Both TNF-α and MMP-9 are known to be tumour supportive cytokines, which result in more aggressive tumour growth and angiogenesis [27]. The chemokines CXCL10/IP-10 and CCL5/RANTES, however, are important in T_H1-polarized effector cell recruitment [28]. Furthermore, attempts to in vitro differentiate ercDC from monocytes,

showed that addition of CXCL8/IL-8, IL-6 and VEGF, which are highly expressed within the RCC, is sufficient to induce this RCC DC subtype [29]. These findings suggest that the tumour milieu is able to attenuate DC function and thereby enables one mechanism for RCC to escape from immune surveillance.

1.4 Wnt signalling

The Wnt-signalling pathway has been the focus of an increasing number of studies. This pathway plays important roles in a variety of cellular processes, e.g. embryogenesis, cancer development, tissue repair, and neural as well as immunological processes [30]. Depending on tissue milieu, cell type, and receptor profile, the 19 lipid-modified Wnt-ligands can activate a complex system of (Wnt-) signalling cascades, historically subdivided into “canonical-“and a subset of “non-canonical” signalling pathways. There at least 15 different Wnt-receptors and co-receptors, including the Frizzled-receptors (Fzd) [31], low-density lipoprotein receptor-related protein 5 and 6 (LRP 5/6) [32], receptor-like tyrosine kinase (RYK) [33], protein tyrosine kinase 7 (PTK7) [34], receptor Tyr kinase-like orphan receptor (ROR) [35], VANGL planar cell polarity protein (VANGL) [36] and many more.

While the Frizzled-receptors are the largest group of Wnt-receptors, it is not yet known whether they can function without a co-receptor. In addition, it is also difficult to distinguish between “receptors” and “co-receptors”, as some receptors can act in both ways [37]. The Frizzled-proteins are a group of 10 different seven-transmembrane domain receptors which can act as G-protein-coupled receptors, depending on cell type, receptor setting and the downstream cascade [38]. They are involved in β-Catenin-dependent and independent signalling, and bind Wnt-ligands via a cysteine-rich domain (CRD), which is also found in other receptors, such as the muscle-specific receptor tyrosine kinase (MUSK), neuronal specific kinase (NUSK2), ROR1 and ROR2 [39]. Similar to the Fzd-receptors, it cannot be said with certainty that the other receptors, often wrongly referred to as “co-receptors”, solely activate β-Catenin independent pathways. ROR1/2 for example are single-pass transmembrane receptors Tyr kinases, which can bind Wnt5a and mainly activate the PCP-pathway and the Ca^{2+}-pathway [37]. However, under certain tissue settings ROR can also transduce β-Catenin dependent signalling. The same can be said about the divergent receptor tyrosine kinase RYK and PTK7 [40].

A complex system of intra- and extracellular processes, e.g. inhibitors and phosphorylation, decides which pathway is activated by a specific Wnt-ligand. Consequently, it can be difficult to predict whether a specific Wnt-ligand is a "canonical" or a "non-canonical" ligand. Furthermore, the ligand-receptor (Wnt-Fzd) functional specificity is not well understood. A recent study showed that while Wnt3a has intermediate to strong binding to most Fzd-receptors, other Wnt-ligands including Wnt 4, 5a, 5b appear more selective in regard to their Fzd-receptor binding [41]. The current paradigm suggests that Wnt1, Wnt3a and Wnt8 preferentially activate β-Catenin dependent Wnt-signalling, while Wnt4, Wnt5a and Wnt11 are more associated with β-Catenin independent Wnt-cascades.

1.4.1 Canonical Wnt-pathway

Upon Wnt-β-Catenin or "canonical-pathway" activation, β-Catenin accumulates in the cytoplasm, translocates into the nucleus, and binds to TCF/LEF-transcription factors resulting in the modulation of target genes. At the beginning of this signalling cascade, a Wnt-ligand binds to a Fzd-Receptor and the (single-pass transmembrane) co-receptor LRP5/6 forming an oligomeric complex, called signalosome [42], which in turn initiates calveolin-mediated receptor endocytosis. The scaffolding protein dishevelled (Dvl) is then recruited to the cellular membrane and co-recruits glycogen synthase kinase 3 (GSK3) and casein kinase 1 (CKIα), which phosphorylate LRP5/6 and thereby further recruit AXIN and adenomatosis polyposis coli (APC). Hereby the β-Catenin-destruction complex (APC/Axin/GSK3β) is disrupted and inhibited, β-Catenin is not further phosphorylated, and recognised by the Ubiquitin-Ligase, and thus escapes proteasomal degradation. In the absence of Wnt-signalling, Axin, together with other components of the destruction complex GSK3, CKI and APC, orchestrates the sequential phosphorylation of β-Catenin. The phosphorylation enables β-transducin-repeat-containing protein (β-Trcp), an E3 ubiquitin ligase subunit, to ubiquitylate β-Catenin and thereby mark it for proteasomal degradation [43, 44].

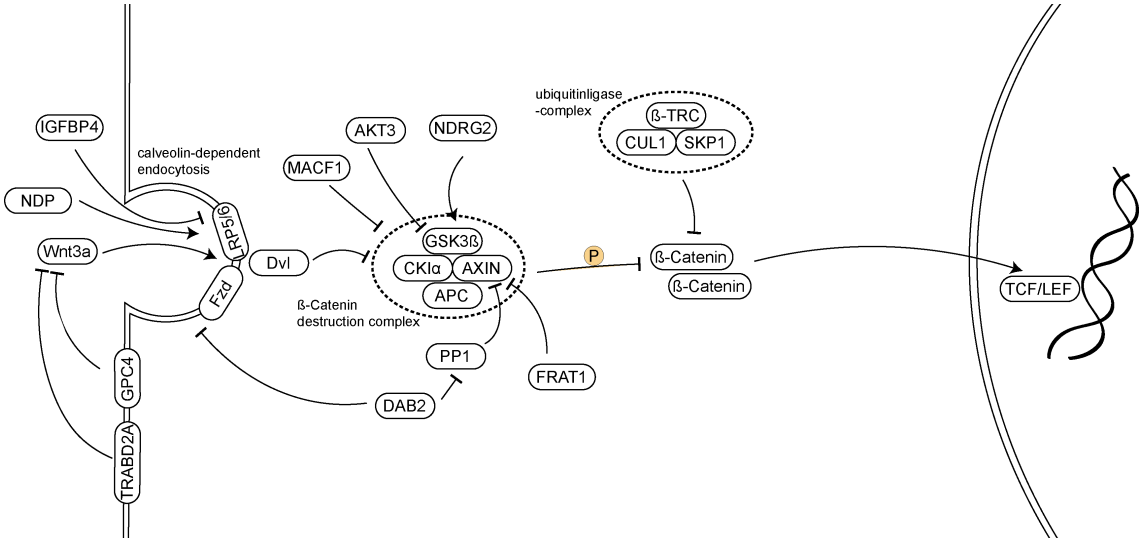

Fig. 1: ***The Wnt – β-Catenin dependent signalling.*** *The graph summarises main interactions within the canonical Wnt-signalling pathway. Boxes indicate gene products, arrows either activation or inhibition and "P" phosphorylation of the enzyme.*

1.4.2 Non-canonical Wnt-pathway

Apart from β-Catenin dependent signalling, there are also a number of β-Catenin independent pathways, referred to as "non-canonical", which include the Planar cell Polarity pathway (PCP), Wnt-Ca^{2+} pathway and other tissue specific Wnt activated signalling cascades. These pathways become activated when Wnt-ligands bind to Fzd-receptors, RYK, ROR, PTK7, MUSK, VANGL and others or a combination of Fzd with the other receptors acting as co-receptors.

The planar cell polarity pathway plays a role in epithelial orientation, as seen during embryogenesis and in the structural orientation of multicellular tissues. It is also associated with human diseases, such as neural tube defect, cystic renal diseases [45] and cancer development. The planar cell polarity pathway regulates cytoskeletal rearrangements as well as the transcription of target genes. When a Wnt-ligand, for example Wnt5a or Wnt11, binds to a Fzd-receptor, RYK or ROR1/2, VANGL and Dvl are recruited to the plasma membrane and dishevelled-associated activator of morphogenesis 1 (Daam1) is activated. In order to induce cell polarity, so-called "core PCP" proteins are asymmetrically organised in an apical-basal manner within a cell or between cellular formations upon Wnt stimulation [46]. While Dvl is recruited to the apical side towards the activated Fzd-receptor, VANGL is recruited to the basal side of the cell [47] by physical interaction with receptor for activated C kinase 1 (Rack1) [48]. Furthermore, it has been shown that a Wnt5a-ligand gradient is transduced into a VANGL2 phosphorylation by forming a ROR2-VANGL2 receptor complex, which seems to be of importance for the PCP-signalling pathway [49]. Downstream of Dvl ras homolog family member A (RHOA), Rho-associated coiled-coil containing protein kinase (ROCK), ras-related C3 botulinum toxin substrate 1 (RACI), c-JUN N-terminal kinase (JNK) and cell division control protein42 homolog (CDC42) can be activated and affect cytoskeletal rearrangement, as well as transcription of target genes [50, 51].

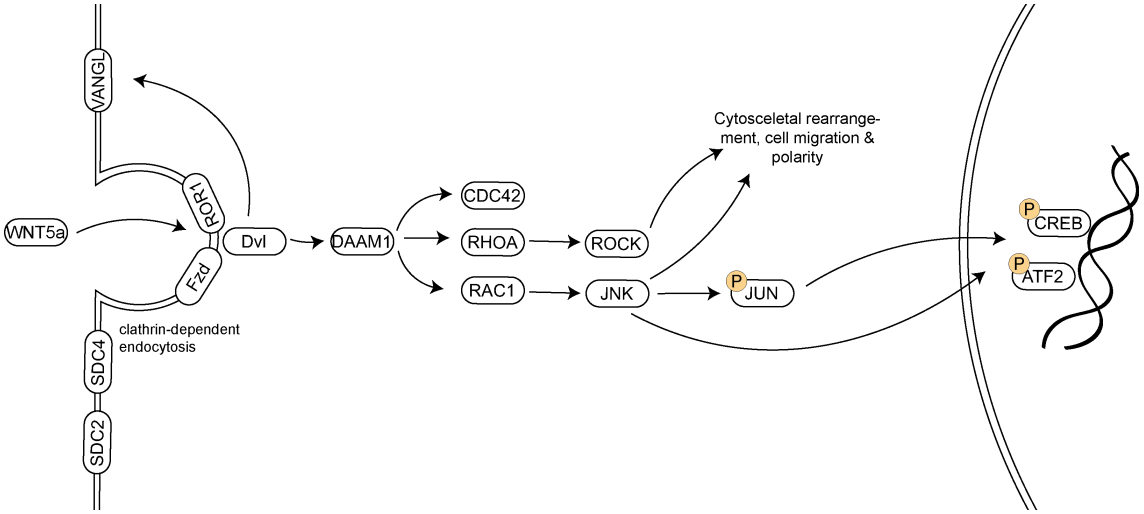

Fig. 2: ***The Wnt – Planar cell polarity pathway****. The graph summarises main interactions within the non-canonical Wnt- PCP pathway. Boxes indicate gene products, arrows either activation or inhibition and "P" phosphorylation of the enzyme.*

Wnt5a stimulation can also induce an intracellular increase in Ca^{2+}, Inositol-1,4,5-triphosphate (IP3) and Diacylglycerol (DAG) by activating Phospholipase C through Wnt-Fzd and ROR receptor interaction. IP3 then diffuses through the cytosol and releases Ca^{2+} from the endoplasmic reticulum [52]. The increase in Ca^{2+} and DAG activate Calcium sensitive calmodulin-dependent protein kinase II (CAMKII), proteinkinase C (PKC) or calcineurin. Downstream of CAMKII, PKC and calcineurin various effector proteins are activated by dephosphorylation, such as nuclear factor kappa-B (NFkB), cAMP responsive element binding protein (CREB) and nuclear factor associated with T cells (NFAT), which act as nuclear transcription factors. Re-phosphorylation of NFAT by GSK3 leads to its export from the nucleus and ending of its activation [53]. CAMKII can also activate nemo-like-kinase (NLK), which enters the nucleus and inhibits β-Catenin signalling by phosphorylation and degradation of TCF/LEF, the transcription factors of the β-Catenin dependent signalling pathway [54]. Furthermore Wnt-Fzd interaction can activate phosphodiesterase (PDE) in a Ca^{2+} dependent manner, regulating intracellular cyclic nucleotide concentrations through hydrolysis of cGMP to its nucleoside 5-prime monophosphates [55].

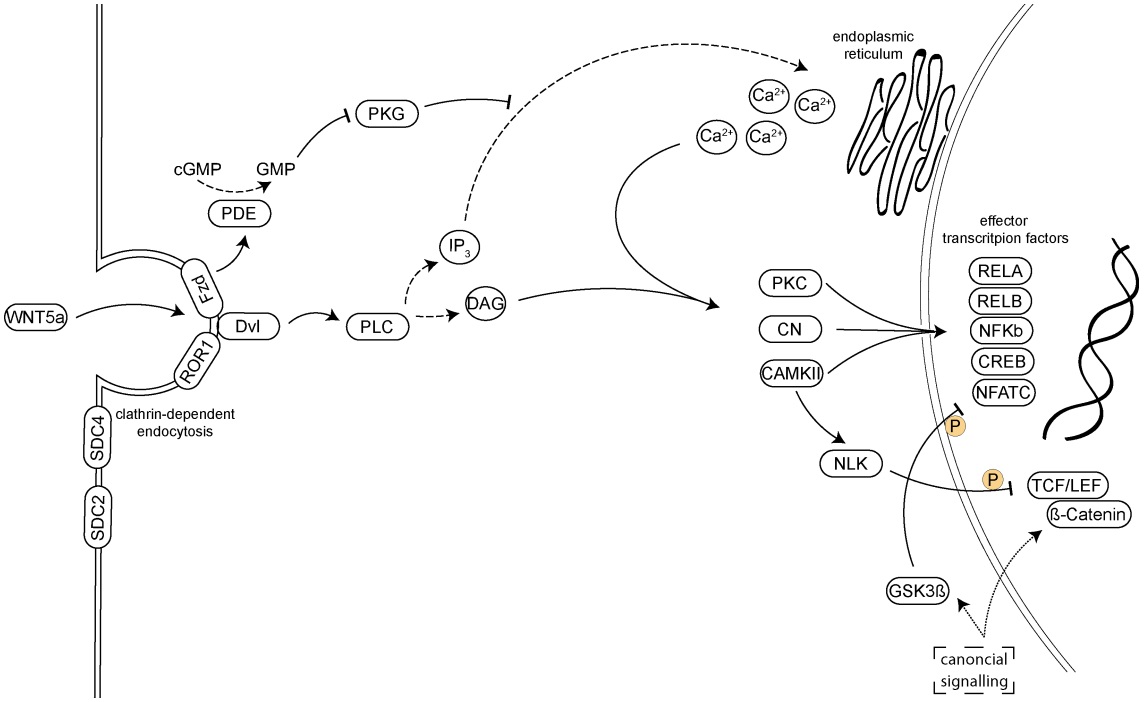

*Fig. 3: **The Wnt – Ca^{2+} pathway**. The graph summarises main interactions within the non-canonical Wnt- Ca^{2+}-pathway. Boxes indicate gene products, circles additional molecules involved, arrows either activation or inhibition and "P" phosphorylation of the enzyme.*

1.4.3 Complexity of Wnt-signalling

The Wnt-signalling pathway is a complex intracellular signalling network with cross-talk between different cascades and other signalling pathways, e.g. the Sonic Hedgehog pathway [56], rather than a single linear signalling pathway [57]. In order to achieve this network and the activation of differing downstream signalling cascades, a number of context dependent modifiers are required. The full extent of this network, as well as the exact mechanisms are not yet fully understood and are still under continuing research.

A number of different mechanisms of cascade activation have been suggested. Following Grumolato et al. the activation of β-Catenin dependent versus β-Catenin independent signalling depends on the ability to couple a Fzd-receptor with an endogenous co-receptor [58]. In this study it was shown that Dvl not only acts as a specific downstream scaffolding protein, but also as a switch between β-Catenin dependent and independent signalling, by enabling the phosphorylation and activation of specific co-receptors, LRP5/6 and ROR1/2, via GSK3β and Axin. Furthermore it has been suggested that Wnt5a inhibits β-Catenin dependent signalling via ROR2 signalling [59] or the Siah/APC-cascade [60]. Thrasivoulou et al. investigated the mechanisms of nuclear translocation of β-Catenin and proposed a convergent model of

Wnt-signalling in which an increase in intracellular and nucleoplasmic Ca^{2+} depolarizes the nucleoplasmic envelope and thereby enables and increases β-Catenin translocation into the nucleus. This was shown for a number of Wnt ligands (3A, 4, 5A, 7A, 9B, and 10B) in different mammalian cell lines and suggests a coupled mechanism of Wnt/Ca^{2+} and β-Catenin dependent pathway [61]. In another study it was shown that JNK inhibits Wnt3a-induced β-Catenin signalling by inducing the nuclear export of β-Catenin and thereby inhibiting the β-Catenin dependent expression of target genes [62]. Although these findings seem opposing it could be explained by further mechanism that are not yet known and need further investigation.

In addition to intracellular mechanisms, that decide on cascade activation or inhibition, there are also a number of soluble extracellular proteins that influence Wnt-signalling. This includes Wnt-inhibitors such as the Dickkopf-proteins (DKK), soluble frizzled related proteins (sFRP), Wnt-inhibitor factors (WIF) and Cerberus. DKK-proteins bind the Wnt-coreceptors LRP5/6 and thereby modify β-Catenin dependent Wnt-signalling. While DKK 4 acts as Wnt- antagonist [63], DKK1, DKK2 and DKK3 can either antagonize or potentiate Wnt-signalling depending on cell type and receptor profile [64]. Kremen, a single-pass transmembrane receptor, can negatively regulate Wnt-signalling via the LRP5/6 co-receptor in the presence of Dickkopf by mediating LRP internalisation, but can also facilitate Wnt-signalling in the absence of DKK [65].
Other Wnt-antagonists, such as sFRPs, WIF and Cerberus bind to Wnt-ligands and are thought to inhibit Wnt-signalling by competing with Fzd-receptors for Wnt-ligand binding or direct interaction with Wnt-receptors. The sFRPs have a Cystein rich domain (CRD), which is similar to that of Fzd receptors, and WIF have a Wnt interacting domain similar to that of the RYK-receptor, which allows their interaction with the Wnt-ligand. However, there is also evidence that sFRPs might be able to enhance Wnt-signalling by enabling Wnt-ligand distribution [66] and LRP phosphorylation [67]. Hence, the view of Wnt-antagonists solely acting as inhibitors of Wnt-signalling has to be renewed and a more complex system should be applied.

Positive influencers of Wnt-signalling are collagen triple helix repeat containing 1 (CTHRC1) and R-spondins. CTHRC1, a secreted glycoprotein is involved in the selective

activation of the PCP-pathway possibly by forming a CTHRC1-Wnt-Fzd/Ror2 complex [68] and thereby stabilizing ligand-receptor interaction. R-spondins can act as Wnt-agonists, which potentiate Wnt-signalling in the presence of Wnt-ligands. A number of different receptors, such as the syndecans and leucine-rich repeat-containing G protein-coupled receptors (LGRs), have been suggested for R-spondin interaction [37]. Ohkawara et al. investigated a possible molecular mechanism for R-spondin and syndecan interaction, suggesting clathrin-mediated endocytosis of the Wnt-receptor complex upon SDC4 and R-spondin3 binding, allowing Wnt/PCP-activation [69]. This ligand-receptor internalisation is not only associated with Wnt/PCP-signalling, but also other Wnt-cascades. Heparan sulphate proteoglycans (HSPG), notably glypicans and syndecans, can act as Wnt-Coreceptors and enhance Wnt-signalling by binding both ligand and receptor, allowing endocytosis and enhancement of Wnt-signalling [37]. syndecans and glypicans can act as Co-receptors in a variety of different cellular signalling cascades by interacting with e.g. Fzd. in Wnt-signalling, Hedgehog receptors and transforming growth factors β (TGF-β) receptors [70].

In summary, it can be said that Wnt-signalling is represented by a complex set of different signalling cascades, including extensive cross-talk within these cascades and with other signalling pathways. There are 19 different Wnt-ligands, over 15 receptors and many more co-receptors and extracellular as well as intracellular Wnt-modulators that make it difficult understand and predict Wnt-signalling. To simplify, one can distinguish between β-Catenin dependent and β-Catenin independent signalling, which in turn consists of Wnt-PCP and Ca^{2+} signalling. However, making this distinction requires a profound understanding: Considering that this is only a simplified model, it is clear that there are many more factors and interactions that are not yet fully understood and under on-going research.

2 Aim of the present study

Wnt-signalling has been studied in the context of a variety of cellular processes and has been linked to the development and differentiation of immune cells with especially strong ties to myeloid biology. The aim of this study was to characterize the differences in activation status of Wnt-signalling in different myeloid cells with special emphasis on cDC and ercDC. We hypothesized that as myeloid cells undergo activation to different effector subtypes including cDC and the resident ercDC, they alter the Wnt-activation status and that these changes may be linked to their effector function. As a first step, we therefore performed transcriptomic analyses on primary human peripheral blood monocytes from healthy donors and in vitro generated M1, M2, cDC and ercDC. Differential gene expression within the canonical and non-canonical Wnt-signalling cascades was selectively investigated.

The effects of altering Wnt-signalling via inhibition or stimulation, on the functional abilities of cDC and ercDC, were evaluated with special emphasis on their essential functional abilities, including migration and cytokine production.

3 Materials

3.1 Instruments

Name	Manufacturer
BD™ LSR II	Becton Dickinson (BD), Franklin Lakes (USA)
Eppendorf „Centrifuge“ 5417 R	Eppendorf, Hamburg
Fluorescence Microscope *DMRBE*	Leica, Wetzlar
HERAcell® 240i CO_2-Incubator	Heraeus Instruments, Hanau
Irradiator HWM-D-200, (radiation source: Caesium^{137})	Gammacell® 40, Ottawa (Canada)
Jenoptik ProgRes CCD camera	Jenoptik, Jena
Laminar flow working bench	BDK, Sonnenbühl-Genkingen
Leica DM IL microscope	Leica Microsystems, Wetzlar
LightCycler® Instrument 480	Roche Life Science, Unterhaching
MACS Multistand (quadro MACS)	Miltenyi Biotec, Bergisch Gladbach
Magnetseparator, SPRIPlate Super Magnet Plate	Beckman Coulter, Brea (USA)
Milli-Q® Integral Water Purification System	Merck Millipore, Billerica (USA)
Microwave	Milestone Medical, Kalamazoo (USA)
Mikrozentrifuge Biofuge Pico	Heraeus Instruments GmbH, Hanau
Multichannel pipette	Thermo Scientific, Waltham (USA)
Neubauer Chamber	GLW, Würzburg
Nitrogen tank	Messer Griesheim, Krefeld

Nunc-Immuno™ Washers	Nunc, Wiesbaden
Pipetus® battery	Hirschmann Laborgeräte, Eberstadt
Power supply PowerPac300	Biorad, München
QubitTM fluorometer	Invitrogen, Karlsruhe
Rotator	VWR international, Westchester (USA)
SpeedVac Univapo 150 ECH	Montreal Biotech, Montreal (Canada)
Spectrophotometer sunrise	Tecan Group AG, Männedorf (Switzerland)
Thermomixer comfort	Eppendorf, Hamburg
UV Transilluminator	Bachofer, Reutlingen
Vortexer	Heidolph Instruments, Schwabach
Water bath	Köttermann, Uetze
Zentrifuge Megafuge 2.0/2.0 R	Heraeus Instruments GmbH, Hanau

3.2 Consumables

Name	Manufacturer
Butterfly (Ecoflo)	Dispomed Witt oHG, Gelnhausen
Cell scraper S (24cm)	TPP, Trasadingen (Switzerland)
Cell scraper mini	LEAP Biosciences Corp., Palo Alto (USA)
Cell strainer (700/100 µM)	BD, Franklin Lakes (USA)
Cell culture flasks (75/175cm^2)	Greiner bio-one, Kremsmünster (Austria)
ELISA plates	Greiner bio-one, Kremsmünster (Austria)
Eppendorf tubes (0,5/1,5/2 ml)	Eppendorf, Hamburg
FACS-tubes (1,5ml, polypropylen)	Greiner bio-one, Kremsmünster (Austria)
Falcon tubes (15/50 ml)	BD, Franklin Lakes (USA)
MACS Separation Columns, 25 LS	Miltenyi, Biotec, Bergisch Gladbach

Nunc™ Well Plates (Flat & Round Bottom (6-, 24-, 96-well)	Nunc, Wiesbaden
Pasteurpipettes, glas	Peske OHG, Aindling
Pipette tips	Eppendorf/Gilson, Zentrallager Helmholtz-Zentrum, Neuherberg
QIAshredder	QIAGEN, Venlo (Netherlands)
"Safe-lock tubes" (1,5ml, RNAse free)	Eppendorf, Hamburg
scalpel	Aesculap AG, Tuttlingen
Serological Pipettes (2 ml, 5 ml, 10 ml und 25 ml)	Greiner bio-one, Kremsmünster (Austria)
µ-Slide Chemotaxis	Ibidi, Planegg/Martinsried
Syringe (5/50ml)	BD, Franklin Lakes (USA)
Taqman plates	Sarstedt, Nümbrecht
Taqman cover	Sarstedt, Nümbrecht
Trans-well 24 well plate, 5 µM pore size	Costar, Corning (USA)
Vortexer	neo-Lab,München

3.3 Media, chemicals, reagents and additives

Name	Manufacturer
AccuCheck counting beads	Invitrogen, Thermo Fisher Scientific, Waltham
Acetic acid	Merck KGaA, Darmstadt
Agarose, ultrapure	Invitrogen, Thermo Fisher Scientific, Waltham
AIM-V	Life Technologies, Carlsbad (USA)
7-Amino-Actinomycin D (7-AAD)	Sigma-Aldrich, St.Louis (USA)
Aqua ad injectabilia	Braun, Melsungen
ß-Mercaptoethanol	Roth, Karlsruhe
Bovines serumalbumin (BSA)	Sigma Aldrich, St.Louis (USA)
CD14 Microbeads	Miltenyi Biotec, Bergisch-Gladbach

Collagen I Bovine Protein, 5 mg/ml	GIBCO, Thermo Fisher Scientific, Waltham (USA)
CompBeads (anti-mouse/anti-rat Ig, κ; FCS)	BD, Franklin Lakes (USA)
3,3'-diaminobenzidine (DAB)	Sigma Aldrich, Taufkirchen
Dimethylsulfoxid (DMSO)	Merck KGaA, Darmstadt
Dithiothreitol (DTT)	Invitrogen, Karlsruhe
Ethanol	Merck KGaA, Darmstadt
Ethylenediaminetetraacetic acid (EDTA)	Sigma Aldrich, St.Louis (USA)
Ficoll® (Biocoll, concentration 1,077 g/ml)	Biochrom AG, Berlin
First-strand buffer (5x)	Invitrogen, Thermo Fisher Scientific, Waltham
Fetal calf serum (FCS)	Life Technologies, Carlsbad (USA)
Heparin 2500 IE	Essex Pharma GmbH, München
HEPES, 1M	Invitrogen, Carlsbad
Hexanucleotides	Roche Diagnostics, Mannheim
Human serum (HS) (different healthy donors)	IMI Helmholtzzentrum, München
Hydrogen peroxide solution, 30%	Merck KGaA, Darmstadt
Ibidi freezing medium classic, serumfree	Ibidi, Planegg/Martinsried
L-Glutamine	Life Technologies, Carlsbad (USA)
Lipopolysaccharid (LPS) E.coli	Sigma Aldrich, St.Louis (USA)
Magnesiumchloride	Fermentas, St.Leon-Rot
Methanol	Merck KGaA, Darmstadt
Methyl green	Fluka, Schnelldorf
MoDC-differentiation medium, human (contains FCS, RPMI 1640, L-Glutamine, IL-4, GM-CSF)	Miltenyi Biotec, Bergisch-Gladbach
Non-essential amino acids (NEAA) (100x)	Life Technologies, Carlsbad (USA)
dNTP set	Fermentas, St.Leon-Rot

Paraformaldehyd (PFA)	Merck KGaA, Darmstadt
Penicilline/Streptomycine (100x)	Life Technologies, Carlsbad (USA)
Phosphate buffered saline (PBS)	Life Technologies, Carlsbad (USA)
Polysorbat-20 (Tween 20)	Sigma Aldrich, St.Louis (USA)
Propidiumjodid (PI)	Sigma Aldrich, St.Louis (USA)
RNAsin – ribonuclease inhibitor	Promega, Madison, USA
Rox reference dye (25x)	Invitrogen, Thermo Fisher Scientific, Waltham
RPMI 1640 Medium	Sigma Aldrich, St. Louis (USA)
Sodium azide	Sigma Aldrich, St.Louis (USA)
Sodiumcarbonat, hydrogencarbonat	Merck KGaA, Darmstadt
Sodiumchloride	Merck KGaA, Darmstadt
Sodium pyruvate	Life Technologies, Carlsbad (USA)
SYBRgreen I (250x)	Fluka, Schnelldorf
Trishydroxymethylaminomethan (Tris)	Merck KGaA, Darmstadt
Trypan blue	ICN Biomedicals GmbH, Eschwege
Trypsin-EDTA (10x)	Life Technologies, Carlsbad (USA)
Taq buffer without detergent (10x)	Fermentas, St.Leon-Rot
VectaMount Permanent Mounting Medium	Vector Laboratories, Burlingame, Carlifornia (USA)
Xylol	Merck KGaA, Darmstadt

3.4 Prepared buffers and solutions

Name	Preparation
ELISA – blocking buffer	PBS +10%FCS
ELISA – coating buffer	0,1 M Carbonatebuffer pH 9,5: 8,4 g NaHCO3 3,56 g Na2CO3 ad 1 L Milipore-water

ELISA – washing Buffer	PBS + 0,05% Tween 20
FACS – acid-buffer	PBS + 2 mM EDTA + 0,1% sodium azide + 2% FCS
MACS – buffer	PBS + 2 mM EDTA + 0,5% FCS
Trypsin – EDTA – solution (2x)	PBS + 20% 10x Trypsin-EDTA
Loading buffer	H_2O + 0.25% Bromphenol blue + 0.25% Xylene cyanol + 30% glycerol
SYBRgreen I solution	1:100 in H2O with 20% DMSO, (-20°C)
SYBRgreen Mastermix	20% Taq buffer without detergent + 375 µM NTPs + 4% Rox referencedye + 40% PCR Optimizer + 2% BSA + 0.4% SYBRgreen I solution + 6 mM MgCl2

3.5 Prepared media

Name	Preparation
RPMI – basismedium	RPMI 1640 + 2 mM L-Glutamine + 1 mM Sodium pyruvate + 1 mM NEAA
LCL – medium (L929-CD40L-cells)	RPMI – basismedium + 10% FCS

RCC – medium (RCC-26-Zellen)	RPMI – basismedium + 12% FCS
AIM-V – medium (myeloid cells)	AIM-V (serumfree) + 2 mM L-Glutamine

3.6 Enzymes and enzyme solutions

Name	Manufacturer
DNAse I	Qiagen, Hilden
RNase A (10 mg/ml)	Roche Diagnostics, Mannheim
Taq DNA – polymerase (5U/µl)	NEB, Frankfurt a.M.
Streptavidin-Horseradish peroxidase	Vector Laboratories, Burlingame, USA

3.7 Antibodyies

Name	Manufacturer
Mouse anti-Wnt5a antibody	abcam®, Cambridge, UK
Biotinylated goat anti-mouse IgG	Jackson ImmunoResearch Laboratories, West Grove, USA

3.8 qPCR Primer

Name	Manufacturer
Hs_CAMK2D_1_SG QuantiTect Primer Assay	Qiagen, Hilden
Hs_CELSR1_1_SG QuantiTect Primer Assay	Qiagen, Hilden
Hs_DAAM1_1_SG QuantiTect Primer Assay	Qiagen, Hilden
Hs_FRAT1_1_SG QuantiTect Primer Assay	Qiagen, Hilden
Hs_FRAT2_1_SG QuantiTect Primer Assay	Qiagen, Hilden
Hs_FZD5_1_SG QuantiTect Primer Assay	Qiagen, Hilden
Hs_GPC4_1_SG QuantiTect Primer Assay	Qiagen, Hilden
Hs_HIPK2_1_SG QuantiTect Primer Assay	Qiagen, Hilden
IL10, human, TaqMan® Gene Expression Assay	Thermo Fisher Scientific, Waltham (USA)

IL12A, human, TaqMan® Gene Expression Assay	Thermo Fisher Scientific, Waltham (USA)
IL12B, human, TaqMan® Gene Expression Assay	Thermo Fisher Scientific, Waltham (USA)
Hs_NFATC1_1_SG QuantiTect Primer Assay	Qiagen, Hilden
Hs_RELA_1_SG QuantiTect Primer Assay	Qiagen, Hilden
Hs_RELB_1_SG QuantiTect Primer Assay	Qiagen, Hilden
Hs_SDC2_1_SG QuantiTect Primer Assay	Qiagen, Hilden
Hs_SDC3_1_SG QuantiTect Primer Assay	Qiagen, Hilden
Hs_TCF7L2_1_SG QuantiTect Primer Assay	Qiagen, Hilden
Hs_TLE3_1_SG QuantiTect Primer Assay	Qiagen, Hilden
TNFa, human, TaqMan® Gene Expression Assay	Thermo Fisher Scientific, Waltham (USA)
Hs_WNT5A_1_SG QuantiTect Primer Assay	Qiagen, Hilden

3.9 Cytokines, chemokines and stimulants

Name	Manufacturer
fMLP	Sigma-Aldrich, Taufkirchen
rhu CCL19	Peprotech, Hamburg
rhu IL-1ß	PromoKine, Heidelberg
rhu IL-6	Promokine, Heidelberg
rhu PGE2	Sigma-Aldrich, Taufkirchen
rhu TNF-α	Sigma-Aldrich, Taufkirchen
Lipopolysaccharid (LPS) E.coli	Sigma Aldrich, Taufkirchen
rh-sFRP1 (250μg/ml)	R&D systems, Minneapolis (USA)
rh-sFRP5 (100μg/ml)	R&D systems, Minneapolis (USA)
rh/m-Wnt5a (100μg/ml)	R&D systems, Minneapolis (USA)

3.10 Kits

Name	Manufacturer
Avidin/Biotin Blocking kit	Vector Laboratories, Burlingame, USA
Human IL-10 BD OptEIATM ELISA Set	BD, Franklin Lakes (USA)
Human IL-12 (p70) BD OptEIATM ELISA Set	BD, Franklin Lakes (USA)
Human IL-12 (p40) BD OptEIATM ELISA Set	BD, Franklin Lakes (USA)
Human TNFa BD OptEIATM ELISA Set	BD, Franklin Lakes (USA)
PureLink® RNA Mini Kit	Ambion, Life technologies, Carlsbad (USA)
Quant-iTTM RNA Assay kit	Invitrogen, Karlsruhe
RNeasy Mini (50) kit	Qiagen, Hilden
Taqman® Universal PCR Master mix	Applied Biosystems, Darmstadt

3.11 Cells

Cells	Description	Source	Medium
„classical“ DC (cDC)	Differentiated from monocytes of healthy human donors	generated in the lab	MoDC-Diff.-Medium, AIM-V-Medium (1% HS) + IL-4 + GMCSF
„enriched in renal cell carcinoma“ DC (ercDC)	Differentiated from monocytes of healthy human donors through addition of RCC-26-CM	generated in the lab	AIM-V-Medium (3% HS), VLE-Medium (6% HS) with respectively 25 % RCC-26-CM
L929-CD40L	Mouse-fibroblast-cell line, transfected with human CD40L, adherent	P. Garrone (1995)	LCL-Medium

Peripheral blood mononuclear cells (PBMC)	Isolated from human whole blood of healthy donors	Not cultured	Healthy donors
RCC-26	Human renal cell carcinoma cell line, HLA-A2-positiv, adherent	RCC-Medium	IMI, Helmholtz Zentrum München

3.12 Blood samples

Whole blood samples were kindly donated by healthy human donors. All blood drawls were performed by authorised and qualified personnel. The donors' informed consents and the full approval of the ethics commission were obtained beforehand.

3.13 Array data

For transcriptomic analysis in vitro and ex vivo, myeloid microarray expression data were kindly provided by the group of Prof. Dr. Elfriede Nößner from IMI Helmholtz Zentrum Munich. Microarray expression data of healthy kidney samples and renal cell carcinoma samples were provided by PD Dr. Matthias Maruschke from the Department of Urology of the University of Rostock [71]. Subsequent analyses were performed in the laboratory of Prof. Dr. Peter Nelson, Klinische Biochemie, Medizinische Poliklinik der LMU.

3.14 Kidney sections for immunohistochemistry

Kidney sections of healthy human kidney and human renal cell carcinoma were provided by Prof. Dr. Hermann-Josef Gröne, head of Department of Cellular and Molecular Pathology at the DKFZ Heidelberg. Sample preparation and immunohistochemistry were performed in the laboratory of Prof. Dr. Nelson.

3.15 Software

Name	Manufacturer
Adobe Illustrator	Adobe, San Jose (USA)
Affymetrix® Expression Console™	Affymetrix, Santa Clara (USA)
BD FACSDivaTM	BD, Franklin Lakes (USA)
Endnote X7.0.2	Thomson Reuters, New York (USA)
FlowJo	TreeStar Inc., Ashland (USA)
Graph Pad Prism 6	Graphpad Software, La Jolla (USA)
ImageJ 1.49v (Plugins: Manual Tracking, Chemotaxis Tool)	National Institute of Health, Bethesda (USA)
MADMAX	Bioinformatics, Wageningen UR, Wageningen (Netherlands)
Microsoft Office 2010	Microsoft, Redmond (USA)

4 Method

4.1 Cell culture

4.1.1 General cell culture

The culture of cells was performed with a laminar flow hood and only sterile materials, solutions and mediums were used in order to avoid contamination. Cells were cultivated in an incubator at 37°C, 6,5% CO_2 and 95% air humidity. Unless stated otherwise, all centrifugations were performed at 1500rpm for 5min with the Heraeus Megafuge 2.0.

4.1.2 Freezing and thawing of cells

The freezing medium was prepared by adding Dimethylsulfoxid (DMSO) to the cell medium. As DMSO is toxic to cells all steps were performed quickly on ice to avoid damage of the cells. Cells were centrifuged, the sediment resuspended in 500µl cooled FCS and then transferred into a cryotube. Thereafter, another 500µl 20%DMSO freezing medium was added to the cryotube, leading to a final concentration of 10% DMSO, and cooled down to -80°C over a period of 24 or 48h, and later transferred to the gas-phase of a liquid nitrogen tank for long-term storage at approximately -196 °C. In order to freeze RCC-26-cells, the pellet was resuspended in 1ml Ibidi freezing medium, which also contains DMSO.

When thawing cells, the cryotube was rapidly thawed in at 37°C water bath until 2/3 of the suspension was thawed, which indicated a temperature of 4°C. Immediately 2ml of FCS were added and the suspension transferred into a 15ml tube for centrifugation. The pellet was then resuspended in cell medium and transferred into a culture plate.

4.1.3 Counting of viable cells

Cells were counted using a Neubauer counting chamber. An aliquot of the cell suspension was taken and mixed with Trypan Blue in the required ratio in order to stain dead cells blue. When preparing whole blood for PBMC extraction, 3% acetic acid was added to enable the bursting of Erythrocytes, which facilitates PBMC counting. The cover slip of the Neubauer counting chamber had to be attached to the chamber in such a way so that the “Newton rings” were visible. The distance between chamber and slip

is defined and enables counting. Only living cells were then counted in all quadrants and cells per ml could be calculated, regarding the dilution factor:
Cell no./ml = mean cell no. of the 4 large quadrants x dilution factor x 10^4

4.1.4 Cultivation of RCC-26 cells

In order to in-vitro differentiate ercDC from $CD14^+$ Monocytes, RCC-26 conditioned medium (RCC-26-CM) was required. The RCC-26 cell line is an adherent growing cell line and was cultured in lying cell culture flask with filter cover. Depending on the size of the culture flask (T75 with 75 cm^2 or T175 with 175cm^2 growing surface) respectively 10 or 15ml of AIM-V growth medium were used for cultivation. The cell medium had to be renewed every 3-4 days, in order to avoid lack of nutrition. Furthermore, cells were split when 80-100% confluence was reached to avoid overgrowth. For this purpose, the medium was completely removed and cells washed with 5ml PBS. Then 1ml (T75) or 2ml (T175) Trypsin-EDTA solution was added to detach cells from the surface, which was confirmed by microscopy. Thereafter fresh culture medium with FCS was added, which inhibits Trypsin and its reaction, and the solution was transferred into a tube and centrifuged. The supernatant was then discarded, the pellet resuspended in fresh culture medium and the cells could be split and seeded into fresh flasks for further cultivation.
In order to obtain RCC-26-CM, $2x10^6$ RCC-26-cells were cultured in a T75 flask with 10ml AIM-V medium for 10 days. Thereafter the supernatant was collected, centrifuged for 10min at 2000rpm, sterile filtered through a 0.2µm pore filter and frozen at -20°C.

4.1.5 Isolation of peripheral blood mononuclear cells from whole blood

Whole blood was donated from healthy donors and the PBMCs were isolated through Ficoll® density centrifugation. Ficoll® is a hydrophilic polysaccharide, which is commonly used to separate blood into its components and the isolation of PBMCs. The Ficoll® density centrifugation is based upon the density differences between the mononuclear cells and other components of the blood. After centrifugation the whole blood is separated into plasma (top layer, very low density), PBMCs and thrombocytes

(interphase, low density) and polymorphonuclear cells, such as neutrophils and eosinophils, and erythrocytes (bottom layer, high density).

In order to avoid coagulation of the whole blood, the 50ml syringes were prepared with 1000 Units Heparin/50ml blood (100µl per syringe) previous to the blood draw. Heparin is an anticoagulant, which inhibits the coagulation of blood by binding to and activating antithrombin and thereby inactivating thrombin and other proteases involved in blood clotting. The whole blood was then one-to-one diluted with RPMI 1640-Medium, i.e. 200ml whole blood with 200ml RPMI 1640-Medium, and each 35ml of the diluted blood layered over 15ml Ficoll® in a 50ml Falcon tube. Subsequently, the whole blood was separated into its components by centrifugation for 20min at 2000rpm without break. The interphases, just over the Ficoll®, containing the PBMCs were collected with a 10ml pipette into a 50ml Falcon-tube, again one-to-one diluted with RPMI 1640-Medium and remaining Ficoll® washed away through centrifugation for 12min at 1900rpm.

4.1.6 Isolation of $CD14^+$ monocytes

Magnetic Cell Sorting (MACS) was used to isolate CD14+ monocytes from PBMCs. The Principle of MACS separation is based upon the magnetic labelling of target cells. In this case monocytes were labelled with CD14 Micro beads. The CD14 receptor, which is strongly expressed on most monocytes and macrophages, but not on other cells, is part of a LPS receptor complex, but does not transduce signalling due to its lack of a cytoplasmic domain. The cell suspension is separated in a column, which is placed in the magnetic field of the MACS separator. While the unlabelled cells pass through the column, the $CD14^+$ labelled cells retain in the column and can later be eluted when removing the column from the magnetic field.

The following steps were carried out on ice. The supernatant of the washed PBMCs isolated through Ficoll density centrifugation was decanted and the pellets carefully resuspended in 10ml cold MACS buffer and summed up in a 50ml Falcon tube. Unnecessary pipetting was avoided in order to prevent cell activation and lump formation. The tubes were rinsed again with 10ml MACS buffer. The cell suspension was then loaded onto a cell strainer filter (100µm pore size) placed on a 50ml falcon tube in order to eliminate cell aggregations and big particles, filled up to 50ml with MACS buffer and centrifuged for 12min at 1900rpm and 4°C. The supernatant was decanted

and the pellet resuspended in 80µl MACS buffer/ 10^7 cells. Hereafter 10-15µl CD14 Micro beads/ 10^7 were added and thoroughly mixed. The suspension was then rotated for 15min at 4°C.

Surplus unbounded beads were removed by adding 10 times volume of MACS buffer and 12min centrifugation at 1900rpm and 4°C. The supernatant was decanted, the pellet re-suspended in 5ml cold MACS buffer and then loaded onto the MACS column, which was equilibrated with 3ml MACS buffer and clamped in the MACS separator. The CD14 negative cells were collected and the column washed three times with 3ml MACS buffer. The column was then removed from the MACS separator and placed on a 15ml Falcon collecting tube. The $CD14^+$ cells were eluted with 5ml MACS buffer and the help of a piston. Thereafter the cell suspension was centrifuged for 12min at 1900rpm and 4°C. Again the supernatant was discarded, the pellet re-suspended in 3ml AIM-V medium/1% L-glutamine and a small aliquot was taken for cell number determination. The CD14+ yield varied between 15 x 10^6 to 30 x 10^6/100 ml depending on the blood donor.

4.1.7 In vitro generation of cDC and ercDC

In order to generate $CD209^+$ $CD14^+$ conventional DC (cDC) the isolated monocytes, $CD14^+$ cells, were differentiated using Miltenyi's Mo-DC differentiation medium. Miltenyi's differentiation medium is based on RPMI 1640 Medium and contains the two cytokines IL-4 and GM-CSF. The monocytes were cultured in a 6 well Nunc® plate in a concentration of 5 x 10^6 cells/ 5ml Miltenyi's Mo-DC differentiation medium per well. On day three of culture another 5ml Miltenyi's Mo-DC differentiation medium was added to each well. The cells were then either used as immature cells on day 7 or maturated using the "Jonuleit cocktail" [72] on day 6. For maturation on day 6, the immature cDC were harvested and re-suspended in 1ml/1 x 10^6 AIM-V medium/1% L-glutamine plus "Jonuleit cocktail". The "Jonuleit cocktail" is a defined cocktail of interleukin-1ß (IL-1ß, 10ng/ml), TNF-α (25ng/ml), IL-6 (1µg/ml) and prostaglandin E2(PGE2, 12.5ng/ml), which has been found to be optimal for the maturation of cDC.

For in vitro generation of triple positive $CD209^+CD14^+CD163^+$ ercDC, Figel et al. showed that RCC-26-CM is able to induce this phenotype. Hence isolated $CD14^+$ monocytes were cultured in a 6 well Nunc® plate at a cell density of 7 x 10^6 cells/3ml AIM-V/3%HS/1%

L-glutamine plus 1ml RCC-26-CM per well. On day 2 and on day 5 respectively 1ml RCC-26-CM was added to each well. ErcDC were harvested as immature cells on day 7, or maturated adding the "Jonuleit cocktail" on day 6. After adding the "Jonuleit cocktail" on day 6, cells were harvested 24h later and used for respective experiments.
Alternatively, immature ercDC were harvested on day 6 and re-suspended in AIM-V/1% L-glutamine without RCC-26-CM and matured by adding "Jonuleit cocktail". This variation allowed investigating the effects of stimulation with i.e. Wnt5a, without possible inhibiting factors in the RCC-26-CM.
Where indicated, recombinant proteins, such as Wnt5a (250ng/ml), sFRP5 (500ng/ml) and sFRP1 (500ng/ml) were added to the cDC and ercDC suspension during differentiation.

4.2 Functional Tests

4.2.1 Signal-3-Assay

The signal-3-assay, previously described by Mailliard et al., is a functional test of DC to determine the cytokine production of DC after T-cell contact (signal-3) [73]. For this purpose, DC were co-cultured with stimulating cells, which mimic T-cells. To mimic the interaction with CD40L-expressing T_H-cells, the mouse-fibroblast cell line L929-CD40L, which was transfected with human CD40L (CD40 ligand/CD154), was utilized. To ensure no further proliferation during the co-culture, the L929-CD40L-cells were inactivated through Caesium-irradiation (100Gy) and thereafter cultivated for 48h in a 96-well-plate with a density of $5x10^4$cells/100µl LCL-medium. The medium was then removed and $2x10^4$ DC/200µl AIM-V medium (1%HS) added. As a control either L929-Cd49L-cells or DC alone were used. After 24-h incubation at 37°C and 6.2% CO_2, the cells were centrifuged at 2000rpm for 10min and the supernatant collected for further cytokine determination with ELISA.

4.2.2 LPS-Assay

Lipopolysaccharide (LPS), which can be found in the membrane of gram-negative bacteria, has been shown to be able to induce DC maturation. Upon stimulation with LPS, DC increase their Antigen uptake, migration ability and secretion of pro-

inflammatory cytokines. Hence, LPS can be used as a good experimental set up to simulate and investigate DC changes during maturation.

To investigate the differences between cDC and ercDC and the effects of Wnt5a, sFRP5 and sFRP1 on cytokine levels, DC were differentiated and harvested on day 6 of differentiation. Thereafter the growth medium was removed and they were resuspended in AIM-V (+1%HS + 1% L-Glutamine) with LPS at a concentration of 10μl/ml and cultured at a density of $2x10^5$ DC/200μl in a 96-well-plate for 24h hours at 37°C and 6.2% CO_2. As a control DC in AIM-V (+1%HS + 1% L-Glutamine) without LPS were used. After 24h incubation the cells were centrifuged at 2000rpm for 10min and the supernatant collected for further cytokine determination with ELISA.

4.2.3 Enzyme-linked immunosorbent Assay

The Enzyme-linked Immunosorbent Assay (ELISA) is commonly used for the detection and quantification of proteins. In this thesis, the so-called "Sandwich ELISA" was used. For this purpose, the target protein in the sample is captured by a target specific capture antibody, which is bound onto the surface of an ELISA plate. After washing to remove any unbound target protein, a second specific detection antibody and an enzyme conjugate, Streptavidin-horseradish peroxidase (SAv-HRP), is added, which also binds to the captured antigen. After another washing step to remove unbound antibody-enzyme conjugates and the addition of a substrate, a combination of hydrogen peroxide and 3,3‘,5,5‘-Tetramethylbenzidin (TMB), a colour change can be observed. The reaction is stopped upon addition of phosphoric acid and the measured absorbance, with the Spectrophotometer sunrise at 450nm, can be used to quantify the amount of antigen present. For this purpose, a standard curve must be run with each assay.

The cytokine detection of IL-10, IL12p40, IL12p70 and TNF-α were performed with the BD OptEIATM ELISA Set according to the manufacturers‘ instructions.

4.2.4 Boyden chamber assay to determine DC chemotaxis

Upon maturation, through for example antigen uptake, DC express the chemokine receptor CCR7, which allows migration towards the chemokines CCL19 and CCL21. Thereby CCL19 and CCL21 allow DC trafficking towards lymphoid organs where they

then can interact with T-cells [74]. In order to measure DC migration towards the chemoattractant CCL19 the Boyden Chamber Assay was used. A cylindrical cell culture insert, acting as a trans-well, is placed inside the wells of a 24 well cell culture plate and thus creating a two-compartment system. Cells are seeded in the trans-well insert and can migrate through the porous membrane into the lower compartment towards the chemoattractant. The bottom of the polycarbonate trans-well insert consists of a thin, translucent membrane with a defined pore size. Since DC chemotaxis was investigated, a pore size of 5µm was chosen. It is important to choose the correct pore size, as the pore must be large enough to allow active migration, but small enough to avoid passive passage.

DC used for the boyden chamber assay were maturated on day 6 and harvested, re-suspended with AIM-V/1% L-glutamine and adjusted to 1000 DC/µl on day 7. The trans-well insert was incubated for 1 hour with 100µl AIM-V/1% L-glutamine prior to the experiment. The base well was then filled with 400µl AIM-V/1%L-glutamine with or without CCL19 (concentration of 200ng/ml) and 200µl of the cell suspension were added to the trans-well insert after removal of the incubation medium. For migration the plate was then incubated at 37°C and 6.5% CO2 in the cell incubator for 3 hours. In order to release the few DC which might be stuck on the trans-well membrane, 50µl of 0.1M EDTA was added to each well and the plate placed on a horizontal shaker (200 shakes/min) at room temperature for 10 min. Thereafter the trans-well insert was removed and 20µl AccuCheck counting beads (960 beads/µl) were added to the cell suspension in the base well. The suspension containing migrated cells and counting beads was then transferred into a 1.5ml FACS tube and centrifuged for 7min at 538g. After aspiration of the supernatant to about 100µl, 1µl of Propidium iodide (PI) was added. PI is a fluorescent, which intercalates with double-stranded nucleic acids. As it is excluded by viable cells and can only penetrate the cell membrane of dying or dead cells, it is used to identify dead cells.

Finally, the LSR-II flow cytometer was used to determine the number of migrated cells. In order to calculate the absolute number of migrated cells, an electronic gate counting all beads on forward scatter (FSC) and sideward scatter (SSC) dot plot was created. AccuCheck counting beads are composed of two different fluorospheres, A and B beads. These two different beads are used as a double internal standard. The proportion of the

two beads, counted in two differentiate bead gates, should agree with the manufacture's indicated proportion. The acquisition of events was stopped when 10 000 events were recorded in the bead gate. Knowing the concentration of the beads, the absolute number of cells was then obtained by relating the number of cells counted to the number of bead events. See formula below:

$$abs.cell\ no. = \left(\frac{no.of\ measured\ migrated\ cells}{no.of\ measured\ beads}\right) \times no.of\ beads/well$$

The number of beads per well is given by the number of beads/µl as indicated by the manufacturer (960 beads/µl).
For better comparability the relative migration was calculated by division of the abs. cell migration by the abs. cell migration of cDC without stimulation.

4.2.5 3D Chemotaxis assay using µ-Slide Chemotaxis^{3D}

The µ-Slide Chemotaxis^{3D} by IBIDI can be used for observing the chemotactic response of cells embedded in a gel matrix and exposed to a chemical gradient. For this purpose, two large-volume reservoirs are connected by a small gap, filled with the gel matrix. By adding a chemoattractant, CCL19, to one of the reservoirs and not the other, a linear concentration gradient inside the gap can be established and the behaviour of the cells within the gap observed by video microscopy. The aqueous gel matrix hinders the connective flow of liquid, but at the same time allows diffusion in order to establish a concentration gradient. The experimental set up followed the instructions of Chemotaxis 3D application note 17 of IBIDI. For DC migration a 1.6mg/ml Collagen gel based on RPMI medium was used. The composition of the gel for 3 gaps each with 6µl is shown in the following table:

1,6 mg/ml Collagengel			with RPMI
	4,54	µl	H_2O
	2,50	µl	10x RPMI
	0,25	µl	200mM L-Glutamin
9µl gelmedium	0,67	µl	7,5% NaHCO
	0,40	µl	1M NaOH
	0,39	µl	HEPES
	0,25	µl	BSA
16 µl Collagen			Collagen 5mg/ml
25 µl cells			cell suspension

Experiments were performed with a CCL19 concentration of 1.25µg/ml. The obtained data was analysed with the ImageJ plugins “Manual tracking” and “Chemotaxis and Migration tool” by IBIDI.

4.3 Gene-expression analysis

Gene-expression analyses performed in this thesis are based upon raw Affymetrix Gene Chip® Array data kindly provided by the laboratory of Prof. Dr. Nößner and Prof. Cohen. These arrays were performed on “Affymetrix GeneChip® Human Gene 1.0 ST“, which allow the detection of 29000 genes with an average of 26 probes per gene. These probes, which are artificially created multiple short oligonucleotides specific for the transcript of interest, are able to hybridise to the investigated cDNA by complementary base paring. This allows to detect absolute gene expression levels through the emitted amount of fluorescence during hybridisation.

Analysis steps included quality control, normalization using the RMA-algorithm (Robust-Multi-array-Average) [75], clustering analysis, annotation of individual genes based on CustomCDF [76] and statistical analysis. All these steps were performed using the MADMAX (Management and Analysis Database for Multi-platform microArray eXperiments) platform (https://madmax.bioinformatics.nl), University of Wageningen) [77]. Quality control and normalisation were performed in order to assess sample and hybridization quality and to remove non-biological variation to enable comparability between different microarrays. The RMA-algorithm used for normalisation includes background correction through perfect match probes, log2 transformation, quantile normalization and median polish. In order to compare average expression levels

between the different groups, Fold Changes based on mean RMA – PLM (probe level model) values were calculated. A Fold Change above 1.5 was considered a differential gene expression.

In addition, the arrays were analysed using Affymetrix Expression console with the DABG algorithm to determine genes detected above background, as the RMA-algorithm only allows for the comparison between experimental groups. Individual DABG p-values were filtered using a cut-off of $p<0.05$ to detect statistically significant gene expression.

4.4 Verification of microarray results on the mRNA level

For verification of microarray data, qPCRs were performed for a chosen set of genes. Therefore, cDC, ercDC and DC stimulated with Wnt5a were differentiated and stimulated as before. Immature cells were harvested on day 6 and maturated cells on day 7 after addition of the "Jonuleit cocktail".

4.4.1 RNA-Purification

In order to isolate RNA, the PureLink® RNA Mini Kit was used according to the manufacturer instructions. This kit includes lysis, homogenisation and isolation of the RNA. An optional digestion step with DNase I, following the RNeasy Mini Handbook instruction, was included instead of step 6 & 7, to ensure high quality of RNA and to remove any residual DNA. The RNA was eluted in 30 µl RNase free water.

4.4.2 Quantification of RNA

For quantification of RNA, the Quant-iT™ RNA assay for the Qubit™ fluorometer was utilised. Measurements followed the manufacturer's protocol.

4.4.3 Reverse transcription

As qPCR only allows the measurement of the amount of cDNA, the isolated RNA was transcribed into cDNA through reverse transcription. Usually primers are cDNA specific and do not measure genomic DNA. However, for some genes, for example S18-RNA, it is not possible to design cDNA specific primers. Considering this and to exclude genomic DNA contamination of the sample, a RT- sample was used as negative control. This

sample contained H_2O instead of the of the reverse transcription enzyme, Superscript II. Any produced signal in this sample therefore had to originate from a combination of a cDNA unspecific primer or genomic DNA contamination.

In order to reversely transcribe 2μg of RNA into cDNA the following reverse transcription reaction mixture was prepared for each sample. The RT- reaction mixture only contained 0.2μg of RNA.

Reagent	**RT+**	**RT-**
RNA	2μg	0.2μg
First-strand buffer (5x)	1x	1x
dNTPs	2mM	2mM
DTT	0.5mM	0.5mM
Rnasin	0.025U/μl	0.025U/μl
Acrylamid, linear	62.5ng/ml	62.5ng/ml
Hexamer nucleotides (10x)	1x	1x
Superscript II	0.1 U/μl	-
RNAse free water	ad 40μl	ad 40μl

The reaction tubes were then incubated at 42°C and slowly shaken on a thermo block for 1.5h. Thereafter the RT+ cDNA was 1:10 diluted for further qPCR experiments and all tubes stored at -20°C, until further use.

4.4.4 Quantitative – PCR

The quantitative polymerase chain reaction (qPCR), also called real time PCR (RT-PCR), allows the measurement/quantification of the amount of specific cDNA in a sample. This is based upon a fluorescent signal which is emitted during each amplification cycle of the sample and detected by the thermal cycler, in this case the LightCycler® Instrument 480. For this thesis two different methods for qPCR were used, the Taqman assay and the SYBRgreen assay. The Taqman assay is based upon the annealing of a primer and a probe, which is labelled with a quencher and a fluorescent dye, to the cDNA. Only if the primer and probe are bounded and the Taq-polymerase amplifies the strand, the

fluorescent dye is released from the quencher through hydrolysis of the probe. The quencher free probe, which is labelled with FAM or VIC, emits a fluorescent signal which is then detected by the LightCycler.

The SYBRgreen method uses the ability of the dye to intercalate especially with double-stranded cDNA. Through amplification of the cDNA product with each cycle, the intercalated SYBRgreen increases and hence increases the fluorescent signal emitted with each cycle. Performing a melting curve analysis after the amplification cycles, ensured that the product is specific.

For the SYBRgreen reaction mixture 1x QuantiTectPrimer and 0.03U/µl Taq-Polymerase were added to 1x SYBRgreen mastermix, as described in materials, and H_2O was added to reach a final volume of 18µl. For the TaqMan Assays, 1x TaqMan Assay was mixed with 1x TaqMan Universal PCR Mastermix and again H_2O added to reach a final volume of 18µl. 2µl of either RT+ (1:10) dilution or RT- sample were then plated to the ground of a taqman plate and the 18µl reaction mixture added to each sample. Each sample was tested as duplicate. Experiment were performed with the LightCycler® Instrument 480 and expression levels normalized to the reference gene 18S rRNA.

The cycle threshold (CT) value calculated by the LightCycler software, describe the detected fluorescence above a certain threshold, which is individually adjusted for every gene. The CT values can then be used representative for the gene expression. A high CT value, indicates a low expression of the gene, as a signal was only detected in a late cycle of the PCR. The opposite can be applied for a low CT value.

4.5 Immunohistochemistry

Immunohistochemistry allows the detection and visualisation of an Antigen in a tissue sample by specific antibody binding. Paraffin embedded and formaldehyde-fixed samples were kindly provided by Prof. Dr. Hermann-Josef Gröne, head of Department of Cellular and Molecular Pathology at the DKFZ Heidelberg.

4.5.1 Sample preparation

In order to remove the paraffin from the tissue, samples were washed three times for five minutes in xylol. Thereafter rehydration was performed by incubation three times

in 100% Ethanol, two times in 96% Ethanol and once in 70% Ethanol for three minutes each. To prevent background reactions endogenous peroxidase was blocked through incubation in a dilution of 20ml H_2O_2 (30%) in 180ml Methanol for 20 min. To remove any residuals a washing step with PBS followed. For unmasking of the antigen, 3 ml of antigen unmasking solution in 300ml distilled water were brought to a boil and then autoclaved with the sample for 20min at 1bar. Samples were then cooled down to room temperature and again washed in PBS. After antigen retrieval samples were encircled with a liquid blocker pen and ready for antigen detection.

4.5.2 Detection of the antigen

All steps were performed in a humid chamber, consisting of a metal box covered with a wet pulp and a cover, to prevent dehydration of the tissue samples during incubation. Endogenous biotin was blocked using the Avidin/Biotin Blocking kit. The primary antibody, in this case Anti-Wnt5a antibody, was then added and incubated for 1h at room temperature or at 4°C over night. The samples were then twice washed in PBS before the secondary biotinylated antibody, at a dilution of 1:300 in PBS, could be added for 30 minutes. The secondary antibody was again washed off using PBS. To increase sensitivity of the staining the avidin-biotin-complex method was employed and the slide incubated with 15µl of reagent A and 15µl of reagent B in 1ml PBS for 30 minutes at room temperature. A washing step in PBS and one in Tris for 5 minutes each followed. Staining was performed using a mixture of 500µl 3% H_2O_2, 4ml 3,3'-diaminobenzidine (DAB) and 1ml NiCl in 200ml Tris pre-warmed to 37°C. Following the counterstaining with ethyl green, the slides were then quickly dehydrated in an ascending alcohol series (from 96% upwards) and washed in xylol. In a final step the samples were covered with the mounting medium VectaMount™ for permanent preservation and ready for microscopy.

4.6 Statistical analyses

Statistical analyses were performed using the Graphpad Prism 6 software. The level of significance is denoted by an asterisk, with * ($p < 0.05$), ** ($p < 0.01$), *** ($p < 0.001$), **** ($p < 0.0001$) and ns for non-significant. Tests were utilised as indicated in the

corresponding result section. When values were normally distributed, parametric tests were applied, i.e. the paired student T-test for paired data. For non-Gaussian distributed data, the unpaired Wilcoxon-Mann-Whitney-test was applied.

5 Results

5.1 Array-analysis

To investigate Wnt-signalling in myeloid cells, Affymetrix DNA-microarrays were performed on peripheral blood monocytes (PBMs) and in vitro generated Macrophage1 (M1), Macrophage2 (M2), GMCSF, cDC and ercDC in the laboratory of Prof. Nößner. Quality control, clustering analysis and normalisation were performed as described in methods. The DABG algorithm was applied to detect statistically significant gene expression and fold changes (FC) were calculated in order to compare average gene expression levels between different groups. A FC above or below 1.5/-1.5 was considered a differential gene expression.

As a central focus of the study was to investigate Wnt and related signalling pathways in the context of myeloid cell differentiation, a gene list was compiled from literature that included canonical and non-canonical Wnt genes (ligands, receptors, inhibitors, pathway genes and downstream targets). As these pathways are not yet fully understood, the gene lists do not include all genes that have ever been associated with the pathways, but only the most essential genes. The objective was to identify all relevant genes in respect to ligands, receptors, co-receptors and downstream effector proteins, as well as modulators of the signalling pathway as they relate to different myeloid subtypes, but with a specific focus on the ercDC subtype identified ex vivo from human renal cell carcinoma samples. These gene lists were then used as a mask to analyse the array data in respect to expression levels of different myeloid subtypes (see supplementary table 1).

5.1.1 Differential expression of ligands, receptors and extracellular regulators

The Wnt-signalling gene list consisted of 198 genes. It quickly became apparent that the most significant differential gene expression was associated with the β-Catenin independent (non-canonical) Wnt-pathway. Altered expression within the β-Catenin-dependent pathway did not appear to affect the core-genes associated with this signalling pathway, but rather other associated target genes.

Only moderate differential gene expression was detected for most Fz-receptors, co-receptors and no significant changes were found for LRP5/6. By contrast, the syndecans (SDC) and some glypicans (GPC) were strongly regulated in the activated myeloid cells (M1, M2, ercDC, cDC) as compared to PBMs. Both, SDCs and GPCs, are part of the heparan sulphate proteoglycan family (HSPG) and are anchored to the cellular membrane either as type 1 transmembrane proteins or via a glycosylphosphatidylinositol modification. They can act as co-receptors for a variety of different extracellular ligands, such as growth factors, chemokines, angiogenic factors and for morphogens such as the Wnt- and Hedgehog-ligands. In terms of Wnt-signalling, HSPG are thought to be involved in ligand gradient formation and in signal transmission by promoting receptor-ligand internalization and thereby positively as well as negatively affecting Wnt-signalling [70]. In this array of myeloid subsets, significant differential gene expression was found in SDC2, 3, 4 and GPC4, but not in SDC1 and other GPCs. Especially SDC2 was highly expressed in all myeloid subsets compared to Monocytes. The highest FC was found in cDC compared to Monocytes (26.8) and in M2 compared to monocytes with 25.5.

With regards to the extracellular and membrane-bound Wnt-antagonists and positive Wnt-modulators, the different myeloid subsets showed only moderate differential gene expression. Only the Wnt-antagonists IGFBP4 and TraB domain containing 2A (TRABD2A) showed strong differential expression. IGFBP4, a canonical Wnt-antagonist, is highly expressed in the M1 macrophages and showed a FC of 27 compared to all other subsets. TRABD2A, also known as Tiki, showed an over three-fold increase in cDC compared to the other subsets.

Positive extracellular modulators of Wnt-signalling are Norrin (NDP) and the R-spondin family. While there is no up-regulation in R-spondins, Norrin is slightly higher expressed, with a FC of 2.6, in cDC. Norrin is a secreted protein with a cysteine-knot motif, which acts as a high affinity ligand for Fz4 and LRP5/6 and thereby activates β-Catenin dependent signalling with downstream TCF/LEF transcription factors [78]. This Fz4 activation is Wnt-ligand independent.

Among the Wnt-ligands, Wnt5a was found to be strikingly differentially expressed within the myeloid populations. It showed a five-fold increase in cDC as compared to all other investigated subsets of myeloid cells including the ercDC. Furthermore,

application of the DABG-Algorithm showed that Wnt5a was only expressed in cDC, but not in the other investigated myeloid subsets. Wnt5a is a classic non-canonical Wnt-ligand. It is able to bind to a number of different Fz-receptors and co-receptors [79]. Canonical Wnt-ligands, however, were not differentially regulated.

Differential gene expression within the canonical Wnt-pathway is summarized in a schematic diagram in order visualize differences within different myeloid subsets (Fig. 4).

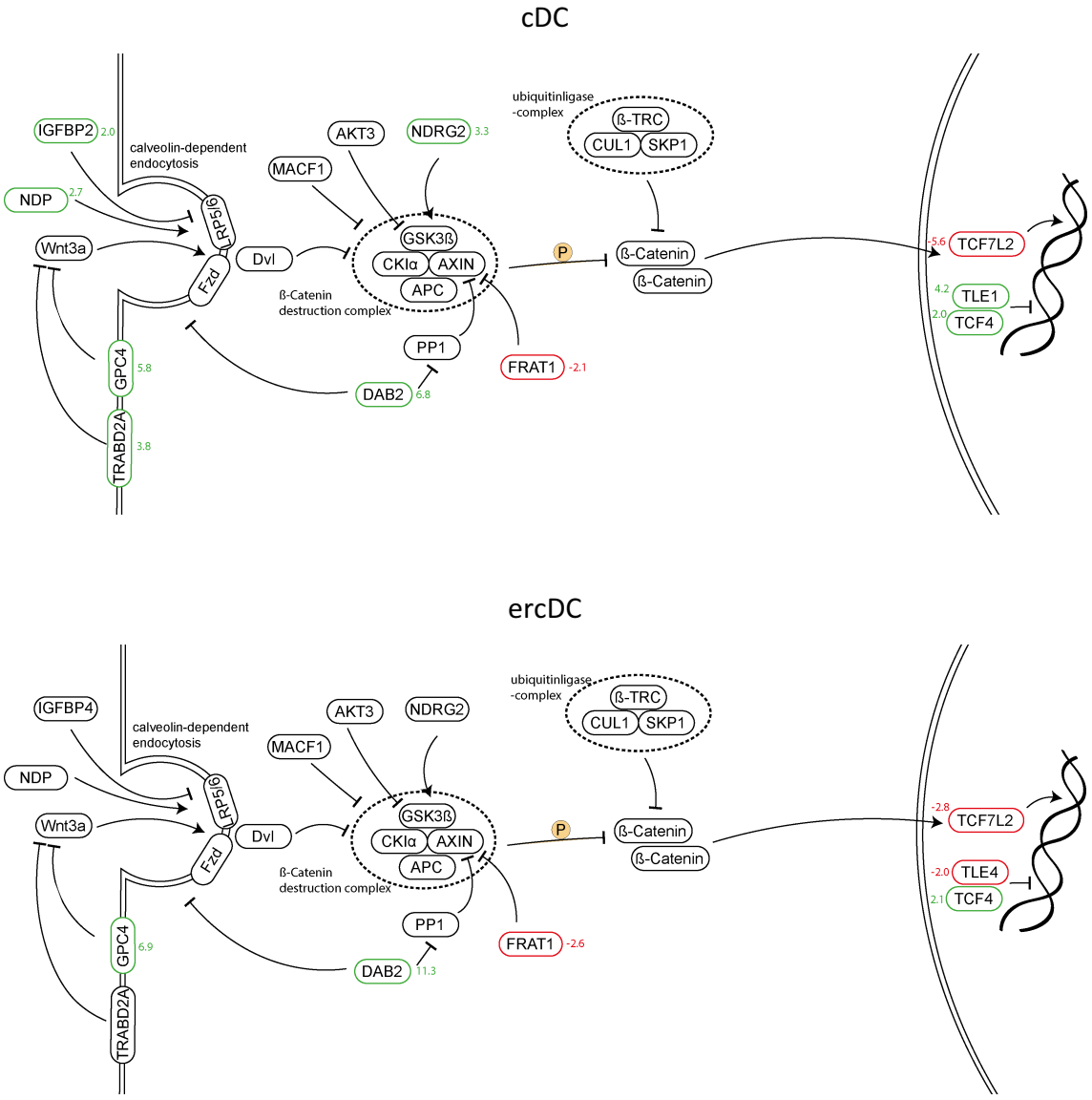

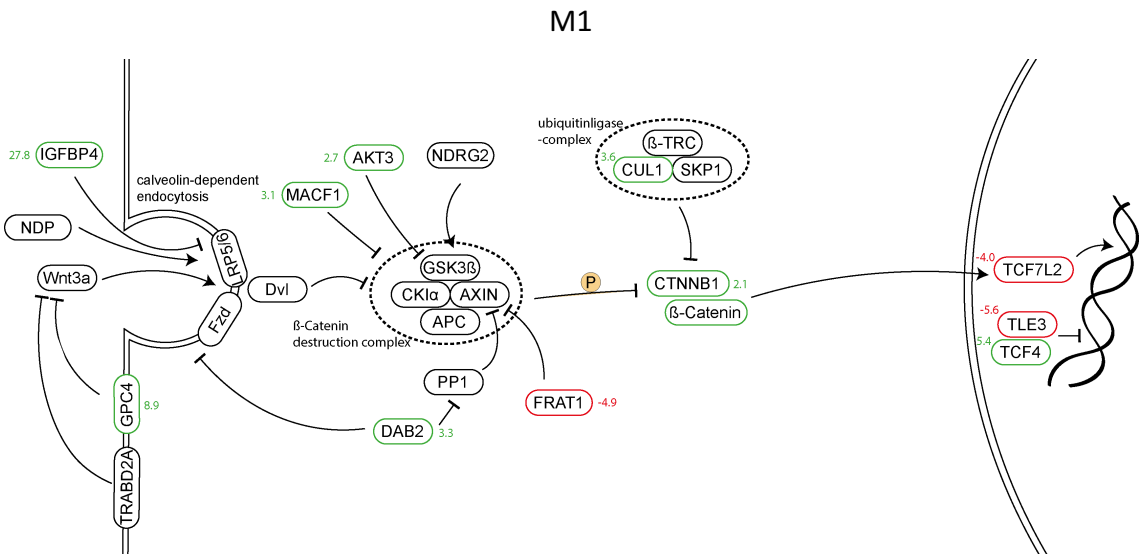

Fig. 4: ***Microarray analysis of β-Catenin signalling pathway.*** *The scheme display microarray data integrated into a modified version of the β-Catenin signalling pathway. Significant differential gene expression is presented by green (up-regulation) or red (down-regulation) boxes and the corresponding fold changes in comparison to monocytes. Fold changes were generated using the RMA-Algorithm and a FC >1.5 was considered significant differential expression.*

5.1.2 Non-canonical Wnt-signalling

The molecular mechanisms underlying the PCP and the Ca^{2+}-signalling cascade are not well characterized. The gene lists used to study their regulation included the 20 most well-known and investigated genes linked to the PCP-cascade, and 37 genes associated with the Ca^{2+}-cascade. Within the PCP-cascade, differential gene expression was found in the M1 transcriptome. Dishevelled-associated activator of morphogenesis 1 (DAAM1) is a downstream target of Dvl, and is activated by Dvl upon e.g. Wnt5a binding to a Fzd or the Co-receptor ROR2. DAAM1 can activate RHO, Rac and Cdc42 and thereby influence cytoskeletal rearrangements, cell migration and polarity. The array showed a cDC up-regulation of DAAM1 by two fold compared to monocytes, whereas M1 showed a -2.4 fold down-regulation. Furthermore, M1 also showed a -2.8 fold down-regulation of RHOB and a -6.7 fold down-regulation of RAC2. RHOB was also slightly down-regulated by two fold in cDC and M2. Again, this could suggest a down-regulation of Wnt-signalling within the M1. However, the regulations of the PCP-cascade are not as strong as for the other cascades and assumptions have to be drawn carefully, also because not all regulating genes are yet known and included in this analysis.

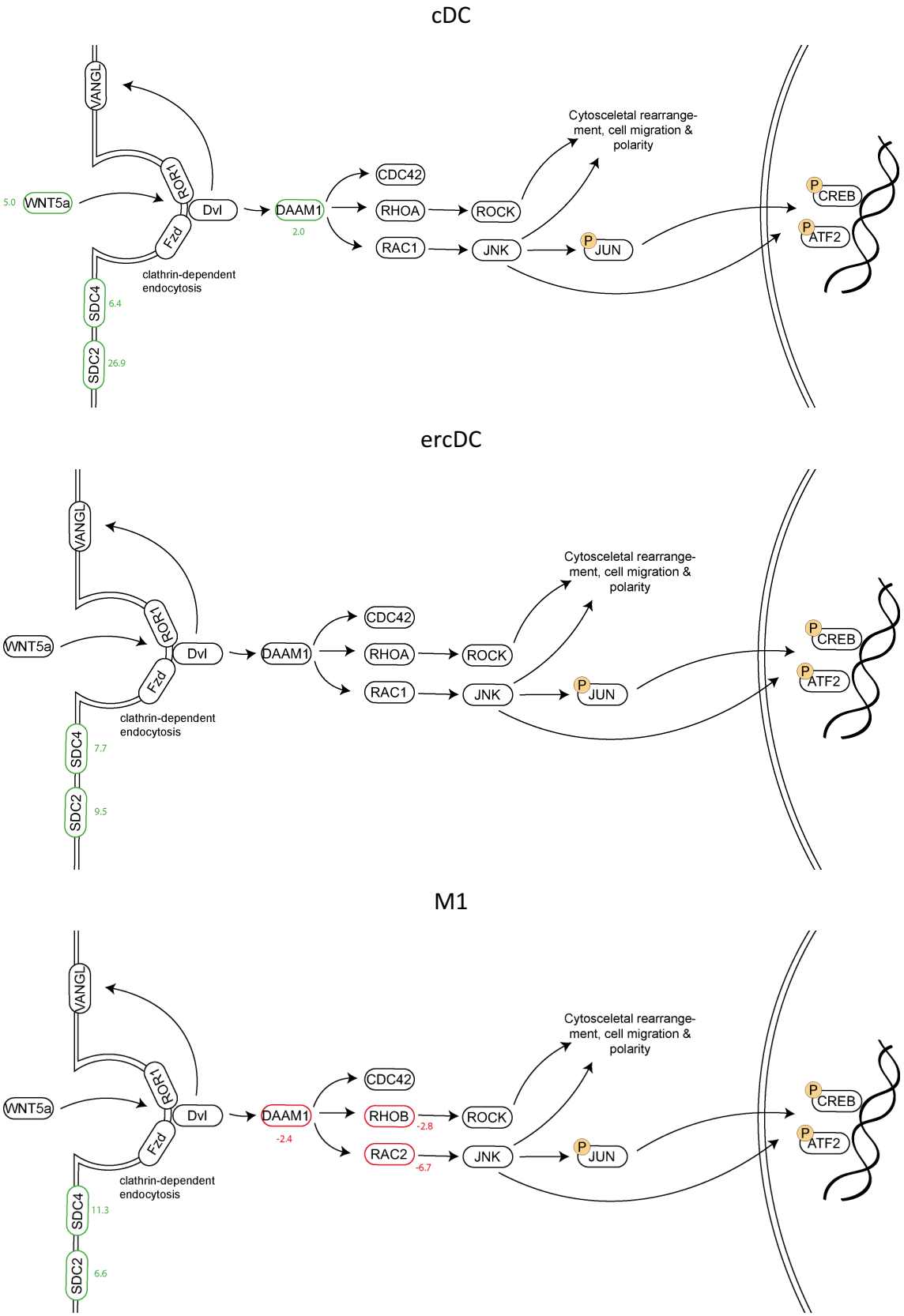

Fig. 5: ***Microarray analysis of PCP-signalling pathway.*** *The scheme displays microarray data integrated into a modified version of the PCP-signalling pathway. Significant differential gene expression is presented by green (up-regulation) or red (down-regulation) boxes and the corresponding fold changes in comparison to monocytes. Fold changes were generated using the RMA-Algorithm and a FC >1.5 was considered significant differential expression.*

Within the Ca^{2+}-signalling cascade differential gene expression was found for key regulating genes. Phospholipase C beta1 (PLCB1), which forms inositol 1,4,5-trisphosphate (IP3) and diacylglycerol (DAG) from phosphatidylinositol 4,5-bisphosphate upon Wnt-receptor binding, is strongly down-regulated in all myeloid subsets compared to monocytes. Furthermore, PLCB2 is also very strongly suppressed in M1 (FC -15.9) and slightly in GMCSF (FC -2.9). The formation of IP3 initiates the release of Ca^{2+} from the endoplasmic reticulum, which in turn activates proteinkinase C (PRKC), calcium sensitive calmodulin-dependent protein kinase II (CAMKII) or calcineurin. While PRKCA is 3.4 fold up-regulated in cDC, PRKCB is down-regulated in all myeloid subsets and strongest again in M1 with a FC of -6.1. M1 also showed a -2.7 fold down-regulation of CAMK2G and a -4.4-fold suppression of calcineurin (PPP3CA). Moreover, NFkB2, RELA and RELB, which are downstream effector transcription factors of the Wnt-Ca^{2+}-cascade, were up-regulated in M1 with a FC of 3.0, 3.5 and 2.5 respectively. NFATC1 and NFATC2, however, were slightly up-regulated with a FC of 2.3 in M2 and cDC. It has been shown that the non-canonical cascades can inhibit the canonical-signalling cascade via different mechanism. One mechanism is the TAK1-NLK pathway, which is activated by CAMKII in the Ca^{2+}-cascade. The NLK, which is 2.2 fold up-regulated in cDC, phosphorylates TCF/LEF and thereby inhibits TCF/LEF transcriptional activation upon ß-Catenin binding [54].

cDC

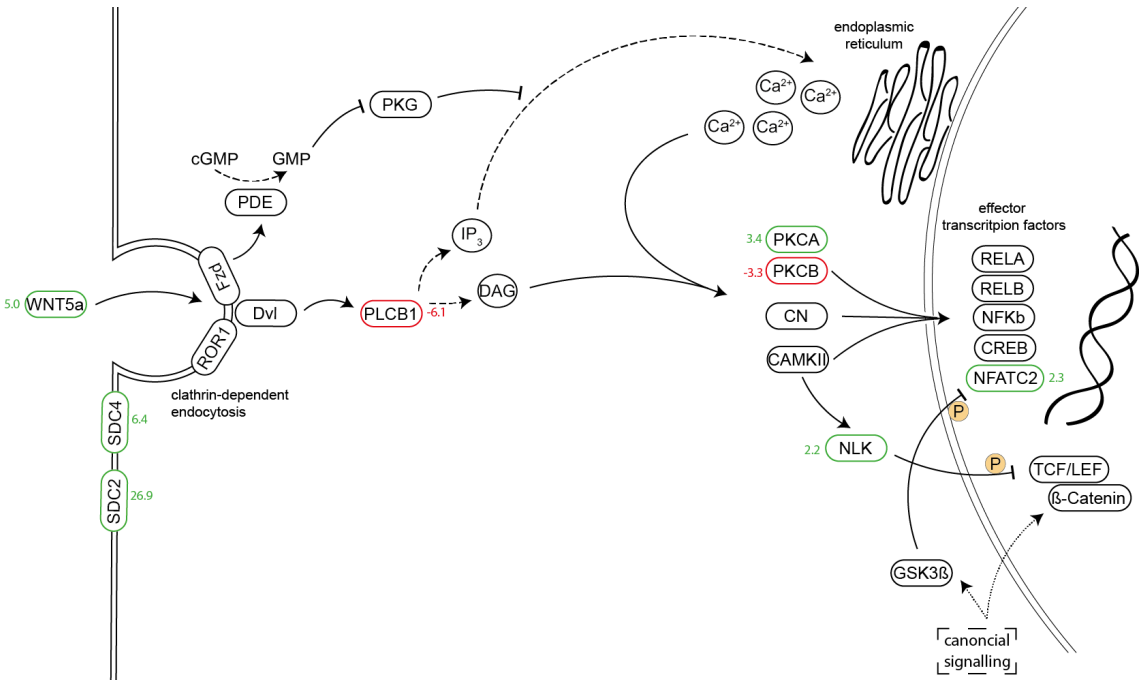

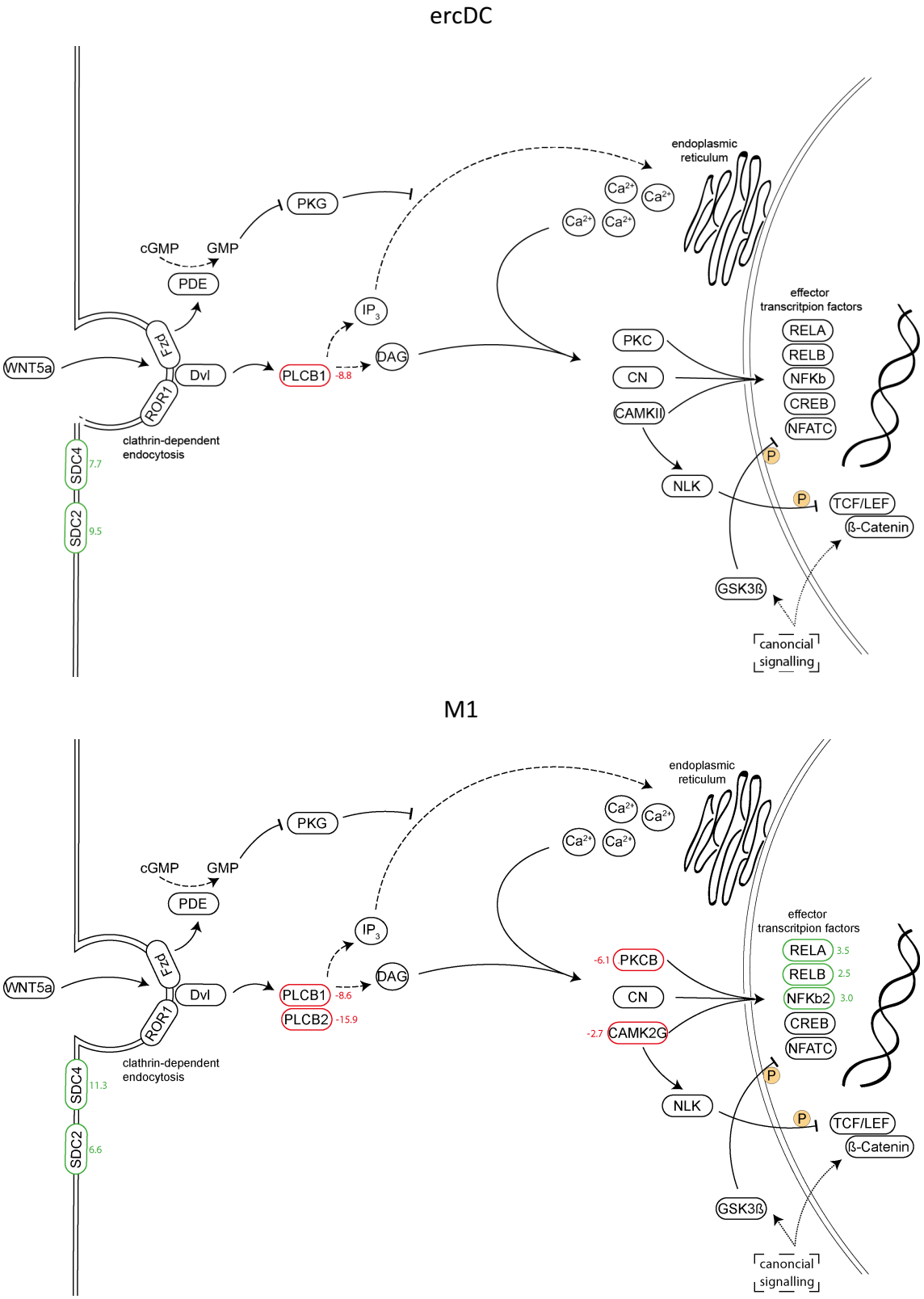

Fig. 6: ***Microarray analysis of the Ca^{2+}-signalling pathway.*** *The scheme displays microarray data integrated into a modified version of the Ca^{2+}-signalling pathway. Significant differential gene expression is presented by green (up-regulation) or red (down-regulation) boxes and the corresponding fold changes in comparison to monocytes. Fold changes were generated using the RMA-Algorithm and a FC >1.5 was considered significant differential expression.*

Transcriptomic analysis identified differential gene expression within the Wnt-signalling pathway. While only moderate changes in expression were found within the PCP-signalling cascade, the differential expression was found in the β-Catenin-dependent and the Ca^{2+}-cascade pathways. Changes in pathway regulation was strongly associated with cDC and M1 myeloid subtypes. A potential reduction in canonical Wnt signalling with a corresponding increase in the Ca^{2+}-signalling pathway was seen in cDC. The dysregulation in M1 macrophages was difficult to assign to specific pathways, but it could be concluded that regulation is evident. Interestingly, only few differential gene expressions could be observed when comparing ercDC to monocytes, suggesting for similarities and a possible explanation for differences between ercDC and cDC.

Among the ligands, only Wnt5a, a non-canonical Wnt-activator, was strongly up-regulated in cDC. A strong up-regulation of syndecans and glypicans in all myeloid subsets was also found as compared to monocytes. These HSPG are thought to act as Wnt-Co-receptors and have been shown to be involved in non-canonical signalling, e.g. by influencing Wnt5a autocrine signalling and signal transduction.

As average expression levels of the different myeloid subsets were compared to monocytes, and all myeloid subsets were generated from peripheral blood monocytes, it becomes evident that Wnt-signalling changes during myeloid differentiation. Depending on the myeloid subset Wnt-signalling varies and canonical or non-canonical signalling pathways show either activation or suppression. Hence we hypothesize, that Wnt-signalling is of importance in myeloid differentiation and functioning. As Wnt-ligands are lipid-modified glycoproteins, they mainly signal in a paracrine or autocrine manner. While cDC showed very strong differential regulation within the Wnt-pathway, ercDC revealed only little regulation. Baring this in mind, the question arose whether Wnt-signalling could in part be responsible for the functional differences and impairment between cDC and ercDC.

5.2 RT-PCR

In order to validate the data obtained by transcriptomic analysis, qPCRs of key Wnt-signalling genes were performed on immature cDC, ercDC and maturated cDC. Additionally, immature cDC and ercDC stimulated with Wnt5a on day zero of differentiation were investigated to assess the effect of Wnt5a-signalling on gene-expression levels. As differential gene-expression was especially found within the non-canonical pathways, investigated genes were chosen subsequently.

All obtained qPCR results supported our findings in the DNA-microarrays (see Fig. 7). Wnt5a could be shown to be only expressed in cDC, but not in ercDC. Furthermore, evidence of decreased expression of Wnt5a in maturated cDC was found. Contrary, the Wnt-receptor Fzd5, a suggested Wnt5a receptor, was expressed in both cDC as well as ercDC, suggesting the presence of non-canonical Wnt-signalling machinery in ercDC. The results of SDC2, which was shown to be strongly differentially expressed within cDC, ercDC and monocytes in the microarray, could be validated by qPCR and showed higher expression in cDC, than ercDC. SDC3 and GPC4, also belonging to the family of HSPG, showed similar expression levels for cDC and ercDC. DAAM1, part of the PCP-signalling pathway, and NFATC2, belonging to the Ca-Pathway, were both up-regulated in cDC compared to ercDC. All other by qPCR investigated genes showed similar expression levels between cDC and ercDC (not shown here).

Furthermore, a tendency of down-regulation in maturated cDC compared to immature cDC was found for several genes, including for example Wnt5a, CAMK2D, SDC2 and SDC3. This could suggest a possible change within the Wnt-signalling cascade and consequently in the Wnt-response of cDC during maturation. Addition of Wnt5a on day zero of differentiation of cDC as well as ercDC did not result in changes of gene-expression levels for investigated genes.

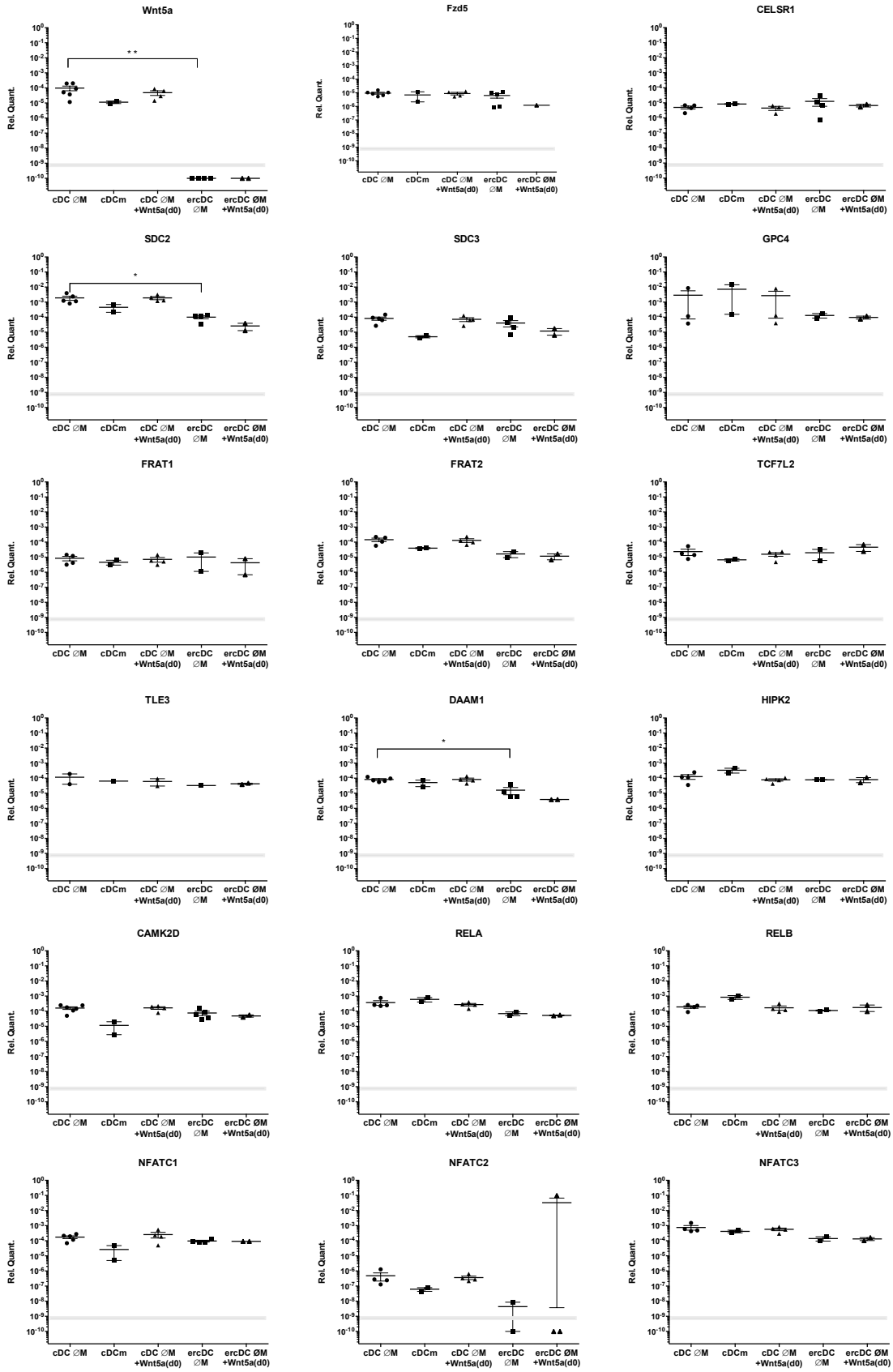

Fig. 7: ***Validation of gene expression.*** *Expression data of Wnt-signalling genes after qPCR advanced relative quantification analysis of immature and maturated cDC, ercDC and stimulation with Wnt5a(d0). Graphs display ΔΔCT-values, mean and the standard error of mean (SEM). The grey bar at 10^{-9} indicates borderline expression and values*

at 10^{-10} non-detectable expression levels. For statistical analysis the unpaired Mann-Whitney-test was applied. Significant differences are denoted by an asterisk.

5.3 Immunohistochemistry

As we detected high levels of Wnt5a in cDC, but not in ercDC, we hypothesized, that Wnt5a might affect DC differentiation and functioning. As it has previously been shown that Wnt5a is expressed in other tumours, we wondered whether Wnt5a is also present in RCC. Immune-histological staining of Wnt5a in RCC samples revealed a strong overexpression of Wnt5a in these samples, hence suggesting a possible source of Wnt5a. This Wnt5a could act in an autocrine, paracrine and juxtacrine manner and affect the differentiation of myeloid cells within the RCC. Subsequently, we aimed to examine the effects of Wnt5a on DC function.

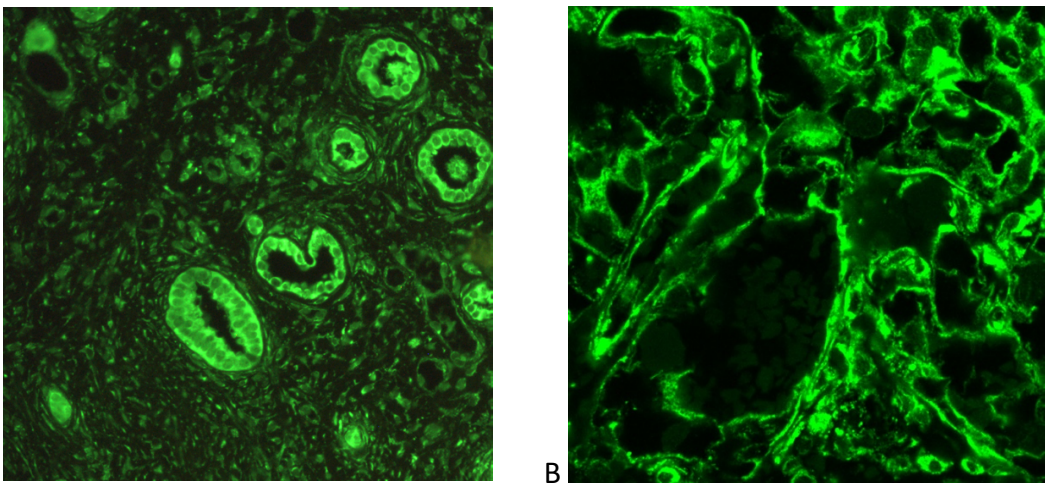

*Fig. 8: **Immunohistochemical staining of Wnt5a**. Immunohistochemical staining of Wnt5a in normal kidney (A) and RCC (B), showing a strong overexpression of Wnt5a and hence suggesting a possible source for Wnt5a.*

5.4 Cytokine pattern on gene expression level

As we found that cDC and ercDC differ in Wnt-gene expression pattern, we hypothesized that Wnt-signalling may influence their differentiation and functionality. In a first step, we investigated cytokine gene expression levels of cDC compared to ercDC, and the impact of Wnt-signalling modulation. We therefore performed qPCRS of IL-10, TNF-α and the subunits IL12A (syn. IL12p35) and IL12B (syn. IL12p40) of the heterodimeric cytokine IL-12 (syn. IL12p70) on cDC and ercDC in an immature as well as maturated state and upon stimulation with Wnt5a on day zero. Maturation was performed by

addition of the "Jonuleit cocktail" on day 6 of differentiation (see methods). Interestingly no differences in cytokine expression levels were found between immature cDC and ercDC. Upon maturation, however, the cytokine expression levels of cDC changed significantly. TNF-α levels were lowered significantly (p-value: 0.0159) and also IL-10 levels showed a decreased tendency, but could not be shown to be significant (p-value 0.057). IL12B levels of maturated cDC were increased significantly (p-value 0.0159). Contrary to maturated cDC, maturated ercDC did not change the gene expression levels of these cytokines. Hence, suggesting an altered response of ercDC towards maturation and a probable maintaining of a rather immature state. Interestingly, Wnt5a did not show a significant effect on the gene expression levels in neither cDC or ercDC in the immature or maturated state. Evaluation of IL12A levels was difficult as the obtained data often showed values below detection level.

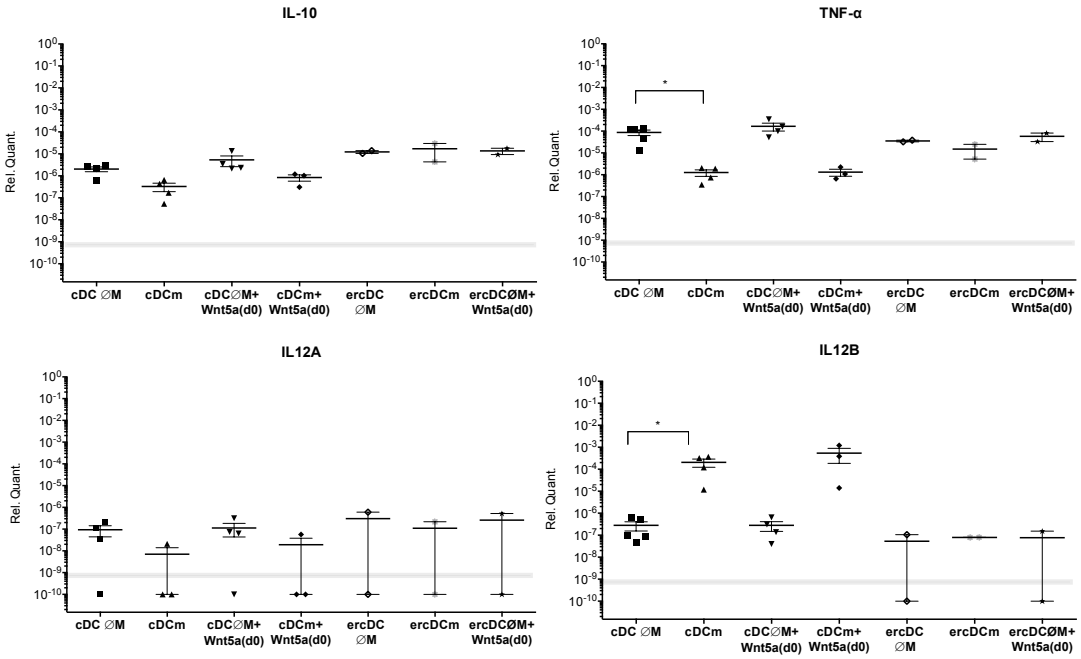

Fig. 9: ***Cytokine gene expression levels.*** *Gene expression levels of IL-10, TNF-α, IL12A and IL12B after qPCR advanced relative quantification analysis of immature and maturated cDC, ercDC and stimulation with Wnt5a(d0). Graphs display ΔΔCT-values, mean and the standard error of mean (SEM). The grey bar at 10^{-9} indicates borderline expression and values at 10^{-10} non-detectable expression levels. For statistical analysis the unpaired Mann-Whitney-test was applied. Significant differences are denoted by an asterisk.*

5.5 Cytokine secretion

In a next step we investigated the cytokine secretion, as protein levels, of cDC compared to ercDC, and the impact of Wnt-signalling modulation with enzyme-linked immunosorbent-assays (ELISA). Hence the secretion of IL12p70, IL12p40, IL-10 and TNF-α were measured upon LPS and CD40L stimulation. IL-12 is a heterodimeric cytokine, which acts as a link between innate and adaptive immune response. It is able to induce IFN-γ production by CTL and NK and activate their phagocytic capacity, but also to induce the generation of T_H1 $CD4^+$ cells [80, 81]. IL-10, however, acts as a regulator and suppressor of the immune system and can counteract IL-12 production [82]. It reduces inflammation and prevents overshooting immune reactions. Furthermore, it has been implicated in $CD8^+$ T-cell priming and suggested as a possible mechanism for cancers to escape immune surveillance [83]. TNF-α is a pro-inflammatory cytokine and involved in immune regulation, inflammation, cellular homeostasis and inhibition of tumourigenesis and viral replication.

A first general comparison between cDC and ercDC revealed that ercDC produce significantly more IL-10 and TNF-α when stimulated with LPS than cDC. This, however, could not be shown for CD40L stimulation, as no distinctive results were obtained. Contrary, IL12p40 secretion upon CD40L stimulation was higher in cDC than ercDC, although this could not be shown to be significant by paired t-test. These differences between cDC and ercDC could in part explain findings of impaired ercDC ability to activate and induce proliferation of T-cells and to escape immune surveillance. While TNF-α is mainly known to carry out antitumourigenic properties, low dose, chronic secretion of TNF-α has been detected in RCC and suggested to promote tumour growth and metastasis. Furthermore, the detection of TNF-α in RCC has been associated with poor prognosis [84]. Our findings could hence suggest a possible source of TNF-α in RCC by ercDC.

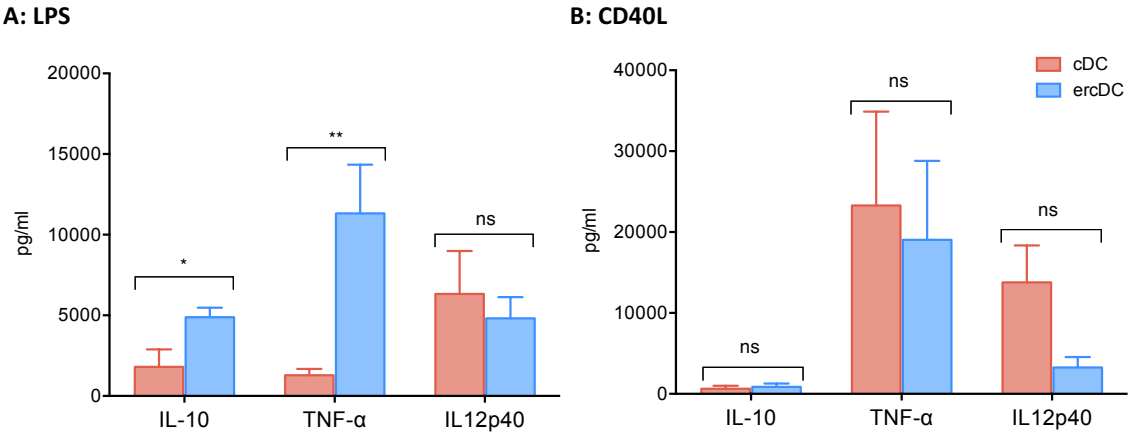

Fig. 10: ***Enzyme linked immunosorbent assay.*** *IL-10, TNF-α and IL12p40 secretion of cDC and ercDC upon LPS (A) and CD40L (B) stimulation for 24h. The graphs display mean and SEM of several experiments. For the purpose of statistical analysis, the parametric paired t-test was applied.*

Following these findings, Wnt-signalling modulation with the non-canonical agonist Wnt5a and the antagonists sFRP1 and sFRP5 were performed. Wnt5a, sFRP1 and sFRP5 were respectively added to the growth medium on day zero of differentiation to be present throughout the whole differentiation process.

As Wnt5a was up-regulated in cDC compared to ercDC, it was expected that addition of Wnt5a to ercDC, or blockage of Wnt5a by sFRP5 and sFRP1 in cDC, would alter the cytokine secretion pattern. Yet, addition of Wnt5a did not show any significant effects on ercDC. The obtained data was not distinct and no tendency could be detected. Contrary, however, Wnt5a showed significant effects regarding IL-10, TNF-α and IL12p40 secretion in cDC. Addition of Wnt5a to cDC showed increased secretion levels of IL-10 upon LPS as well as CD40L stimulation. Increased levels upon addition of Wnt5a could also be detected for IL12p40 stimulated with CD40L. A tendency of increased levels were also seen for IL12p70 upon CD40L stimulation, but were not found to be significant. Furthermore, Wnt5a did decrease TNF-α secretion upon LPS, but not upon CD40L stimulation. While the effects of Wnt5a on IL-10 secretion of cDC did resemble the higher secretion of ercDC compared to cDC, the effects on TNF-α and IL-12, however, were rather contrary. Hence, Wnt5a within the tumour milieu could only in part be responsible for the altered phenotype of ercDC differentiated from monocytes.

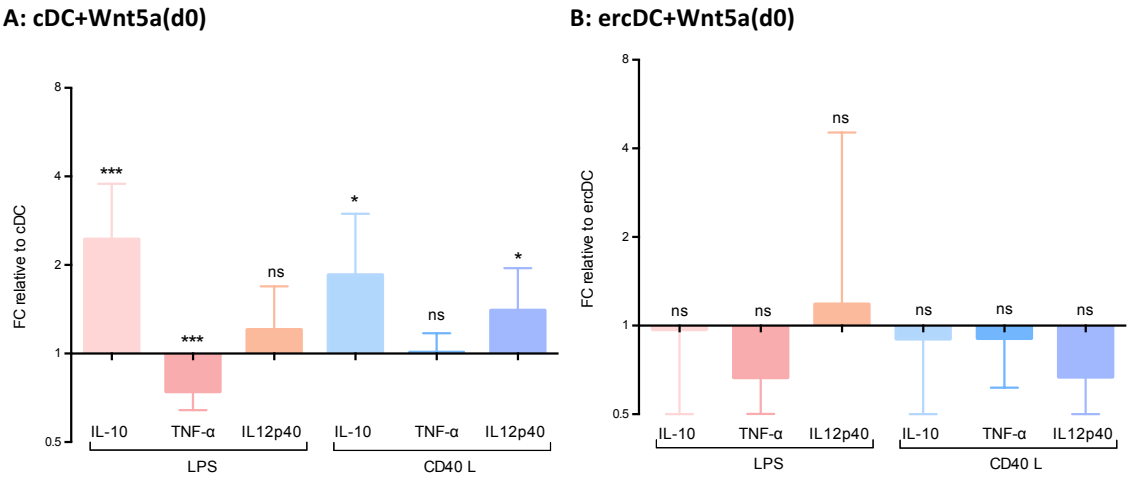

Fig. 11: ***Enzyme linked immunosorbent assay.*** *Wnt5a(d0) effect on IL-10, TNF-α and IL12p40 secretion of cDC (A) and ercDC (B) upon LPS and CD40L stimulation for 24h. The graphs display the geometric mean FC of cDC and ercDC + Wnt5a(d0) in comparison to control cDC and the 95% Confident interval of several experiments. Statistical significance was tested by one-sample t-test of log-transformed FCs.*

Through their cysteine rich domain (CRD) sFRPs can physically interact with Wnt-ligands and act as inhibitors of Wnt-signalling. sFRP5 and sFRP1 have both been proposed as possible inhibitors of Wnt5a. In this work, addition of either sFRP5 or sFRP1 did not have any significant effects on IL-10, IL-12 and TNF-α secretion in cDC or ercDC. Unlike expected, they did not influence cytokine patterns in cDC, which secrete Wnt5a themselves or ercDC, which might be influenced through Wnt-signalling within the tumour milieu.

Furthermore, sFRP5 and sFRP1 did not abrogate the effects of Wnt5a on cDC, as combination of Wnt5a and sFRP5 or sFRP1 respectively did not reduce the IL-10, IL-12 or TNF-α effects of Wnt5a.

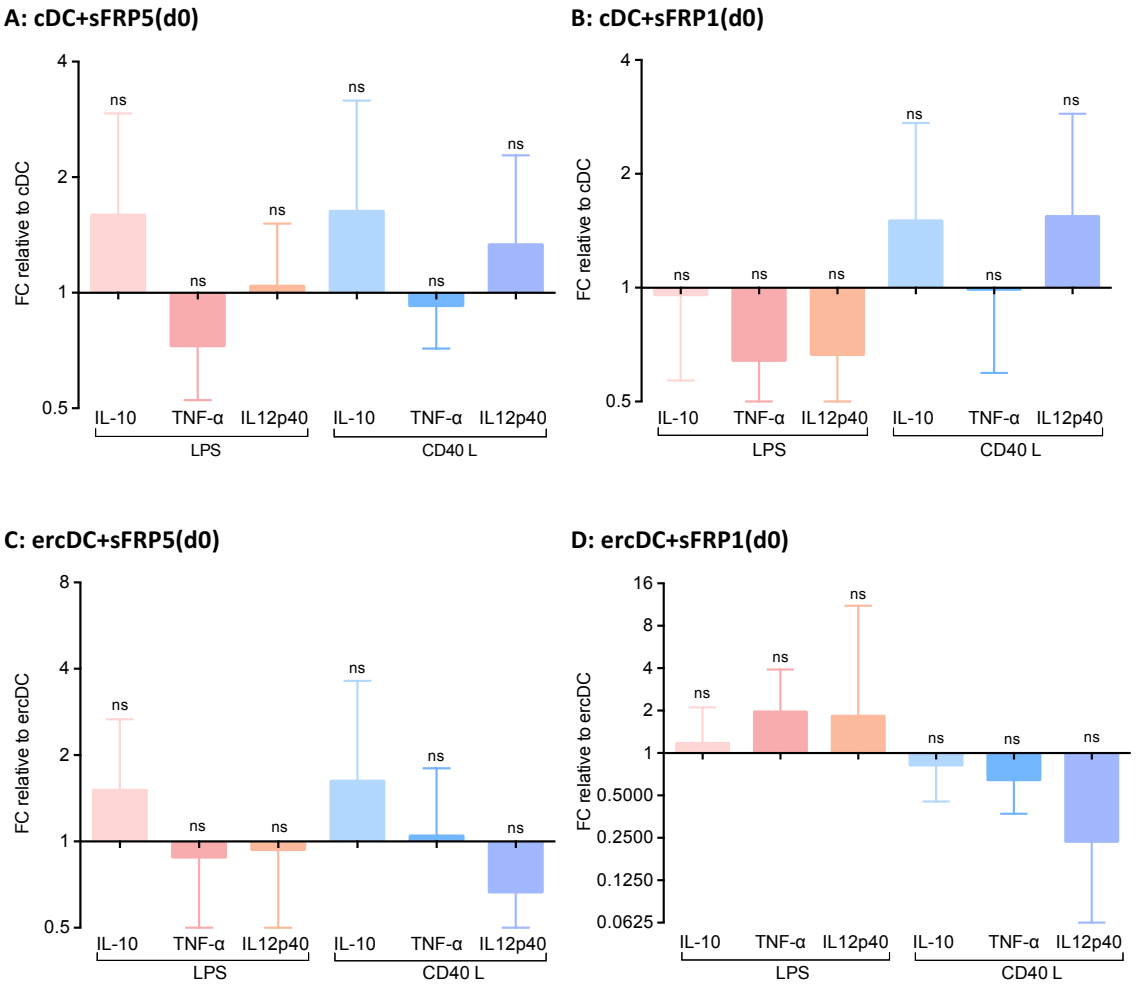

Fig. 12: ***Enzyme linked immunosorbent assay.*** *sFRP5 and sFRP1(d0) effect on IL-10, TNF-α and IL12p40 secretion of cDC (A, B) and ercDC (C, D) upon LPS and CD40L stimulation for 24h. The graphs display the geometric mean FC in comparison to control cDC and ercDC and the 95% Confident interval of several experiments. Statistical significance was tested by one-sample t-test of log-transformed FCs.*

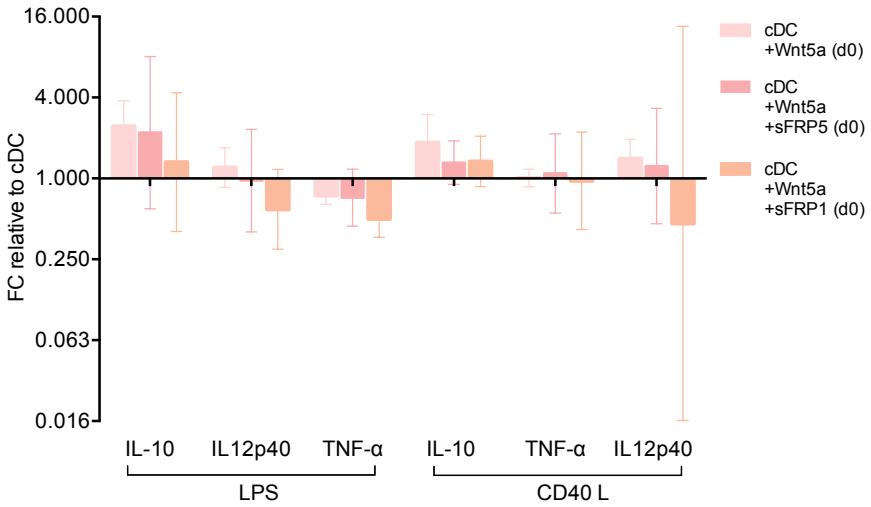

Fig. 13: ***Enzyme linked immunosorbent assay.*** *Effect of Wnt5a and its combination with sFRP5 and sFRP1(d0) on IL-10, TN-Fα and IL12p40 secretion of cDC upon LPS and CD40L stimulation for 24h. The graphs display the geometric mean FC in comparison to control cDC and ercDC and the 95% Confident interval of several experiments.*

5.6 Migration assay

An important function of DC is their migration towards regional lymph nodes after antigen uptake and consequent maturation. This enables the DC to move from the site of inflammation to the site of activation of the adaptive immune system, i.e. activation of T-cells. CCL19 is one of the key chemokines involved in recirculation and homing of lymphocytes. By binding to the chemokine receptor CCR7 on target cells, e.g. DC, B-cells and T-cells, it enables their trafficking towards the thymus and secondary lymphoid organs.

5.7 Boyden chamber migration assay

Using the Boyden chamber migration assay (MA), we investigated the differences of migration ability of cDC as compared to ercDC, and the potential influence of Wnt-signalling modulation on the ability of these DC subtypes to respond to migration stimuli. It could be shown that cDC migrate strongly towards CCL19, whereas ercDC where not attracted by this chemokine (but do express the CCR7 receptor). Furthermore, by addition of CCL19 in the trans well, as well as in the base well, we could verify that the migration of cDC towards CCL19 was a directed migration, i.e. chemotaxis, and not chemokinesis.

cDC produce Wnt5a, but not ercDC. However, as was shown earlier, RCC strongly produce Wnt5a. Thus, Wnt5a stimulation of ercDC may occur within the tumour milieu through paracrine signalling. To test the effect of Wnt5a signalling on the ercDC phenotype, it was added to the cells on day 5, just before onset of the maturation process. While some experiments showed a slight increase in the ability of ercDC to migrate, this effect could not be shown to be consistent and significant. Hence, based on the Boyden chamber MA, no significant effect of Wnt5a on the migration ability of ercDC could be shown.

In order to inhibit the Wnt5a produced by cDC, and investigate the potential importance of Wnt5a regarding cDC migration, sFRP1 and sFRP5 were added to cDC differentiation medium on day 3. Again no significant effect could be detected with the Boyden chamber MA.

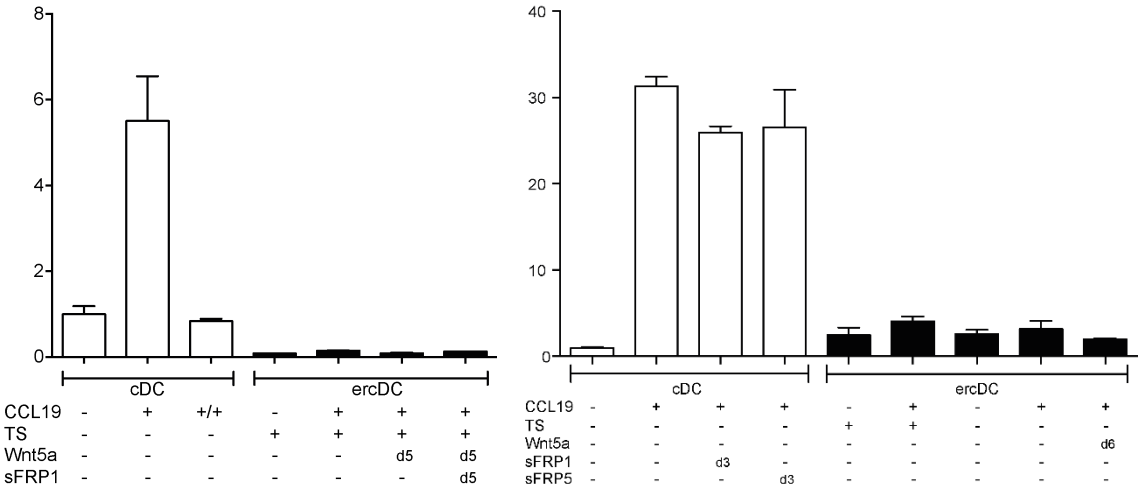

Fig. 14: ***Boyden chamber migration assay.*** *Two representative examples of Boyden chamber MA. The graphs display fold changes in comparison to unstimulated cDCm without CCL19. Addition of CCL19 to the base well results in strong directed Migration of cDCm, but not of ercDCm. No significant effect of Wnt5a, sFRP1, sFRP5, on day 3, 5 or 6 (d3, d5, d6), on cDCm or ercDCm could be detected. By addition of CCL19 to the base well and the transwell (+/+), a chemotactic effect and not only chemokinetic effect could be verified.*

5.8 Ibidi-migration assay

The Boyden chamber MA only enables detection of chemotaxis, by contrast, the µ-Slide Chemotaxis^{3D} by IBIDI also allows investigation of directionality, distance and velocity. DC were first embedded into gel matrices and their migration towards a chemokine gradient, in this case CCL19, was observed by video microscopy every 2 minutes for 3.5h. Analysis steps included the manual tracking of the cells and hence allowing calculation of accumulated as well as euclidean distance [µm], velocity [µm/min], directness, the center of mass and the forward migration index (FMI), using the chemotaxis and migration tool plugin for ImageJ.

The first aim was to validate the results of the Boyden chamber MA, and to then gain further insight into DC migration behaviour. For the IBIDI-MA, the DC required a higher chemokine concentration of 1.25µg/ml, than the Boyden chamber MA. Lower concentrations were not able to induce migration in this assay. Matured cDC (cDCm) migrated strongly towards CCL19. This was represented by a high parallel-FMI (FMI II or y-FMI), i.e. of 0.29, compared to the control without CCL19 (y-FMI around “0”), and a perpendicular FMI (FMI ⊥ or x-FMI) that is close to “0”. The center of mass, which represents the spatial averaged point of all cell endpoints, was shifted strongly along the y-axis. Furthermore, the directionality, calculated by comparing the euclidean distance

to the accumulated distance, was slightly increased. Though the directness cannot be used as a parameter for judging chemotaxis, it can be used to characterize the path of migration. The velocity of the cDC stimulated with CCL19 was only slightly increased.

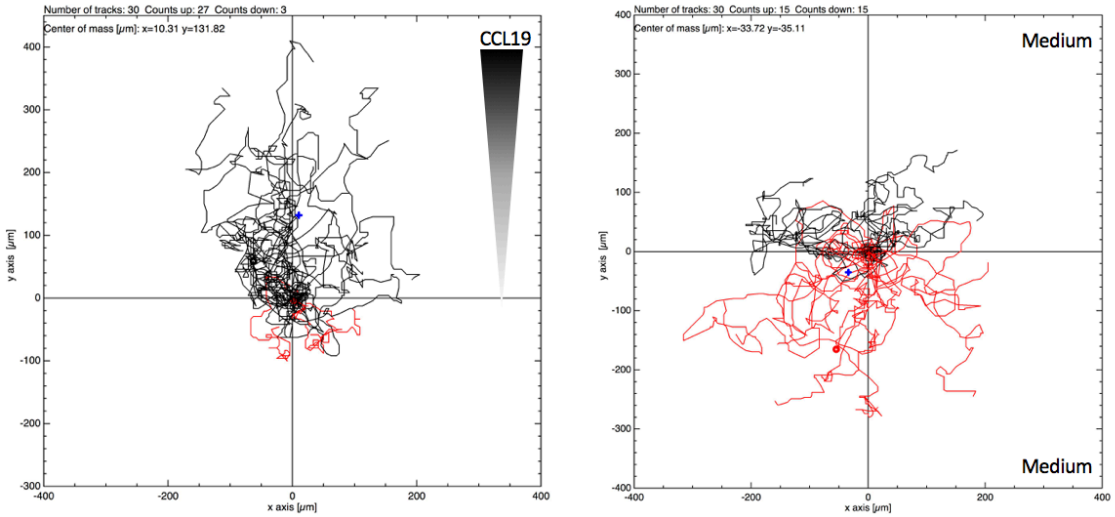

*Fig. 15: **µ-Slide Chemotaxis^{3D}**. cDCm migration with and without the Chemoattractant CCL19. cDCm show a strong chemotactic response to a CCL19-gradient with 1.25µg/ml. Without CCL19, i.e. medium in both chambers, chemokinesis, but no chemotaxis could be observed. The blue cross represents the center of mass, which is shifted upwards on the y-Axis upon CCL19 stimulation. (Analysis with Chemotaxis and Migration tool plug-in for ImageJ)*

In contrast, maturated ercDC (ercDCm) did not increase their y-FMI or directionality, and did not shift their center of mass when stimulated with CCL19. Their accumulated and euclidean distance and velocity, however, did slightly increase upon CCL19 stimulation. These findings basically confirm the results of the Boyden chamber MA, as ercDC do not respond to CCL19 stimulation. Compared to cDCm, ercDCm showed reduced chemokinesis as well as reduced chemotaxis (Fig. 16).

As ercDCm did not migrate towards CCL19 (but still express the CCR7 receptor on their surface), the question was posed whether they have impaired migration abilities. To test this, the migration of ercDC towards formyl-methionyl-leucyl-phenylalanine (fMLP) was investigated. fMLP, a cleavage product of bacteria binds to formyl peptide receptor (FPR) and FPR-like 1 and 2, and acts as a chemoattractant for leukocytes to attract them to the site of inflammation [85]. It was shown that while monocytes and immature DC express FPR, FPR was down-regulated during maturation and maturated DC lost their responsiveness towards fMLP [86]. This could also be shown with the IBIDI MA. While

cDCm did migrate strongly towards CCL19, they did not migrate towards fMLP. The y-FMI was only slightly higher upon fMLP stimulation than unstimulated and did not reach the level of stimulation with CCL19. The center of mass was only slightly shifted along the y-axis. Accumulated and euclidean distance as well as velocity of fMLP stimulation were similar to CCL19 stimulation. Interestingly, ercDCm did migrate strongly towards fMLP. The y-FMI and the Directionality increased and the center of mass shifted along the y-axis upon fMLP stimulation. Also accumulated and euclidean distance and velocity increased slightly. It can therefore be concluded, that ercDCm do not have impaired migration abilities, but impaired abilities to respond towards CCL19. While cDCm down-regulate their fMLP-receptors during maturation, it seems that ercDCm do not and rather retain an immature response towards chemoattractants.

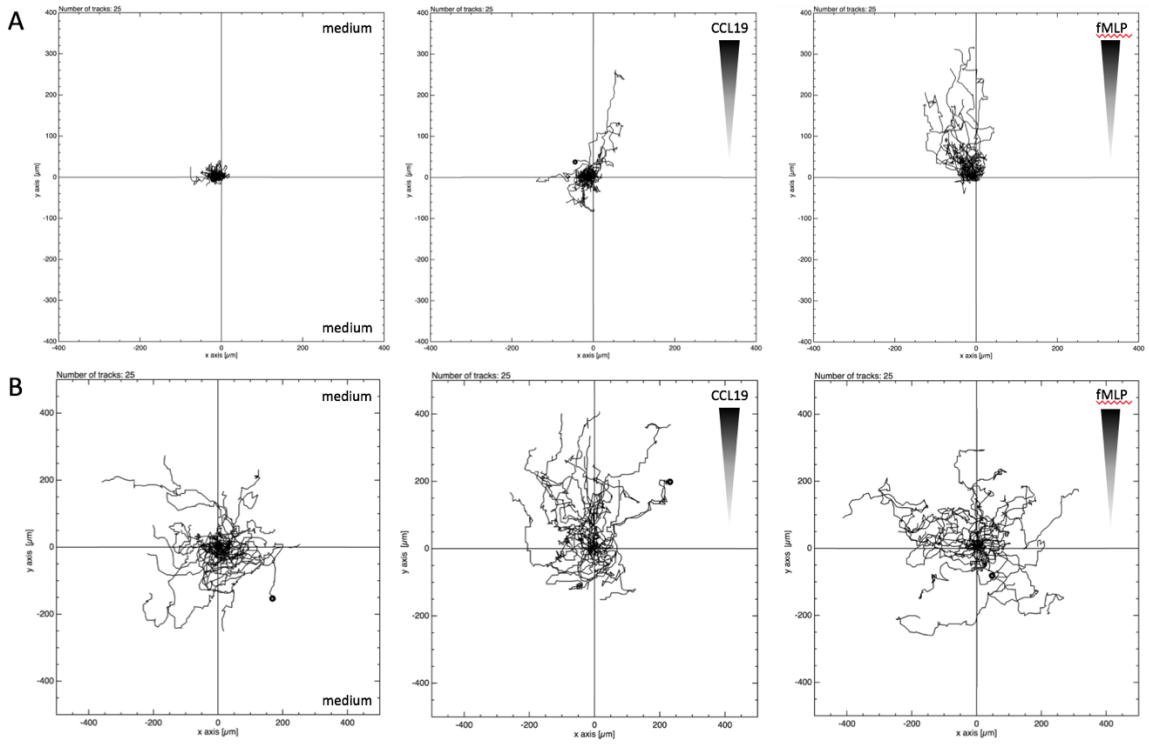

Fig. 16: ***µ-Slide Chemotaxis^{3D}.*** *Chemotactic response of ercDCm (A) and cDCm (B) towards CCL19 and fMLP respectively. While ercDCm show no chemotactic and chemokinetic response towards CCL19, they show a strong response towards fMLP. Contrary, cDCm do not respond towards fMLP, but only towards CCL19 with directed migration. This suggests that ercDCm retain the immature response of DC towards CCL19, and do not have overall impaired migration abilities. Furthermore, it can be noted, that cDCm are more chemokinetic active than ercDCm.*

In a next step, we sought to determine whether immature cDC are less mobile than mature cDC, or generally more mobile than immature ercDC, and whether treatment with Wnt5a could influence this mobility. For this experimental setup, µ-Slide

Chemotaxis^{3D} MAs were performed with cells from the same donor, in an immature state and after maturation. As expected, immature cDC were not able to migrate towards CCL19, and they only gained the ability of directional migration towards CCL19 through maturation. Wnt5a stimulation showed no significant effect on the general mobility of immature cDC. Velocity and accumulated distance were slightly decreased in immature cDC stimulated with Wnt5a (d0) compared to immature cDC without Wnt5a. In their immature state cDC behaved similarly to immature ercDC, which even seemed to be slightly more mobile than cDC with an increased velocity and mean distance.

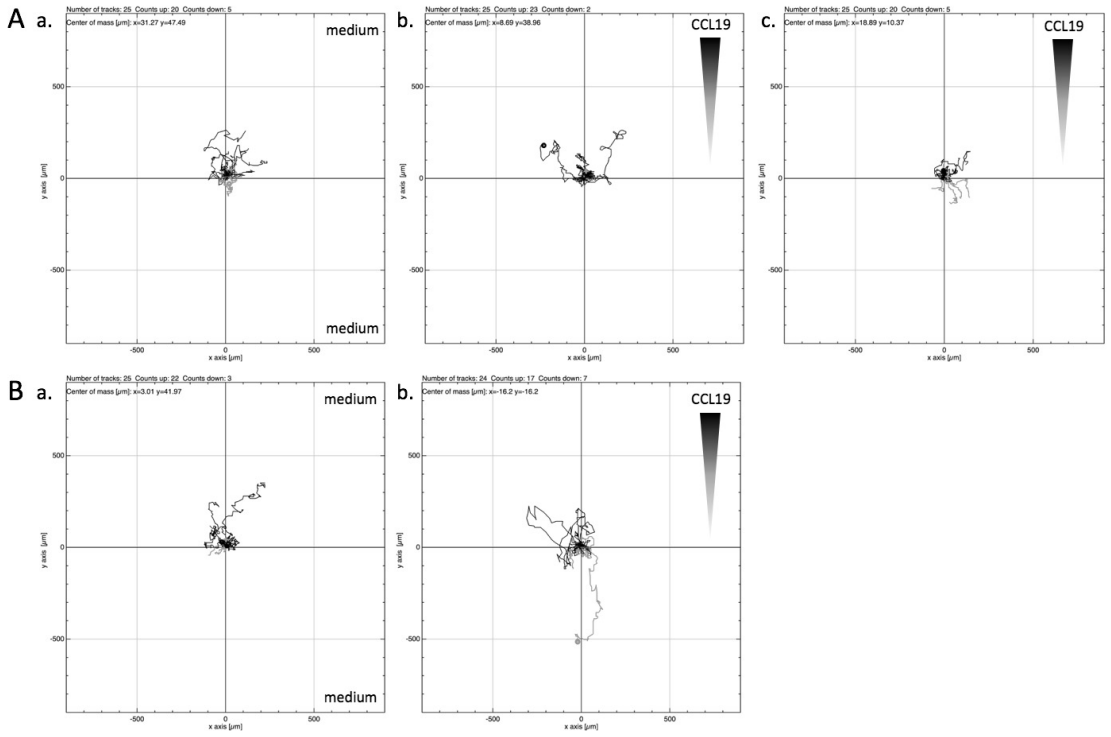

*Fig. 17: **µ-Slide Chemotaxis^{3D}.** Chemotactic response of immature cDC (A) and ercDC (B) towards CCL19, with A c. being immature cDC + Wnt5a(d0). Neither immature cDC nor ercDC show directed migration towards CCL19. In their immature state cDC present similarly to immature ercDC. Addition of Wnt5a(d0) did not show any effect on migration behaviour of immature cDC.*

Once maturated, cDC were able to migrate directional towards CCL19 and increased their accumulated distance and velocity significantly. As expected, the maturation of ercDC did not influence their migration towards CCL19 as compared to their immature state. They showed no directed migration and also distance and velocity remained the same compared to their immature state.

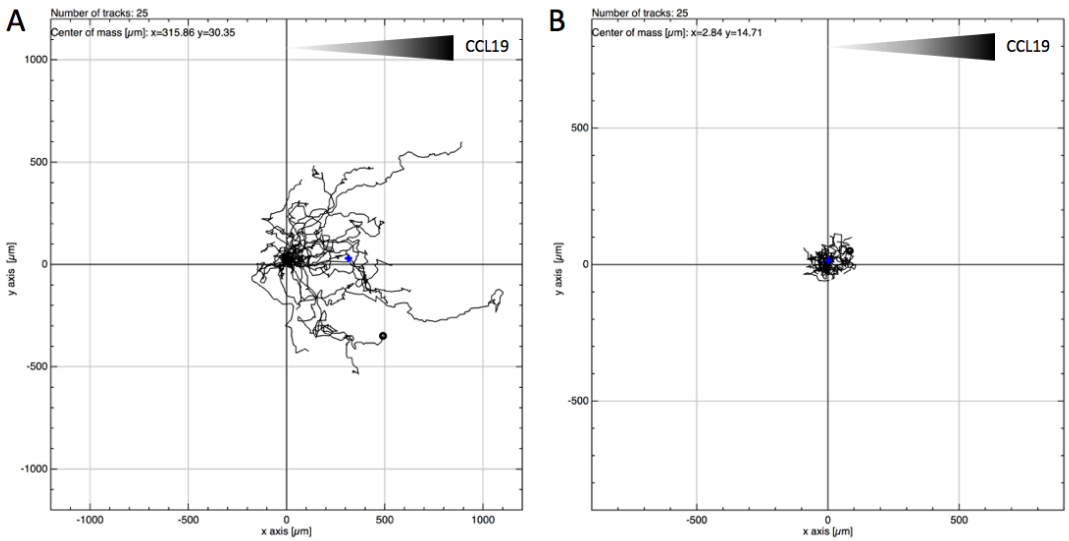

*Fig. 18: **µ-Slide Chemotaxis^{3D}.** Chemotactic response of maturated cDC (A) and ercDC (B) towards CCL19. Cells were derived from the same donor at the same time as experiment Fig. 12. While maturation of cDC enabled strong directional migration towards CCL19, no directional migration could be observed for maturated ercDC.*

5.8.1 Migratory effect of Wnt5a, sFRP5 and sFRP1 on cDC

In order to investigate the specific effects of modulation of Wnt-signalling on the migratory behaviour of cDCm, Wnt5a, sFRP1, sFRP5 or the combination of Wnt5a and sFRP1 were added to the growth medium during differentiation. All stimulants were added on day 0 to ensure their presence throughout the whole differentiation process. Thereafter µ-Slide Chemotaxis^{3D} MAs towards CCL19 was performed and the FMI, directionality, distances and velocity evaluated. As a negative control, cDCm medium-medium migration was performed with each experimental setup. For statistical purposes, the results of several experiments, with different donors were pooled and statistical significance determined using the Mann-Whitney U-test for two-tailed data and cDCm as a reference group. Even though donor specific differences were observed in these experiments, histogram analysis (by Kolmogorov-Smirnov-Test) confirmed Gaussian-distribution of pooled data, justifying their further analysis.

As we previously showed that cDC, but not ercDC, produce Wnt5a, we expected a positive effect of Wnt5a and a possible negative effect of Wnt5a-inhibition on the migratory behaviour of cDCm. Unexpectedly however, Wnt5a significantly reduced the y-FMI, directionality, distances and the velocity. Stimulated with Wnt5a, cDCm showed reduced motility and directed migration towards CCL19. Furthermore, attempted

inhibition of Wnt5a with sFRP5 and sFRP1 did not counteract the effects of Wnt5a, but also showed an inhibitory effect on migration, with reduced FMI, directionality, distance and velocity. The simultaneous stimulation with Wnt5a and sFRP1 also inhibited migration, although this effect was not additive. Overall it could be shown that Wnt-signalling modification seemed to inhibit the migration of cDCm in all investigated aspects. When stimulated the cells showed reduced motility, velocity and directed migration.

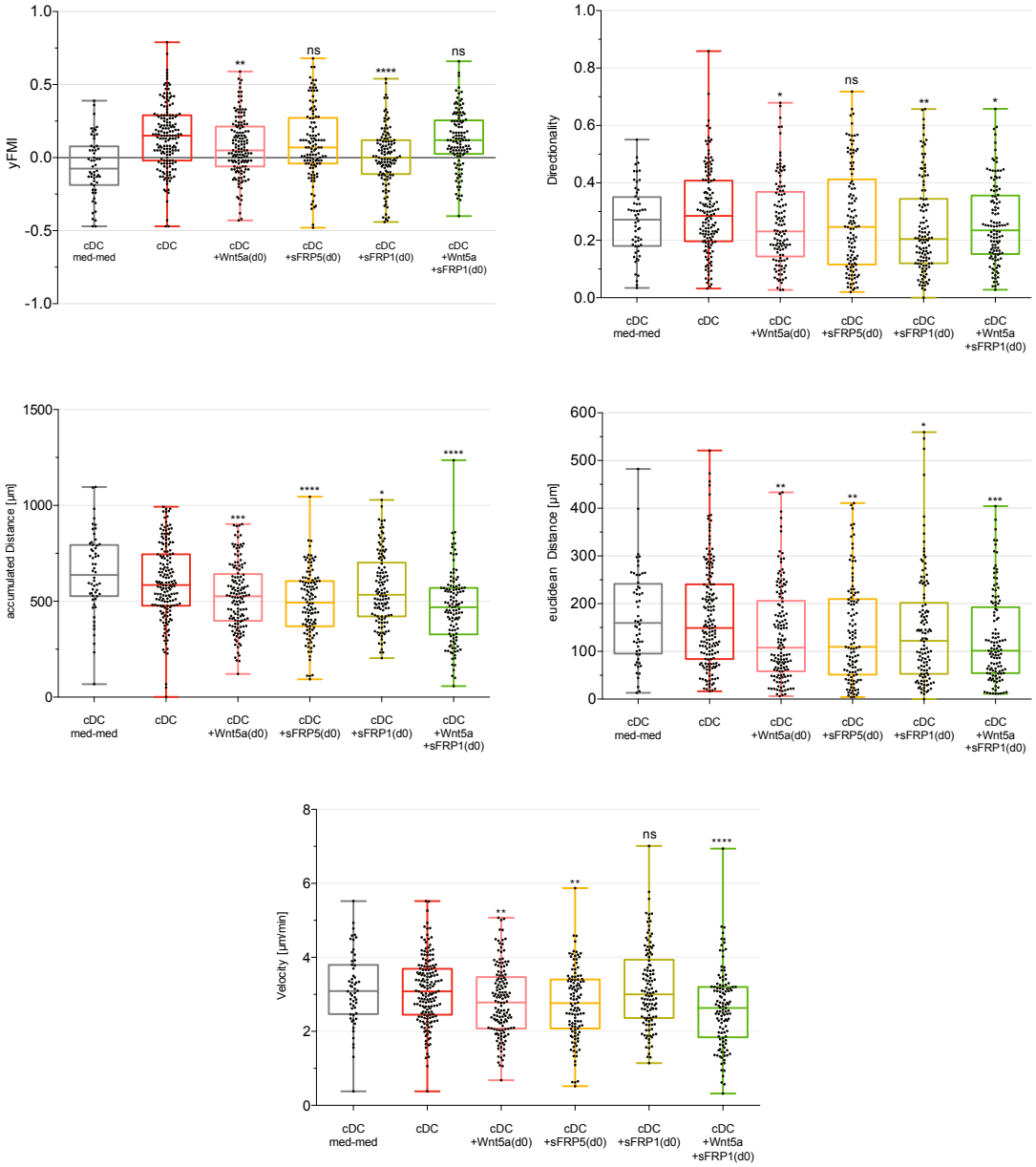

*Fig. 19: **µ-Slide Chemotaxis^{3D}**. Chemotactic and chemokinetic effect of Wnt5a, sFRP5, sFRP1 on cDCm. All stimulants were added on day 0 of differentiation. For statistical analysis the Mann-Whitney U-test for two-tailed data was applied and cDC used as a reference group.*

5.8.2 Migratory effect of Wnt5a, sFRP1 and sFRP5 on ercDC

The same experimental setup was used to investigate the effects of Wnt5a, sFRP1 and sFRP5 on ercDCm. Again all stimulants were added on day 0 of differentiation. Data of several experiments were pooled and the Mann-Whitney U-test for two-tailed data, with ercDCm as reference group, applied in order to test for statistical significance. Contrary to cDCm, however, no significant effects regarding distances, velocity and directionality could be detected. The significant effects on yFMI have to be evaluated carefully, as ercDCm only showed marginal migration, with very short distances, and therefore rather have to be considered as an experimental error.

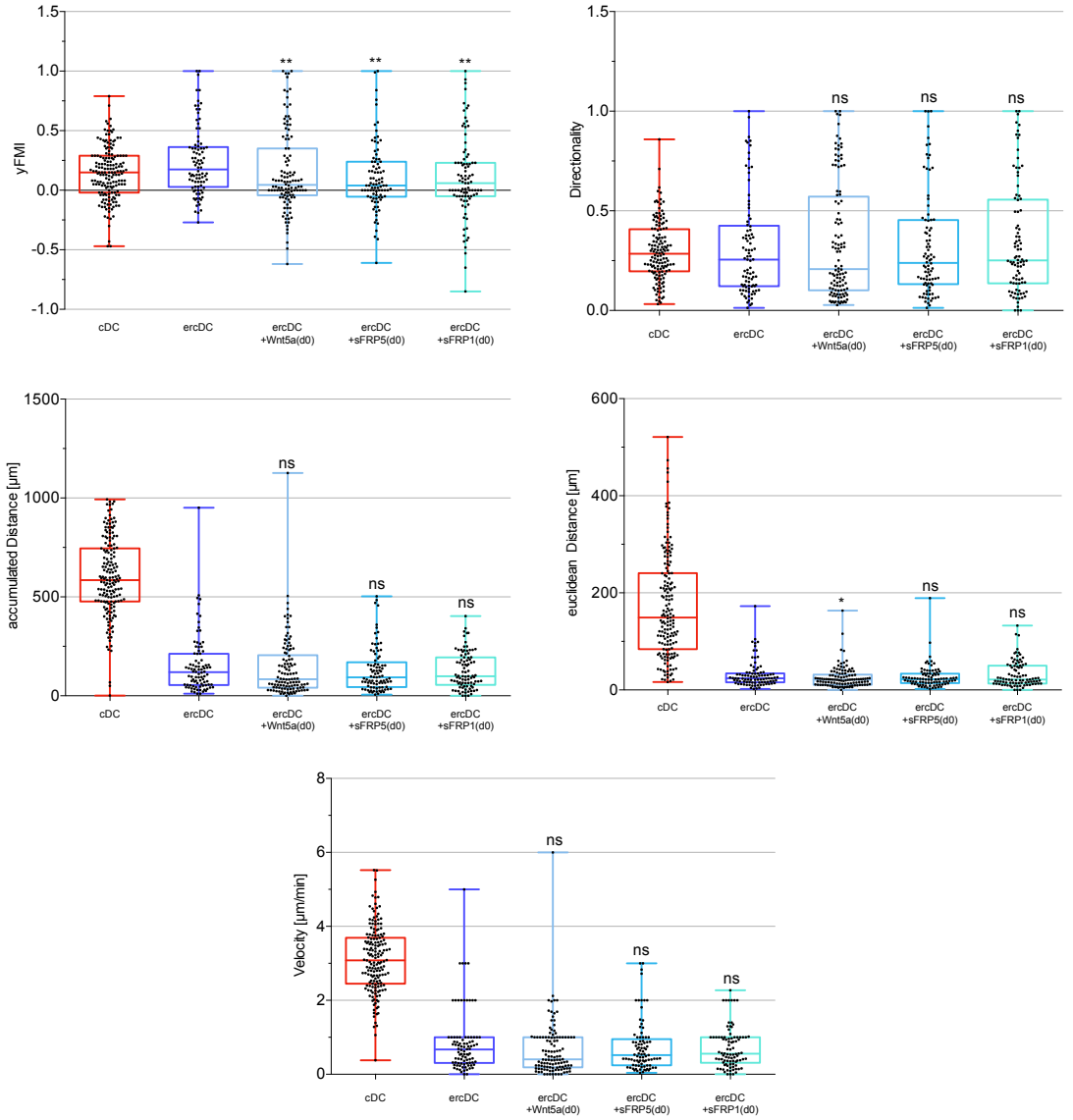

*Fig. 20: **µ-Slide Chemotaxis^{3D}.** Chemotactic and chemokinetic effect of Wnt5a, sFRP5, sFRP1 on ercDCm. All stimulants were added on day 0 of differentiation. For statistical analysis the Mann-Whitney U-test for two-tailed data was applied and cDC used as a reference group.*

5.9 Microarray analysis of ex vivo cDC and ercDC

All initial experiments were performed with in vitro generated PBMC derived cDC, ercDC and MΦ. In a final step we therefore aimed to validate the in vitro transcriptomic analysis with ex vivo derived data. "Affymetrix GeneChip® Human Gene 1.0 ST" array data of ex vivo cDC, ercDC and MΦ were kindly provided by Dorothee Brech. Ex vivo ercDC RCC ($CD209^+CD14^+CD163^+$) and MΦ ($CD209^+CD14^+CD163^+$) were obtained from tissue-suspensions of clear cell RCC samples, while $CD1c^+$ DC ($CD11c^+$, $CD1c^+$, $CD19^-$) and slanDC ($CD11c^+$, $slan^+$, $CD19^-$) were obtained from blood samples of healthy donors. Again quality control, clustering analysis and normalisation using the RMA-algorithm were performed using the MADMAX platform. Fold changes were calculated as before comparing $CD1c^+$ DC, slanDC and MΦ to ercDC_RCC and a fold change >1.5 or <-1.5 was considered differential gene expression. For better comparability, FCs of in vitro cDC compared to ercDC were included in the chart (see supplementary table 2).

Interestingly $CD1c^+$ DC and slanDC compared to ercDC_RCC showed a lot of regulation for canonical as well as non-canonical Wnt-signalling pathways. These differential gene expressions did however, not necessarily resemble the gene expression pattern found for the in vitro cDC compared to ercDC.

Contrary to the in vitro data, no differential gene expression could be observed for any of the Wnt-ligands or receptors and only little for co-receptors, agonists and antagonists. Unlike in vitro cDC, ex vivo $CD1c^+$ DC or slanDC did not show higher expression of Wnt5a compared to ercDC. Interesting, was the differential expression of SDC2, 3 and 4, which showed higher expression in ercDC_RCC compared to $CD1c^+$ DC or slanDC.

Even though this data does not support our findings of increased expression of Wnt5a in in vitro cDC, compared to ercDC, differential expression for core signalling genes of canonical as well as non-canonical signalling was evident and suggest possible mechanism for impaired ercDC functioning.

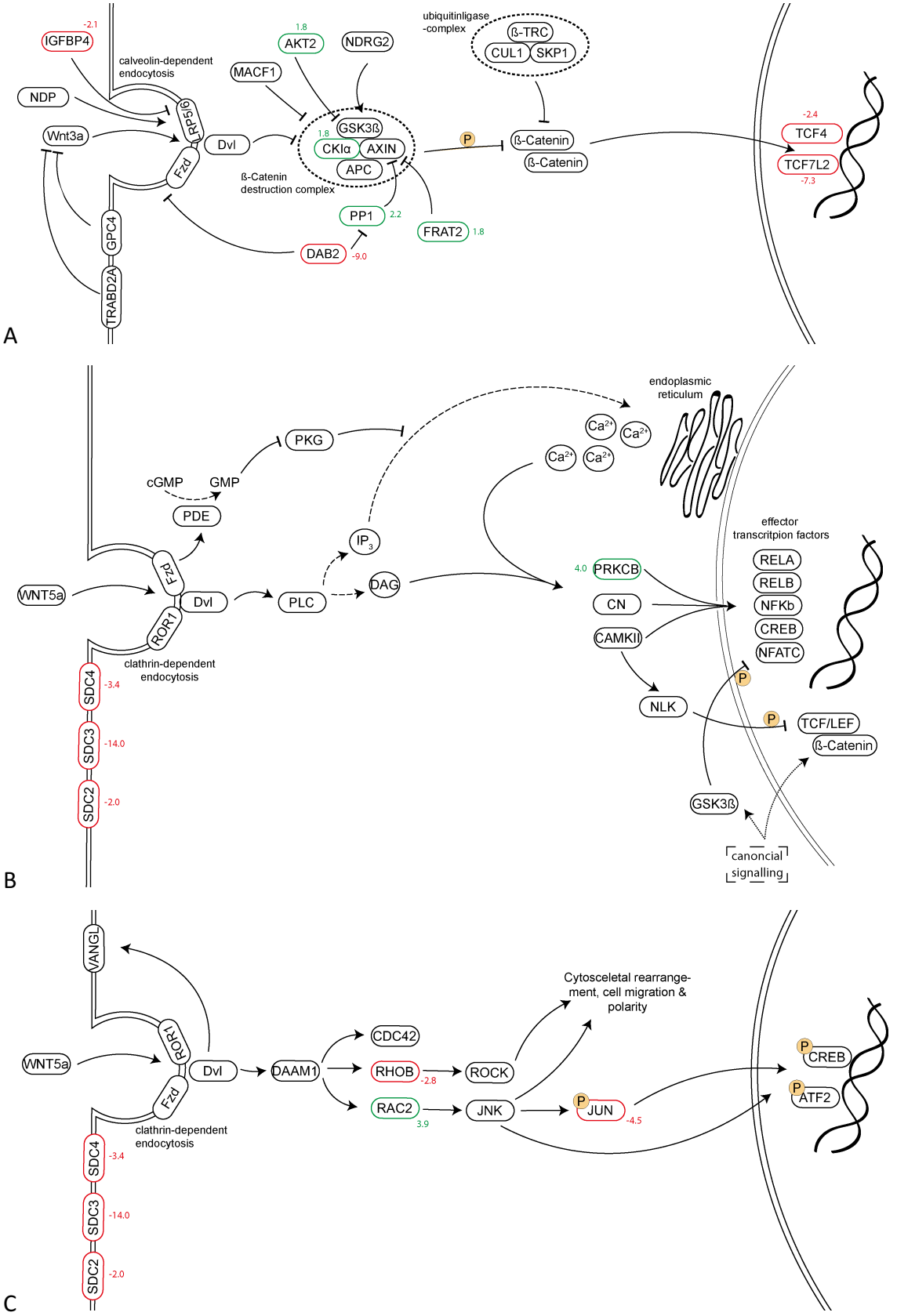

Fig. 21: ***Microarray analysis of CD1c$^+$ DC.*** *The scheme displays microarray data integrated into a modified version of the canonical (A), Ca^{2+} (B) and PCP (C) Wnt pathway. FC were calculated comparing CD1c$^+$ DC (CD11c$^+$, CD1c$^+$, CD19$^-$) to ercDC_RCC (CD209$^+$CD14$^+$CD163$^+$). Significant differential gene expression is presented by green (up-regulation) or red (down-regulation) boxes and the corresponding fold changes in comparison to monocytes. Fold changes were generated using the RMA-Algorithm and a FC >1.5 and <-1.5 was considered significant differential expression.*

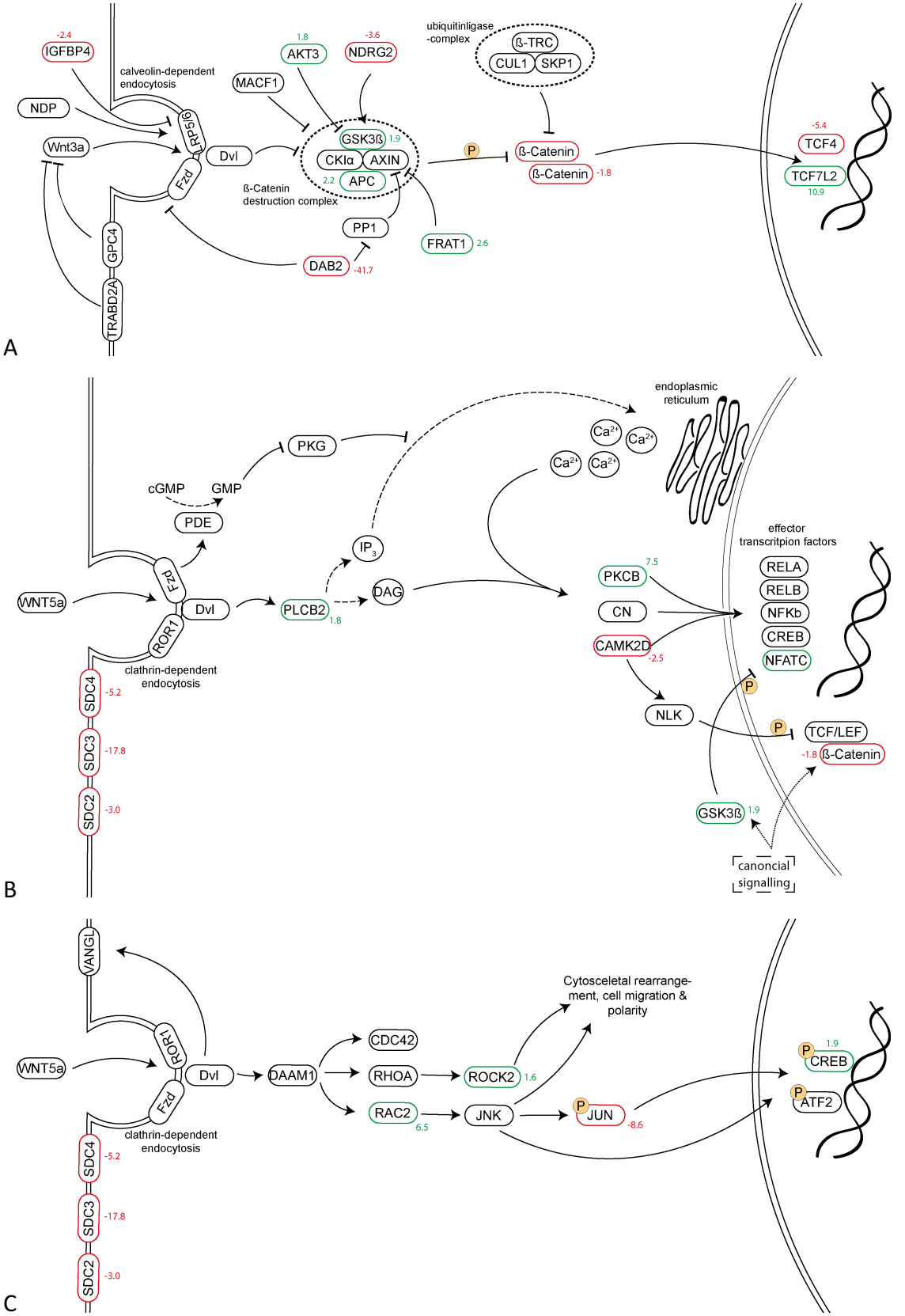

Fig. 22: ***Microarray analysis of slanDC.*** *The scheme displays microarray data integrated into a modified version of the canonical (A), Ca^{2+} (B) and PCP (C) Wnt pathway. FC were calculated comparing slanDC ($CD11c^{+}$, $slan^{+}$, $CD19^{-}$) to ercDC_RCC ($CD209^{+}CD14^{+}CD163^{+}$). Significant differential gene expression is presented by green (up-regulation) or red (down-regulation) boxes and the corresponding fold changes in comparison to monocytes. Fold changes were generated using the RMA-Algorithm and a FC >1.5 and <-1.5 was considered significant differential expression.*

5.10 Wnt-signalling in renal cell carcinoma

In order to further analyse Wnt-signalling in RCC, we performed transcriptomic analysis of the Wnt-signalling pathways in normal kidney and samples of RCC with G1 and G3 nuclear grade, 3-tiered WHO. Data was kindly provided by PD Dr. Matthias Maruschke from the Department of Urology of the University of Rostock. Analysis and FC calculation were performed concordant with previous data (see supplementary table 3).

Supporting the immune-histological findings Wnt5a was strongly up regulated in RCC and even more expressed with higher WHO nuclear grading. Other Wnt-ligands were not differentially expressed, suggesting a possible key role of Wnt5a signalling in RCC. An up-regulation could also be observed for Fzd1 and 2 receptors in RCC, especially G3. Interestingly, the RCC showed a strong down regulation of HSPG, especially glypicans 3 and 4. Our in vitro data of activated myeloid cells (cDC, ercDC, M1 and M2), however, showed high expression of SDC2, 3, 4 and GPC4. High expression for SDC2, 3 and 4 were also observed for ercDC_RCC compared to $CD1c^+$ DC and slanDC. As discussed earlier, HSPG are discussed to be involved with Wnt-ligand gradient formation and can act as co-receptors, especially for non-canonical signalling. The RCC could hence be a possible source of Wnt5a and thereby affect myeloid cells differentiation.

Strong differential expression was also found for several Wnt-antagonists, suggesting strong regulation of specific Wnt-signalling. DKK3, sFRP2, 3, 4, CTHRC1 and IGFBP1 were for example up-regulated, whereas WIF1, sFRP1, Shisa 2, 3 and SOST were down-regulated.

Differential expression of core Wnt-signalling genes was found for β-Catenin-dependent as well as β-Catenin-independent, PCP and Ca, -signalling. Even though regulation was evident, data was not suggestive of specific activation of either canonical or non-canonical signalling.

In conclusion, it can be said that strong differential expression of core Wnt signalling genes and associated genes could be found in clear cell RCC, and differences could also be found depending on grading of the tumour. Interesting was the high expression of Wnt5a in RCC compared to normal kidney. This could suggest a possible mechanism for impaired DC functioning in RCC and even be in part responsible for altered differentiation of ercDC.

6 Discussion

6.1 Renal cell carcinoma and ercDC

As immunogenic tumours, RCC and especially clear cell RCC (ccRCC) are usually highly infiltrated by leukocytes. However, a negative correlation of increased mononuclear cells in the infiltrate with prognosis has been observed, suggesting that the immune cells do not properly function in their role as anti-tumour defence [87]. Recent studies have attempted to investigate the composition of this infiltrate with special emphasis on subtype identification and functionality. A deeper understanding of RCC immunology and the factors involved in tumour escape from an eliminating immune response, could reveal prognostic factors and identify new therapeutic approaches. Schleypen et al. investigated the influence of cytotoxic marker expression and the frequency of natural killer cell infiltrates in samples of RCC, with regards to their functional capacity [88]. Their findings suggested the potential use of NK-infiltrates in RCC as prognostic marker for the clinical outcome of RCC patients. DC, which can function as a switch between immune activation and tolerance, have also been suggested as predictive markers of disease progression. The granulocyte/DC ratio, for example, was proposed as a biomarker for immune monitoring of RCC patients [89]. SlanDC, a proinflammatory subset of myeloid DC, have been shown to accumulate in primary ccRCC, metastatic lymph nodes and metastases [90]. These RCC infiltrating slanDC, however, differ from slanDC found in healthy human blood, as they present an immature phenotype and show impaired ability to induce T-cell proliferation and polarization, and produce reduced levels of proinflammatory cytokines such as TNF-α and IL-12, but higher levels of anti-inflammatory IL-10. While healthy blood slanDC may contribute to an antitumour immune response, these tolerogenic slanDC seem to be involved in tumour growth and immune escape and hence may be used as prognostic marker.

Another DC subtype identified in RCC tissue are the so called ercDC, which co-expresses the DC marker CD209 and the macrophage markers CD14 and CD163. This “DC” subtype was found to be enriched in RCC and with increasing density in advanced tumour stages [91]. Although initially referred to as DC-subtype, further work by D. Brech have positioned the ercDC phenotype within the continuum of the mononuclear phagocyte system, where DC and Mϕ represent opposite extremes. In her work, she has shown

that ercDC resemble DC as well as Mϕ, but based on gene expression analysis, appear to show more similarities to Mϕ, especially to an inflammatory Mϕ subtype found within the ascites produced by ovarian cancer. ErcDC can be generated *in vitro* through addition of CXCL8/IL-8, IL-6 and VEGF, which are highly expressed by RCC [91]. Furthermore, D. Brech has shown that PGE_2, glucocorticoids (GC) and palmitic acid (PA), or a combination of TNF, PGE_2 and Pam3CysSerLys4 found within the tumour milieu influence the differentiation of ercDC and thus could explain the proangiogenic and invasive gene expression of ercDC, which promote tumour progression. Moreover, she identified signs of tolerogenic and protumoural characteristics, such as the impaired ability of ercDC to induce T-cell proliferation.

In the present work, my goal was to further identify differences between ercDC and cDC. As cytokine production plays a pivotal role in influencing cell signalling, immune responses and especially the activation or inhibition of other immune cells, cytokine levels of IL-12, TNF-α and IL-10 were measured. IL-12 and TNF-α are pro-inflammatory cytokines associated with antitumourogenic properties. IL-10 is referred to as an anti-inflammatory cytokine and high levels are assumed to play a role in the tumours escape from an immune response [83]. Recent studies reported a low, chronic secretion of TNF-α in RCC and showed that this correlates with poor prognosis [84]. In support of these findings, my work could show that ercDC produce significantly more TNF-α and IL-10 upon LPS stimulation, and hence could represent a possible source of these cytokines in RCC. IL-12, however, was detected at decreased levels in ercDC compared to cDC. These findings support the hypothesis of ercDC being a myeloid subset, found especially in RCC, which facilitates the tumours escape from the immune surveillance and furthermore possibly promotes tumour growth.

In a next step, the ability of ercDC to migrate towards CCL19 was investigated. CCL19 is an important chemokine involved in the homing of maturated DC towards peripheral lymph nodes. Homing to lymph nodes is crucial in DC biology, as this is where DC activate and prime T-cells for a directed, adaptive immune response. While cDC migrated strongly towards CCL19, ercDC did not respond to CCL19 stimulation although they express the receptor CCR7. To ensure that ercDC have the ability to migrate, ercDC migration towards fMLP was tested. fMLP is a cleavage product of bacteria and attracts leukocytes to the site of inflammation. FPR, the receptor for fMLP, was found to be

expressed on monocytes and immature DC, but down-regulated on maturated DC [86], thereby enabling a switch between site of inflammation and site of adaptive immune response activation. Here we could show that unlike maturated cDC, “maturated” ercDC migrate strongly towards fMLP, but not towards CCL19. This suggests that ercDC retain a rather immature response towards chemoattractants or do not maturate in the same way as cDC. This prohibits the migration of ercDC towards lymph nodes, where they could potentially initiate an adaptive immune response. We hypothesize that this is a second mechanism by which the tumour escapes immune response in which ercDC play a decisive role.

In summary, we found further evidence to support the hypothesis that ercDC may be involved in the tumours ability to escape immune surveillance. We could show that ercDC produce high levels of IL-10 and TNF-α, but lower levels of IL-12. Furthermore, maturated ercDC are not able to migrate towards CCL19. As a next step, we attempted to go deeper into the biology of ercDC, specifically as it relates to their regulation by signalling pathways linked to tumour biology.

6.2 Wnt-signalling in renal cell carcinoma

While Wnt-signalling, especially β-catenin dependent signalling, has been studied extensively in other cancers, such as colorectal cancer, breast cancer and melanoma, only little is known about its involvement in RCC. Controversial results of β-Catenin expression levels have been detected, yet all of these studies confirm the importance of β-Catenin-signalling in RCC. Multilayer-omics studies identified gene mutations and epigenetic as well as mRNA expression alterations of canonical Wnt-signalling in RCC [92]. Increased expression levels of Wnt receptors Fzd5, 7 and 8 [93] and Wnt-ligands, such as Wnt1 and Wnt10A could be detected [94]. Furthermore, decreased expression levels were detected for extracellular Wnt-antagonists, such as DKK, IGFBP4 and sFRPs, which result in increased β-Catenin stabilisation [95]. Downstream alterations include the activation of ubiquitin protein ligase E3C (UBE3C)[96] and the oncogene MYC [93]. Potential implications of Wnt signalling in RCC include changes in apoptosis, proliferation and migration [97].

As little was known about non-canoncial signalling in RCC our one goal of this study was to further elucidate its potential involvement. Immunohistochemistry demonstrated

that Wnt5a is highly expressed within the RCC. Furthermore, it was possible to verify Wnt5a expression in RCC by transcriptomic analysis, and that Wnt5a expression appears to increase with tumour progression suggesting a possible role for Wnt5a.

Although, Shiina et al. and Kruck et al. detected increased levels of canonical Fzd-receptors and Wnt-ligands, these findings could not be verified in our gene array analysis performed on RCC samples. In addition, no differential expression of β-Catenin and only slight variations in other genes linked to canonical Wnt signalling were observed. Possible reasons for these deviations from the published literature include differing sample acquisition, tumour stages and other factors associated with protocol differences. Noteworthy, was the strong up regulation of RAC2, which showed a positive correlation with progressive tumour grading. RAC2 is a small Rho-like GTPase and part of the Wnt PCP pathway. It is involved in cytoskeletal rearrangement by regulating cell adhesion, migration and polarity. Differential expression was also seen for other genes of the Wnt PCP and Ca^{2+}-pathways, suggesting a possible role of non-canonical signalling in RCC. Strong regulation was observed for Wnt-antagonists. While a previous study by Ueno et al. showed an epigenetical down-regulation of DKK3 [98], we could detect an up-regulation of DKK3. DKK3 has been shown to influence canonical, e.g. in lung cancer, as well as non-canonical Wnt signalling in for example prostate cancer, via interference with Wnt receptors and co-receptors. An increase in expression of sFRP2, 3 and 4 in RCC was also seen as compared to normal kidney tissue. sFRP1 and WIF1, both important inhibitors of Wnt-signalling, were down-regulated in RCC, which is in agreement with previous findings by others [99].

Interesting was the differential expression of HSPG, and especially the strong down regulation of glypicans 3 and 5 found in RCC as compared to healthy kidney. Glypicans are HSPGs that are covalently bound to the plasma membrane through a glycosylphosphatidylinositol anchor. They can regulate signalling pathways through ligand-receptor interaction and thereby exhibit inhibitory as well as stimulatory effects. Similarly to Wnt5a, GPC3 is up-regulated during development, but down regulated in most adult tissues, with the exception of mesothelium, breast and ovarian epithelia [100]. GPC3 up-regulation was detected in hepatocellular carcinoma (HCC) and has been shown to promote β-Catenin dependent signalling through direct ligand receptor interaction, e.g. with Wnt3a and Fzd8, and increased ligand concentration at the cellular

membrane [101]. Furthermore, it was shown to be involved in cellular migration and motility in HCC [102]. GPC3 has been shown to have inhibitory effects on β-Catenin dependent signalling, and promote activation of non-canoncial PCP signalling in breast cancer. In this context, it is thought to promote mesenchymal-epithelial transmission (MET), and thereby inhibit metastasis and the invasiveness of tumours [100]. These contrary effects of GPC3 on Wnt-signalling could be explained in part by cellular context, as well as the ligands and receptors involved. Castillo et al. have suggested that GPC3 expression patterns depend on the tumour tissue and its origin. GPC5 shows high homology to GPC3. However, only little is known about its exact role. It has been shown to promote rhabdomyosarcoma proliferation via hedgehog and Wnt1 signalling, but also to exhibit a protective effect on lung cancer [103]. It would be interesting to further elucidate the biologic mechanisms of GPC3 and GPC5 in RCC.

Summarizing, we detected strong differential regulation of non-canonical Wnt-signalling in RCC. Striking was the up regulation of Wnt5a at the protein and mRNA level, and the differential expression of GPC 3, 5 and Wnt-antagonists. Not all of our findings were in concordance with previous studies, especially with regards to the differential expression of Wnt-antagonists. This is also seen across the literature research where sometimes contrary results and functions were described for the same gene. These results underscore the diversity and complexity of Wnt-signalling in tumour biology. The activation of these pathways depend on the intricate interplay of ligands, receptors, co-receptors and down-stream signalling pathways. The detection of mRNA expression levels alone does not allow for prediction of mechanism or effects. Further research would be necessary to identify causes explaining these differences. In addition, patient differences, tumour stages and other unknown factors such as sample acquisition and experimental error have to be kept in mind. As complex and difficult as this seems, it is still vitally important to better understand this biology in the context of RCC biology.

6.3 Wnt-signalling and dendritic cells

The major goal of this thesis was to study the potential role of Wnt-signalling in the context of myeloid biology and specifically, during development of the ercDC phenotype. We hypothesized, that Wnt-signalling may differ between myeloid subsets and that the tumour milieu of the RCC may be able to influence the differentiation of

myeloid cells and thereby promote RCC growth. Transcriptomic analysis of *in vitro* generated monocyte derived DC and Mϕ was used to identify potential differences in Wnt-signalling associated gene expression levels. Interestingly, high expression of Wnt5a was identified in cDC, while it was largely absent in monocytes, Mϕ and ercDC. Other Wnt ligands, however, were not found to be differentially expressed between the myeloid subsets. According to the DABG algorithm, many of the Wnt-ligands, e.g. Wnt2, 3a, 8a, 8b, 10a and 11 were not detected above background in any of the myeloid subsets. Differential expression was found within the Ca^{2+}- and the β-Catenin dependent Wnt -signalling pathways and moderate changes were also seen in the PCP-pathway. A striking up-regulation of SDC2, 4 and GPC4 was seen in activated myeloid cells compared to peripheral blood monocytes. These HSPGs have been shown to enhance and inhibit canonical, as well as non-canonical signalling, depending on ligand and receptor context. These proteins are thought to help concentrate Wnt-ligands at the cellular membrane and thereby promote direct ligand-receptor interaction [70]. SDC4 has been implicated in Wnt/PCP as well as Ca^{2+}-signalling and SDC2 in moderating RhoGTPase activity [104]. Furthermore, SDC4 expression has been shown to correlate with Wnt5a levels and is thought to be essential for Wnt5a autocrine signalling, internalization and signal transduction, especially in non-canonical signalling of melanoma cells [105]. GPC4 has recently been shown to inhibit β-Catenin signalling in cardiomyocytes by possibly affecting Wnt-ligand gradient formation and interaction with Wnt-inhibitor factor 1 (WIF-1) [106]. However, there is also evidence that GPC4 binds to Wnt11 and enhances Wnt-induced migration and that GPC4 can positively and negatively regulate Wnt3a as well as Wnt5a-signalling depending on its membrane localization [107]. The biology of HSPGs is clearly complex and very little is understood about their exact role in myeloid cell biology.

Based on the results of the transcriptomic and pathway analysis, differences in Wnt-signalling pathways were seen between the myeloid subsets. Activation, as well as suppression of canonical and non-canonical signalling was observed depending on the specific myeloid subset. While a more robust differential expression was observed between cDC and M1, when compared to monocytes, only slight differences were seen when comparing ercDC to monocytes. This suggests that Wnt-signalling in ercDC more closely resembles peripheral blood monocytes, but not with cDC or M1 cells. Hence, this

led to the question whether the differences seen in Wnt-signalling could in part be responsible for the functional differences between cDC and ercDC.

6.4 The role of Wnt5a in dendritic cells

The high expression of Wnt5a of in vitro generated myeloid DC, but not of monocytes and Mϕ, has been previously shown by others [108]. Furthermore, Wnt5a addition during the differentiation of monocyte derived DC, has been shown to increase IL-6 secretion, which in turn inhibits DC differentiation resulting in increased $CD14^{+/++}$ $CD16^{+}$ monocytes [109]. As Wnt5a has previously also been shown to induce inflammatory, as well as anti-inflammatory cytokines, and to inhibit IL-6 secretion [110], Bergenfelz et al. proposed that Wnt5a may act as a cytokine inducer with differing effects depending on the cellular and tissue context. Wnt5a secretion by melanoma cells, for example, influences DC to induce T_{reg} development via β-Catenin dependent indoleamine 2,3-dioxygenase-1 activation [111], highlighting that Wnt5a can activate canonical as well as non-canonical signalling in a cell and receptor specific manner. Activation of β-Catenin dependent signalling through Wnt5a promotes DC with tolerogenic features, so called semi-maturate DC [112]. Valencia et al. describe Wnt5a signalling in DC, but distinguish between effects of Wnt5a stimulation during DC differentiation, maturation and function. This emphasises the assumption that Wnt5a signalling is complex, and its effects may differ depending on different cellular conditions. They show that non-canonical Wnt5a signalling skews the cells toward a tolerogenic phenotype during monocyte-derived DC differentiation [113]. They also showed that Wnt5a stimulation could induce IL-12 secretion and enhance $CD4^{+}$ T-cell priming with IFN-γ and IL-2 secretion. Interestingly, the authors showed that the Fzd5 receptor is expressed only during early DC differentiation and that immature DC express an array of Wnt receptors, but show reduced Fzd5 expression, while maturated DC show regulation of Fzd1 and 4. Ryk, a nonconventional Wnt receptor and co-receptor, is expressed by monocytes and DC [114]. It is thought that this helps to conduct differing effects of Wnt5a through changes in receptor status.

6.5 Wnt5a effect on functional abilities of cDC and ercDC

Following the previous results by others and our findings of strong Wnt5a expression in RCC, a goal of this thesis was to elucidate potential effects of Wnt5a signalling on DC subtypes, specifically on the ercDC subtype associated with RCC. Although we hypothesized that Wnt5a may enhance the migratory ability of cDC, we found that Wnt5a addition during differentiation of peripheral blood monocyte derived cDC had the opposite effect, leading to reduced motility, velocity and directed migration. Furthermore, the addition of sFRP5 or sFRP1, both inhibitors of Wnt5a, could not counteract the Wnt5a-driven effects, but instead also led to inhibition of cDC migration. Simultaneous addition of Wnt5a and sFRP5 or sFRP1 respectively inhibited the directed migration of cDC, but not in an additive manner, suggesting that they might act via a similar mechanism. Moreover, we examined whether addition of Wnt5a during ercDC differentiation might restore their migratory capacity towards CCL19. Again, no positive effect of Wnt5a addition during ercDC differentiation could be observed and their ability to migrate towards CCL19 remained poor.

Similarly, Wnt5a did not exert any effects on cytokine secretion of ercDC. However, addition of Wnt5a to cDC resulted in increased IL-10, IL12p40, IL12p70, but decreased TNF-α levels. While the high secretion of IL-10 upon Wnt5a stimulation resembled the high secretion of unstimulated ercDC, the effects on TNF-α and IL-12 were rather contrary. Hence, addition of Wnt5a can only in part explain the impaired functioning and altered phenotype of ercDC. Interestingly, immature cDC and ercDC did not show any differences in cytokine secretion regarding IL-10, IL-12 and TNF-α, while cDC changed their cytokine secretion pattern upon maturation. By contrast, ercDC appeared to remain in an immature state, suggesting impaired maturation of ercDC.

Although a high expression of Wnt5a was detected in cDC and not in ercDC, we could only show an effect of Wnt5a addition on cDC. Wnt5a was found to inhibit the directed migration of the cells, and to alter the cytokine expression of cDC. These results support the hypothesis that Wnt5a stimulation can skew DC towards a tolerogenic phenotype [113] and, in this context, may help facilitate tumour escape from immune surveillance. Contrary to what was expected, the addition of the Wnt inhibitors sFRP5 and sFRP1, showed a similar effect to that seen with Wnt5a. These factors have been previously

reported to inhibit Wnt5a signalling. In the context of this experiment, however, the agents appear to act as agonists. sFRPs exert their function via a similar CRD as the Wnt-ligands. This could be a possible mechanism for the agonistic function. It would be interesting to further elucidate whether the agonistic or antagonistic function of sFRP5 and sFRP1 might be dose dependent. Valencia et al. previously showed not only a time-dependent response, but also a dose dependent effect of Wnt5a. They propose that the dose dependent response of Wnt5a is due to its different affinity towards particular receptors [114]. As little is known about the mechanism of action of sFRPs, this would be an interesting approach to further understand their functioning.

In our experiments, ercDC did not respond to Wnt5a, sFRP1 or sFRP5 treatment during in vitro differentiation. It would be interesting to further evaluate Wnt5a levels during ercDC differentiation. Valencia et al. showed that addition of Wnt5a to immature cDC did not exert the same effect as at earlier stages. They propose that the decreased response is due to low level autocrine Wnt5a signalling of cDC. Thus, the lack of effect seen here could in part be due to a window of sensitivity.

We could show that immature cDC express Wnt5a and respond to Wnt5a stimulation during differentiation by decreased migratory capacity towards CCL19 and TNF-α secretion, but increased production of IL-10 and IL-12. By contrast, ercDC did not express Wnt5a and did not show any measurable effects upon Wnt5a addition. Their migratory capacity remained poor, and the cytokine secretion pattern of ercDC remained similar to that of immature ercDC.

6.6 In vitro generated dendritic cells versus ex vivo derived dendritic cells

Dendritic cell development is influenced through a number of different factors including cytokines and adhesion molecules that act in a paracrine, autocrine and juxtacrine manner. Thus, the tissue environment helps define the development of DC [115]. To study DC biology, a well-established method involving in vitro differentiation of DC from peripheral blood monocytes was used [116]. In the present study we used the MO-DC differentiation medium provided by Miltenyi Biotec. This medium contains FBS, RPMI 1640, L-Glutamine, GM-CSF and IL-4 and allows a lot-to-lot consistent standardized protocol for DC differentiation. However, even though this protocol is often used, the relevance of monocytes as in vivo precursors of DC is not yet fully

understood and other protocols exist [117]. A number of different maturation protocols including addition of LPS, CD40L and TNF-α or the combination of TNF-α, IL-1ß, IL-6 and PGE_2 have been used for the preparation of immunogenic DC. A tolerogenic phenotype can be induced through the addition of IL-10, TGF-β, corticosteroids or Vitamin D_3. This exemplifies how complex DC biology is and that the exact mechanisms of relevant DC differentiation and maturation are still unknown. Hence, any strong conclusion based on in vitro generated DC should be made carefully, especially when transferring the acquired knowledge to biology of in vivo DC.

In order to validate our transcriptomic analysis data based on in vitro generated cDC and ercDC, we compared the obtained results with recent array data from ex vivo, RCC derived cDC and ercDC. While strong differential gene expression between ex vivo cDC and ercDC regarding canonical and non-canonical Wnt-signalling was evident, it did not fully resemble the differential expression found in the in vitro data. No differential expression was found for neither Wnt-ligands nor receptors and only moderate changes for co-receptors, agonists and antagonists. Striking was the differential expression of SDC2, 3 and 4, which showed higher expression in ercDC_RCC compared to $CD1c^+$ DC or slanDC. Even though the high expression of Wnt5a of in vitro generated cDC could not be validated by the ex vivo data, the results of the ex vivo data analysis suggest a possible role of Wnt signalling in DC biology, which could in part explain differences between subtypes, e.g. cDC compared to ercDC.

Following these results, the question arose of how representative the in vitro generated DC are and whether results based upon in vitro studies can be transferred to better understand the complex in vivo DC biology. Royer et al. investigated the effect of differing culture media and adjuvant proteins on DC phenotype and immune capacity. They could show that depending on culture medium and supplements, e.g. HSA or FCS, DC differed regarding surface markers, such as CD80, CD83 and HLA-ABC, but also regarding their functional abilities, such as IL12p70 secretion [118]. While they pointed out, that standardized protocols are important regarding DC differentiation in terms of DC-based vaccines in immunotherapies, we would go further and highlight that results based on in vitro studies should only carefully be transferred to the in vivo situation. Even more, D. Brech notes in her thesis that cluster analysis of externally available data from “GEO” or the “Array Express” homepage with her own data of $CD1c^+$ DC, slanDC

and Monocytes showed clustering depending on the laboratory but not the cell type. This further suggests that not only the in vitro generation of DC depends on the protocol applied, but also the ex vivo acquisition of DC.

In conclusion, our results show differences in Wnt-signalling between different myeloid and especially DC subtypes. Furthermore, we could show effects of Wnt5a-signalling on migration and cytokine secretion pattern of DC. These could in part explain impaired DC functioning in the tumour milieu of RCC and suggest a possible role of Wnt5a in the tumours escape from immune surveillance. However, further experiments regarding exact downstream signalling of Wnt5a and the relevance of Wnt5a signalling in the in vivo situation would be interesting to perform.

7 Abbreviations

7-AAD	7-Amino-Actinomycin
APC	Antigen presenting cells
APC	Adenomatosis polyposis coli
BSA	Bovines serumalbumin
CAMK	Calmodulin-dependent protein kinase
CCL	CC- Chemokine ligand
CCR	Chemokine CC-motif receptor
CD	Cluster of differentiation
cDC	classical Dendritic cells
CDC42	Cell division control protein 42 homolog
cDNA	copy deoxyribonucleic acid
CK	Casein kinase
CRD	Cysteine-rich domain
CREB	cAMP responsive element binding protein
CTHRC	Collagen triple helix repeat containing
CTLA	Cytotoxic T-lymphocyte antigen
CXCL	Chemokine (C-X-C motif) ligand
DAAM	Dishevelled-associated activator of morphogenesis
DAB	3,3'-diaminobenzidine
DABG	Detection above background
DAG	Diacylglycerol
DC	Dendritic cells
DKK	Dickkopf-protein
DMSO	Dimethylsulfoxid
dNTP	Desoxyribonukleosidtriphosphate
DTT	Dithiothreitol
Dvl	Dishevelled
EDTA	Ethylenediaminetetraacetic acid
ELISA	Enzyme-linked immunosorbent assay
EMT	Epithelial-mesenchymal transmission
ercDC	enriched in RCC Dendritic cells
FACS	Fluorescence activated cell scanning
FC	fold change
FcR	Fc-Receptor
FCS	Fetal calf serum
FDR	Formyl peptide receptor
FMI	Forward migration index
fMLP	N-Formylmethionyl-leucyl-phenylalanine
FOXP3	Forkhead box P3
FRAT	Frequently rearranged in advanced T-cell lymphomas
FSC	Forward scatter
Fzd	Frizzled-receptor

GM-CSF	Granulocyte-macrophage colony-stimulating factor
GPC	Glypican
GPI	Glycosylphosphatidylinositol
GSK	Glycogen synthase kinase
HEPES	4-(2-hydroxyethyl)-1-piperazineethanesulfonic acid
HIPK	Homeodomain interacting protein kinase
HLA	Humane leucocyte antigen
HRP	Horeseradish peroxidase
HS	Human serum
HSPG	Heparan sulphate proteoglycans
IFN	Interferon
Ig	Immunoglobuline
IL	Interleukin
IP3	Inositol-1,4,5-triphosphate
JNK	c-JUN N-terminal kinase
LAMP	Lysosomal associated membrane protein
LEF	Lymphoid enhancer binding factor
LPS	Lipopolysaccharid
LRP	Lipoprotein receptor-related protein
M	Molar
M-CSF	Macrophage colony-stimulating factor
MA	Migration assay
MACS	Magnetic activated cell sorting
MADMAX	Management and Analysis Database for Multi-platform microArray eXperiments
MDSC	Myeloid-derived suppressor cells
mg	Milligram
MHC	Major histocompatility complexes
min	Minutes
ml	Milliliter
mm	Millimeter
mM	Millimole
MMP	Matrix metalloproteinase
MoDC	Monocyte-derived dendritic cell
MPS	Mononuclear phagocyte system
mRNA	messenger Ribonucleic acid
MUSK	Muscle-specific receptor tyrosine kinase
MΦ	Macrophage
NEAA	Non-essential amino acids
NFAT	Nuclear factor associated with T-cells
NFkB	Nuclear factor kappa-B
ng	nanogram
NK	Natural Killer cells
NLK	Nemo-like-kinase
NUSK	Neuronal specific kinase

PAMP	Pathogen associated molecular patterns
PBS	Phosphate buffered saline
PCP	Planar cell polarity
PCR	Polymerase chain reaction
PD1	Programmed death 1 receptor
pDC	plasmacytoid Dendritic cells
PDE	Phosphodiesterase
PFA	Paraformaledhyd
PGE	Prostaglandin E
pH	potentia hydrogenia
PI	Propidiumjodid
PKC	Proteinkinase C
PLCB	Phospholipase C beta
PLM	Probe level model
PRC	Pathogen recognition receptors
PTK	Protein tyrosine kinase
RCC	Renal Cell Carcinoma
RCC-26-CM	Renal cell carcinoma-26 conditioned medium
RHOA	Ras homolog familiy member A
Rhu	Recombinant human
RMA	Robust Multi-array Average
RNA	Ribonucleic acid
ROCK	Rho-associated, coiled-coil containing protein kinase
ROR	Receptor Tyr kinase-like orphan receptor
rpm	Rounds per minute
RPMI	Roswell Park Memorial Institute
RT	Room temperature
RYK	Receptor-like tyrosine kinase
SDC	Syndecan
sec	Seconds
SEM	Standard error of the mean
sFRP	soluble Frizzled related protein
slandDC	6-sulfo LacNAc dendritic cells
SSC	Sideward scatter
STAT	Signal transducer and activator of transcription
T-regs	Regulatory T-cells
TAM	Tumour-associated macrophages
TCF	Transcription factor
TCR	T-cell receptor
TGF	Transforming growth factor
TLR	Toll-like receptor
TNF	Tumour necrosis factor
Tris	Trishydroxamethylaminomethan
VANGL	VANGL planar cell polarity protein

VEGF	Vascular epithelial growth factor
WHO	World health organization
WIF	Wnt-inhibitor factor
WNT	Wingless-related integration site
µg	microgram
µl	microliter
µm	micrometer
µM	micromole

8 References

1. Znaor, A., et al., *International Variations and Trends in Renal Cell Carcinoma Incidence and Mortality.* European Urology, 2015. **67**(3): p. 519-530.

2. Fridman, W.H., et al., *The immune contexture in human tumours: impact on clinical outcome.* Nat Rev Cancer, 2012. **12**(4): p. 298-306.

3. Schendel, D.J., et al., *Cellular and molecular analyses of major histocompatibility complex (MHC) restricted and non-MHC-restricted effector cells recognizing renal cell carcinomas: problems and perspectives for immunotherapy.* J Mol Med (Berl), 1997. **75**(6): p. 400-13.

4. Liu, X.D., et al., *Resistance to Antiangiogenic Therapy Is Associated with an Immunosuppressive Tumor Microenvironment in Metastatic Renal Cell Carcinoma.* Cancer Immunol Res, 2015. **3**(9): p. 1017-29.

5. McDermott, D.F. and M.B. Atkins, *Immune Therapy for Kidney Cancer: A Second Dawn?* Seminars in Oncology, 2013. **40**(4): p. 492-498.

6. Rosenblatt, J. and D.F. McDermott, *Immunotherapy for renal cell carcinoma.* Hematol Oncol Clin North Am, 2011. **25**(4): p. 793-812.

7. Matsushita, H., et al., *A pilot study of autologous tumor lysate-loaded dendritic cell vaccination combined with sunitinib for metastatic renal cell carcinoma.* J Immunother Cancer, 2014. **2**: p. 30.

8. Schleypen, J.S., et al., *Cytotoxic markers and frequency predict functional capacity of natural killer cells infiltrating renal cell carcinoma.* Clin Cancer Res, 2006. **12**(3 Pt 1): p. 718-25.

9. Daurkin, I., et al., *Tumor-associated macrophages mediate immunosuppression in the renal cancer microenvironment by activating the 15-lipoxygenase-2 pathway.* Cancer Res, 2011. **71**(20): p. 6400-9.

10. Fridman, W.H., et al., *The immune contexture in human tumours: impact on clinical outcome.* Nat Rev Cancer, 2012. **12**(4): p. 298-306.

11. Gajewski, T.F., H. Schreiber, and Y.-X. Fu, *Innate and adaptive immune cells in the tumor microenvironment.* Nature immunology, 2013. **14**(10): p. 1014-1022.

12. Ostrand-Rosenberg, S., et al., *Cross-talk between myeloid-derived suppressor cells (MDSC), macrophages, and dendritic cells enhances tumor-induced immune suppression.* Semin Cancer Biol, 2012. **22**(4): p. 275-81.

13. Mosser, D.M. and J.P. Edwards, *Exploring the full spectrum of macrophage activation.* Nat Rev Immunol, 2008. **8**(12): p. 958-69.

14. Gautier, E.L., et al., *Gene expression profiles and transcriptional regulatory pathways underlying mouse tissue macrophage identity and diversity.* Nature immunology, 2012. **13**(11): p. 1118-1128.

15. Davies, L.C., et al., *Tissue-resident macrophages.* Nature immunology, 2013. **14**(10): p. 986-995.

16. Sica, A. and A. Mantovani, *Macrophage plasticity and polarization: in vivo veritas.* The Journal of Clinical Investigation, 2012. **122**(3): p. 787-795.

17. Lawrence, T. and G. Natoli, *Transcriptional regulation of macrophage polarization: enabling diversity with identity.* Nat Rev Immunol, 2011. **11**(11): p. 750-61.

18. Mantovani, A., et al., *Tumor-associated macrophages and the related myeloid-derived suppressor cells as a paradigm of the diversity of macrophage activation.* Hum Immunol, 2009. **70**(5): p. 325-30.

19. Banchereau, J. and R.M. Steinman, *Dendritic cells and the control of immunity.* Nature, 1998. **392**(6673): p. 245-52.

20. Collin, M., N. McGovern, and M. Haniffa, *Human dendritic cell subsets.* Immunology, 2013. **140**(1): p. 22-30.

21. Nizzoli, G., et al., *Human CD1c+ dendritic cells secrete high levels of IL-12 and potently prime cytotoxic T-cell responses.* Blood, 2013. **122**(6): p. 932-42.

22. McKenna, K., A.S. Beignon, and N. Bhardwaj, *Plasmacytoid dendritic cells: linking innate and adaptive immunity.* J Virol, 2005. **79**(1): p. 17-27.

23. Frankenberger, B., E. Noessner, and D.J. Schendel, *Immune suppression in renal cell carcinoma.* Semin Cancer Biol, 2007. **17**(4): p. 330-43.

24. Gigante, M., et al., *Dysfunctional DC subsets in RCC patients: ex vivo correction to yield an effective anti-cancer vaccine.* Mol Immunol, 2009. **46**(5): p. 893-901.

25. Movassagh, M., et al., *Selective accumulation of mature DC-Lamp+ dendritic cells in tumor sites is associated with efficient T-cell-mediated antitumor response and control of metastatic dissemination in melanoma.* Cancer Res, 2004. **64**(6): p. 2192-8.

26. Figel, A.M., et al., *Human renal cell carcinoma induces a dendritic cell subset that uses T-cell crosstalk for tumor-permissive milieu alterations.* Am J Pathol, 2011. **179**(1): p. 436-51.

27. Chuang, M.J., et al., *Tumor-derived tumor necrosis factor-alpha promotes progression and epithelial-mesenchymal transition in renal cell carcinoma cells.* Cancer Sci, 2008. **99**(5): p. 905-13.

28. Schreiber, T.H., et al., *Tumor-induced suppression of CTL expansion and subjugation by gp96-Ig vaccination.* Cancer Res, 2009. **69**(5): p. 2026-33.

29. Figel, A.-M., et al., *Human Renal Cell Carcinoma Induces a Dendritic Cell Subset That Uses T-Cell Crosstalk for Tumor-Permissive Milieu Alterations.* The American Journal of Pathology, 2011. **179**(1): p. 436-451.

30. Logan, C.Y. and R. Nusse, *The Wnt signaling pathway in development and disease.* Annu Rev Cell Dev Biol, 2004. **20**: p. 781-810.

31. van Amerongen, R., A. Mikels, and R. Nusse, *Alternative wnt signaling is initiated by distinct receptors.* Sci Signal, 2008. **1**(35): p. re9.

32. He, X., et al., *LDL receptor-related proteins 5 and 6 in Wnt/beta-catenin signaling: arrows point the way.* Development, 2004. **131**(8): p. 1663-77.

33. Fradkin, L.G., J.M. Dura, and J.N. Noordermeer, *Ryks: new partners for Wnts in the developing and regenerating nervous system.* Trends Neurosci, 2010. **33**(2): p. 84-92.

34. Peradziryi, H., N.S. Tolwinski, and A. Borchers, *The many roles of PTK7: a versatile regulator of cell-cell communication.* Arch Biochem Biophys, 2012. **524**(1): p. 71-6.

35. Minami, Y., et al., *Ror-family receptor tyrosine kinases in noncanonical Wnt signaling: their implications in developmental morphogenesis and human diseases.* Dev Dyn, 2010. **239**(1): p. 1-15.

36. Yoshioka, T., et al., *Vangl2, the planar cell polarity protein, is complexed with postsynaptic density protein PSD-95 [corrected].* FEBS Lett, 2013. **587**(10): p. 1453-9.

37. Niehrs, C., *The complex world of WNT receptor signalling.* Nat Rev Mol Cell Biol, 2012. **13**(12): p. 767-79.

38. Koval, A., et al., *Yellow submarine of the Wnt/Frizzled signaling: submerging from the G protein harbor to the targets.* Biochem Pharmacol, 2011. **82**(10): p. 1311-9.

39. Saldanha, J., J. Singh, and D. Mahadevan, *Identification of a Frizzled-like cysteine rich domain in the extracellular region of developmental receptor tyrosine kinases.* Protein Sci, 1998. **7**(8): p. 1632-5.

40. Hayes, M., et al., *Ptk7 promotes non-canonical Wnt/PCP-mediated morphogenesis and inhibits Wnt/beta-catenin-dependent cell fate decisions during vertebrate development.* Development, 2013. **140**(8): p. 1807-18.

41. Dijksterhuis, J.P., et al., *Systematic mapping of WNT-FZD protein interactions reveals functional selectivity by distinct WNT-FZD pairs.* J Biol Chem, 2015. **290**(11): p. 6789-98.

42. Bilic, J., et al., *Wnt induces LRP6 signalosomes and promotes dishevelled-dependent LRP6 phosphorylation.* Science, 2007. **316**(5831): p. 1619-22.

43. Kimelman, D. and W. Xu, *beta-catenin destruction complex: insights and questions from a structural perspective.* Oncogene, 2006. **25**(57): p. 7482-91.

44. MacDonald, B.T., K. Tamai, and X. He, *Wnt/beta-catenin signaling: components, mechanisms, and diseases.* Dev Cell, 2009. **17**(1): p. 9-26.

45. Goggolidou, P., *Wnt and planar cell polarity signaling in cystic renal disease.* Organogenesis, 2014. **10**(1): p. 86-95.

46. Sebbagh, M. and J.P. Borg, *Insight into planar cell polarity.* Exp Cell Res, 2014. **328**(2): p. 284-95.

47. Babayeva, S., Y. Zilber, and E. Torban, *Planar cell polarity pathway regulates actin rearrangement, cell shape, motility, and nephrin distribution in podocytes.* Am J Physiol Renal Physiol, 2011. **300**(2): p. F549-60.

48. Li, S., et al., *Rack1 is required for Vangl2 membrane localization and planar cell polarity signaling while attenuating canonical Wnt activity.* Proc Natl Acad Sci U S A, 2011. **108**(6): p. 2264-9.

49. Gao, B., et al., *Wnt signaling gradients establish planar cell polarity by inducing Vangl2 phosphorylation through Ror2.* Dev Cell, 2011. **20**(2): p. 163-76.

50. Veeman, M.T., J.D. Axelrod, and R.T. Moon, *A second canon. Functions and mechanisms of beta-catenin-independent Wnt signaling.* Dev Cell, 2003. **5**(3): p. 367-77.

51. Vivancos, V., et al., *Wnt activity guides facial branchiomotor neuron migration, and involves the PCP pathway and JNK and ROCK kinases.* Neural Dev, 2009. **4**: p. 7.

52. De, A., *Wnt/Ca2+ signaling pathway: a brief overview.* Acta Biochim Biophys Sin (Shanghai), 2011. **43**(10): p. 745-56.

53. Schulz, R.A. and K.E. Yutzey, *Calcineurin signaling and NFAT activation in cardiovascular and skeletal muscle development.* Dev Biol, 2004. **266**(1): p. 1-16.

54. Ishitani, T., et al., *The TAK1-NLK mitogen-activated protein kinase cascade functions in the Wnt-5a/Ca(2+) pathway to antagonize Wnt/beta-catenin signaling.* Mol Cell Biol, 2003. **23**(1): p. 131-9.

55. Wang, H., Y. Lee, and C.C. Malbon, *PDE6 is an effector for the Wnt/Ca2+/cGMP-signalling pathway in development.* Biochem Soc Trans, 2004. **32**(Pt 5): p. 792-6.

56. Ma, J., et al., *Downregulation of Wnt signaling by sonic hedgehog activation promotes repopulation of human tumor cell lines.* Dis Model Mech, 2015. **8**(4): p. 385-91.

57. Kestler, H.A. and M. Kuhl, *From individual Wnt pathways towards a Wnt signalling network.* Philos Trans R Soc Lond B Biol Sci, 2008. **363**(1495): p. 1333-47.

58. Grumolato, L., et al., *Canonical and noncanonical Wnts use a common mechanism to activate completely unrelated coreceptors.* Genes Dev, 2010. **24**(22): p. 2517-30.

59. Mikels, A.J. and R. Nusse, *Purified Wnt5a protein activates or inhibits beta-catenin-TCF signaling depending on receptor context.* PLoS Biol, 2006. **4**(4): p. e115.

60. Topol, L., et al., *Wnt-5a inhibits the canonical Wnt pathway by promoting GSK-3-independent beta-catenin degradation.* J Cell Biol, 2003. **162**(5): p. 899-908.

61. Thrasivoulou, C., M. Millar, and A. Ahmed, *Activation of intracellular calcium by multiple Wnt ligands and translocation of beta-catenin into the nucleus: a convergent model of Wnt/Ca2+ and Wnt/beta-catenin pathways.* J Biol Chem, 2013. **288**(50): p. 35651-9.

62. Liao, G., et al., *Jun NH2-terminal kinase (JNK) prevents nuclear beta-catenin accumulation and regulates axis formation in Xenopus embryos.* Proc Natl Acad Sci U S A, 2006. **103**(44): p. 16313-8.

63. Krupnik, V.E., et al., *Functional and structural diversity of the human Dickkopf gene family.* Gene, 1999. **238**(2): p. 301-13.

64. Nakamura, R.E. and A.S. Hackam, *Analysis of Dickkopf3 interactions with Wnt signaling receptors.* Growth Factors, 2010. **28**(4): p. 232-42.

65. Cselenyi, C.S. and E. Lee, *Context-dependent activation or inhibition of Wnt-beta-catenin signaling by Kremen.* Sci Signal, 2008. **1**(8): p. pe10.

66. Mii, Y. and M. Taira, *Secreted Frizzled-related proteins enhance the diffusion of Wnt ligands and expand their signalling range.* Development, 2009. **136**(24): p. 4083-8.

67. von Marschall, Z. and L.W. Fisher, *Secreted Frizzled-related protein-2 (sFRP2) augments canonical Wnt3a-induced signaling.* Biochem Biophys Res Commun, 2010. **400**(3): p. 299-304.

68. Yamamoto, S., et al., *Cthrc1 selectively activates the planar cell polarity pathway of Wnt signaling by stabilizing the Wnt-receptor complex.* Dev Cell, 2008. **15**(1): p. 23-36.

69. Ohkawara, B., A. Glinka, and C. Niehrs, *Rspo3 binds syndecan 4 and induces Wnt/PCP signaling via clathrin-mediated endocytosis to promote morphogenesis.* Dev Cell, 2011. **20**(3): p. 303-14.

70. Pataki, C.A., J.R. Couchman, and J. Brabek, *Wnt Signaling Cascades and the Roles of Syndecan Proteoglycans.* J Histochem Cytochem, 2015. **63**(7): p. 465-80.

71. Maruschke, M., et al., *Expression profiling of metastatic renal cell carcinoma using gene set enrichment analysis.* Int J Urol, 2014. **21**(1): p. 46-51.

72. Jonuleit, H., et al., *Pro-inflammatory cytokines and prostaglandins induce maturation of potent immunostimulatory dendritic cells under fetal calf serum-free conditions.* Eur J Immunol, 1997. **27**(12): p. 3135-42.

73. Mailliard, R.B., et al., *alpha-type-1 polarized dendritic cells: a novel immunization tool with optimized CTL-inducing activity.* Cancer Res, 2004. **64**(17): p. 5934-7.

74. Cyster, J.G., *Chemokines and cell migration in secondary lymphoid organs.* Science, 1999. **286**(5447): p. 2098-102.

75. Irizarry, R.A., et al., *Exploration, normalization, and summaries of high density oligonucleotide array probe level data.* Biostatistics, 2003. **4**(2): p. 249-64.

76. Dai, M., et al., *Evolving gene/transcript definitions significantly alter the interpretation of GeneChip data.* Nucleic Acids Res, 2005. **33**(20): p. e175.

77. Lin, K., et al., *MADMAX - Management and analysis database for multiple ~omics experiments.* J Integr Bioinform, 2011. **8**(2): p. 160.

78. Ke, J., et al., *Structure and function of Norrin in assembly and activation of a Frizzled 4-Lrp5/6 complex.* Genes Dev, 2013. **27**(21): p. 2305-19.

79. Kikuchi, A., et al., *Wnt5a: its signalling, functions and implication in diseases.* Acta Physiol (Oxf), 2012. **204**(1): p. 17-33.

80. Henry, C.J., et al., *IL-12 produced by dendritic cells augments CD8+ T cell activation through the production of the chemokines CCL1 and CCL17.* J Immunol, 2008. **181**(12): p. 8576-84.

81. Heufler, C., et al., *Interleukin-12 is produced by dendritic cells and mediates T helper 1 development as well as interferon-gamma production by T helper 1 cells.* Eur J Immunol, 1996. **26**(3): p. 659-68.

82. Koch, F., et al., *High level IL-12 production by murine dendritic cells: upregulation via MHC class II and CD40 molecules and downregulation by IL-4 and IL-10.* J Exp Med, 1996. **184**(2): p. 741-6.

83. Fu, C., et al., *beta-Catenin in dendritic cells exerts opposite functions in cross-priming and maintenance of CD8+ T cells through regulation of IL-10.* Proc Natl Acad Sci U S A, 2015. **112**(9): p. 2823-8.

84. Ho, M.Y., et al., *TNF-alpha induces epithelial-mesenchymal transition of renal cell carcinoma cells via a GSK3beta-dependent mechanism.* Mol Cancer Res, 2012. **10**(8): p. 1109-19.

85. Murphy, P.M., *The molecular biology of leukocyte chemoattractant receptors.* Annu Rev Immunol, 1994. **12**: p. 593-633.

86. Yang, D., et al., *Differential regulation of responsiveness to fMLP and C5a upon dendritic cell maturation: correlation with receptor expression.* J Immunol, 2000. **165**(5): p. 2694-702.

87. Webster, W.S., et al., *Mononuclear cell infiltration in clear-cell renal cell carcinoma independently predicts patient survival.* Cancer, 2006. **107**(1): p. 46-53.

88. Schleypen, J.S., et al., *Cytotoxic Markers and Frequency Predict Functional Capacity of Natural Killer Cells Infiltrating Renal Cell Carcinoma.* Clinical Cancer Research, 2006. **12**(3): p. 718-725.

89. Riemann, D., et al., *Granulocyte-to-dendritic cell-ratio as marker for the immune monitoring in patients with renal cell carcinoma.* Clinical and Translational Medicine, 2014. **3**(1): p. 1-6.

90. Toma, M., et al., *Accumulation of tolerogenic human 6-sulfo LacNAc dendritic cells in renal cell carcinoma is associated with poor prognosis.* OncoImmunology, 2015. **4**(6): p. e1008342.

91. Figel, A.-M., et al., *Human Renal Cell Carcinoma Induces a Dendritic Cell Subset That Uses T-Cell Crosstalk for Tumor-Permissive Milieu Alterations.* The American Journal of Pathology. **179**(1): p. 436-451.

92. Arai, E., et al., *Multilayer-omics analysis of renal cell carcinoma, including the whole exome, methylome and transcriptome.* Int J Cancer, 2014. **135**(6): p. 1330-42.

93. Shiina, H., et al., *The human T-cell factor-4 gene splicing isoforms, Wnt signal pathway, and apoptosis in renal cell carcinoma.* Clin Cancer Res, 2003. **9**(6): p. 2121-32.

94. Kruck, S., et al., *Impact of an altered Wnt1/beta-catenin expression on clinicopathology and prognosis in clear cell renal cell carcinoma.* Int J Mol Sci, 2013. **14**(6): p. 10944-57.

95. Xu, Q., et al., *Wnt Signaling in Renal Cell Carcinoma.* Cancers, 2016. **8**(6): p. 57.

96. Wen, J.L., et al., *UBE3C Promotes Growth and Metastasis of Renal Cell Carcinoma via Activating Wnt/β-Catenin Pathway.* PLoS ONE, 2015. **10**(2): p. e0115622.

97. Majid, S., S. Saini, and R. Dahiya, *Wnt signaling pathways in urological cancers: past decades and still growing.* Mol Cancer, 2012. **11**: p. 7.

98. Ueno, K., et al., *Wnt antagonist DICKKOPF-3 (Dkk-3) induces apoptosis in human renal cell carcinoma.* Mol Carcinog, 2011. **50**(6): p. 449-57.

99. Kawakami, K., et al., *Functional significance of Wnt inhibitory factor-1 gene in kidney cancer.* Cancer Res, 2009. **69**(22): p. 8603-10.

100. Castillo, L.F., et al., *Glypican-3 induces a mesenchymal to epithelial transition in human breast cancer cells.* Oncotarget, 2016.

101. Capurro, M., et al., *Glypican-3 binds to Frizzled and plays a direct role in the stimulation of canonical Wnt signaling.* J Cell Sci, 2014. **127**(Pt 7): p. 1565-75.

102. Gao, W., H. Kim, and M. Ho, *Human Monoclonal Antibody Targeting the Heparan Sulfate Chains of Glypican-3 Inhibits HGF-Mediated Migration and Motility of Hepatocellular Carcinoma Cells.* PLoS ONE, 2015. **10**(9): p. e0137664.

103. Li, Y. and P. Yang, *GPC5 Gene and Its Related Pathways in Lung Cancer.* Journal of thoracic oncology : official publication of the International Association for the Study of Lung Cancer, 2011. **6**(1): p. 2-5.

104. Lim, H.C. and J.R. Couchman, *Syndecan-2 regulation of morphology in breast carcinoma cells is dependent on RhoGTPases.* Biochim Biophys Acta, 2014. **1840**(8): p. 2482-90.

105. O'Connell, M.P., et al., *Heparan sulfate proteoglycan modulation of Wnt5A signal transduction in metastatic melanoma cells.* J Biol Chem, 2009. **284**(42): p. 28704-12.

106. Strate, I., F. Tessadori, and J. Bakkers, *Glypican4 promotes cardiac specification and differentiation by attenuating canonical Wnt and Bmp signaling.* Development, 2015. **142**(10): p. 1767-76.

107. Sakane, H., et al., *Localization of glypican-4 in different membrane microdomains is involved in the regulation of Wnt signaling.* J Cell Sci, 2012. **125**(Pt 2): p. 449-60.

108. Lehtonen, A., et al., *Gene expression profiling during differentiation of human monocytes to macrophages or dendritic cells.* J Leukoc Biol, 2007. **82**(3): p. 710-20.

109. Bergenfelz, C., et al., *Wnt5a inhibits human monocyte-derived myeloid dendritic cell generation.* Scand J Immunol, 2013. **78**(2): p. 194-204.

110. Oderup, C., M. LaJevic, and E.C. Butcher, *Canonical and noncanonical Wnt proteins program dendritic cell responses for tolerance.* J Immunol, 2013. **190**(12): p. 6126-34.

111. Holtzhausen, A., et al., *Melanoma-Derived Wnt5a Promotes Local Dendritic-Cell Expression of IDO and Immunotolerance: Opportunities for Pharmacologic Enhancement of Immunotherapy.* Cancer Immunol Res, 2015. **3**(9): p. 1082-95.

112. Jiang, A., et al., *Disruption of E-cadherin-mediated adhesion induces a functionally distinct pathway of dendritic cell maturation.* Immunity, 2007. **27**(4): p. 610-24.

113. Valencia, J., et al., *Wnt5a skews dendritic cell differentiation to an unconventional phenotype with tolerogenic features.* J Immunol, 2011. **187**(8): p. 4129-39.

114. Valencia, J., et al., *Wnt5a signaling increases IL-12 secretion by human dendritic cells and enhances IFN-gamma production by CD4+ T cells.* Immunol Lett, 2014. **162**(1 Pt A): p. 188-99.

115. Chorny, A., E. Gonzalez-Rey, and M. Delgado, *Regulation of dendritic cell differentiation by vasoactive intestinal peptide: therapeutic applications on autoimmunity and transplantation.* Ann N Y Acad Sci, 2006. **1088**: p. 187-94.

116. Sallusto, F. and A. Lanzavecchia, *Efficient presentation of soluble antigen by cultured human dendritic cells is maintained by granulocyte/macrophage colony-stimulating factor plus interleukin 4 and downregulated by tumor necrosis factor alpha.* The Journal of Experimental Medicine, 1994. **179**(4): p. 1109-1118.

117. Jeras, M., M. Bergant, and U. Repnik, *In vitro preparation and functional assessment of human monocyte-derived dendritic cells—potential antigen-specific modulators of in vivo immune responses.* Transplant Immunology, 2005. **14**(3–4): p. 231-244.

118. Royer, P.J., et al., *Culture medium and protein supplementation in the generation and maturation of dendritic cells.* Scand J Immunol, 2006. **63**(6): p. 401-9.

9 Supplementary data

9.1 Supplementary table 1: Microarray data of in vitro generated myeloid cells

Supplementary table 1 displays the microarray data of the in vitro generated myeloid cells. It displays calculated Fold changes (FC) of cDC, ercDC, M1, M2 and GMCSF-macrophages compared to monocytes for the canonical and non-canonical Wnt-pathways. Genes are represented by gene-IDs and official gene-symbols. The green colour indicates an up regulation compared to monocytes with an FC of >1.5. The red colour a down regulation with a FC of <-1.5.

Gene:	Entrez-ID:	FC: cDC/Mono	FC: M2/Mono	FC: M1/Mono	FC: GMCSF/Mono	FC: ercDC/Mono
Wnt-ligands						
Wnt 1	7471	1.0478	1.1137	-1.0599	-1.0485	1.0120
Wnt 2	7472	-1.1159	-1.1643	1.0786	-1.0346	-1.1793
Wnt 2b	7482	1.2493	1.3829	1.8945	1.6519	1.5486
Wnt3	7473	-1.0657	-1.0621	-1.2824	-1.1541	-1.0118
Wnt 3a	89780	-1.0484	1.0263	-1.1117	-1.0742	1.0057
Wnt 4	54361	-1.0149	-1.0366	1.0241	1.0444	1.0382
Wnt 5a	7474	5.0499	1.3656	1.2981	-1.0402	-1.0651
Wnt 5b	81029	1.2944	1.1507	-1.0462	-1.1872	-1.0099
Wnt 6	7475	-1.0217	-1.0908	1.0183	1.0577	1.0700
Wnt 7a	7476	-1.0942	-1.1713	1.0001	-1.1834	-1.0997
Wnt 7b	7477	-1.1037	1.0378	-1.0600	-1.0944	-1.1809
Wnt 8a	7478	1.0791	1.2026	1.0383	1.1184	1.0286
Wnt 8b	7479	-1.1196	-1.2019	-1.1273	-1.1105	-1.1273
Wnt 9a	7483	-1.0643	-1.0670	-1.0760	1.0467	-1.0709
Wnt 9b	7484	-1.0681	1.0270	-1.1525	-1.0818	-1.0741
Wnt 10a	80326	-1.1058	1.0172	-1.0888	-1.0502	1.0937
Wnt 10b	7480	-1.1798	-1.1405	1.0292	-1.2164	-1.0193
Wnt 11	7481	1.0567	1.0421	-1.0120	1.0235	-1.0042
Receptors						
Fzd1	8321	-1.1940	-1.0202	1.1876	-1.5238	1.0084
Fzd2	2535	1.0362	-1.1441	-1.1968	-1.2572	-1.1570
Fzd3	7976	1.6825	1.2213	-1.0577	-1.0286	-1.0129
Fzd4	8322	-1.0758	-1.1363	1.0001	-1.0596	1.0678
Fzd5	7855	1.6328	1.6570	2.3540	1.3563	1.5308
fzd6	8323	-1.1244	-1.0507	1.1862	-1.1625	1.0726
Fzd7	8324	1.2094	1.1684	-1.0433	1.6801	1.0872
Fzd8	8325	-1.1847	-1.0675	1.1257	-1.1052	-1.0865
Fzd9	8326	-1.1324	-1.0036	-1.1307	-1.2065	-1.1476
Fzd10	11211	-1.0362	-1.0641	-1.1107	-1.0839	-1.0057
Co-receptors						
LRP5	4041	1.0425	1.0545	1.0456	-1.1117	-1.0982
LRP6	4040	1.0442	-1.1025	1.2047	-1.0164	-1.1069
LRP1	4035	1.0983	1.1279	-4.4389	1.2263	1.1907
Kremen 1	83999	-1.0562	-1.2954	1.3496	1.1663	-1.1561
Kremen 2	79412	-1.1588	-1.0619	-1.1339	-1.2653	-1.0823
RYK	6259	1.5829	1.1947	1.0334	1.2196	1.0210
ROR1	4919	1.2579	1.1067	-1.0999	1.0407	1.1640
ROR2	4920	1.0097	1.0564	1.1123	1.0182	1.1341
VANGL1	81839	-1.0065	-1.0374	-1.0785	1.0427	1.0967
VANGL2	57216	-1.1272	-1.1182	-1.1037	-1.0352	-1.0528
CELSR1	9620	1.3749	1.6053	1.0304	1.6621	1.8117
CELSR2	1952	-1.0571	-1.1768	-1.3285	-1.2005	-1.1994
CELSR3	1951	-1.0029	-1.0239	-1.0833	1.0057	1.0126
PTK7	5754	-1.1457	-1.0947	-1.0110	-1.0483	-1.0982
SDC1	6382	-1.1248	-1.0977	1.0042	1.0102	-1.0464
SDC2	6383	26.8547	25.5374	6.6457	17.9097	9.5164
SDC3	9672	2.3762	2.6069	1.4328	1.4247	2.7031
SDC4	6385	6.4081	10.8838	11.2835	9.3504	7.7408
GPC2	221914	-1.1221	-1.0885	-1.0545	-1.0461	-1.1324
GPC3	2719	-1.0980	-1.0464	1.1636	1.0768	-1.0608
GPC4	2239	5.7710	4.9093	8.9275	7.3588	6.9322
GPC5	2262	1.0140	1.0747	1.5207	1.1036	1.1229
GPC6	10082	-1.1176	-1.1559	-1.1314	-1.0030	-1.1989

GPC1	2817	-1.0188	-1.0845	-1.3223	-1.0810	-1.1129
CD44	960	1.1727	1.0178	1.2675	1.2640	-1.1106
Inhibitors						
Dkk1	22943	-1.2269	-1.1954	-1.1426	-1.0695	-1.2161
Dkk2	27123	-1.1293	1.4759	-1.0151	-1.0348	-1.1505
Dkk3	27122	-1.1490	-1.1092	1.0491	-1.0099	-1.0352
Dkk4	27121	-1.0170	-1.1018	1.1006	1.0211	-1.0639
WIF1	11197	-1.1668	-1.0380	1.0095	1.0290	-1.0021
sFRP1	6422	-1.1427	-1.0632	1.0010	1.0126	-1.2376
sFRP2	6423	-1.0946	1.0135	-1.1346	1.0345	-1.0707
sFRP3	2487	-1.1410	-1.1193	1.0137	1.0502	-1.1478
sFRP4	6424	1.1390	1.2671	1.0846	1.0664	1.1427
sFRP5	6425	1.0184	-1.0106	-1.0684	-1.0486	1.0179
Shisa2	387914	-1.3154	-1.1454	-1.3957	-1.2841	-1.2513
Shisa3	152573	1.0578	1.0007	1.2062	-1.0021	1.1512
CTHRC1	115908	-1.0945	-1.1229	1.0315	-1.1654	1.0169
IGFBP1	3484	-1.1135	-1.0935	1.1107	-1.0644	1.0712
IGFBP2	3485	2.0006	1.2833	1.0485	2.5624	1.1074
IGFBP4	3487	1.0751	1.2708	27.7678	-1.0669	1.4595
IGFBP6	3489	1.2435	-1.0573	1.0969	-1.0126	1.0371
CER1	9350	-1.2912	-1.1755	1.0267	1.0636	-1.1883
SOST	50964	-1.1291	-1.0781	-1.1195	-1.1004	-1.1172
SOSTDC1	25928	-1.1406	-1.2441	-1.0490	-1.1310	-1.0812
TPBG	7162	-1.1712	-1.0196	-1.0649	1.0571	1.0392
APCDD1	147495	-1.7306	-1.8358	-1.6678	-2.0023	-1.9006
TRABD2A	129293	3.7015	-1.0753	-1.0146	1.4683	1.0429
agonists/ positive modulators						
NDP	4693	2.6809	1.1334	1.6308	1.3193	1.1137
RSPO1	284654	-1.0356	1.0406	1.0656	-1.0297	-1.0627
RSPO2	340419	-1.0377	-1.0174	-1.1584	-1.1436	-1.0729
RSPO3	84870	-1.2312	-1.0773	-1.0881	1.0941	-1.0633
RSPO4	343637	-1.2118	-1.2918	-1.2725	-1.1669	-1.2664
ß-Catenin dependent signalling						
Dvl1	1855	-1.0077	-1.0212	-1.1000	-1.0158	-1.0566
Dvl2	1856	1.1384	1.1115	1.0360	1.4196	1.2250
Dvl3	1857	1.0678	1.0474	1.2670	1.0842	1.1509
GSK3ß	2932	-1.1435	-1.2545	-1.0061	-1.0254	-1.0594
Axin 1	8312	-1.0020	1.1640	1.0146	1.1054	-1.1066
Axin 2	8313	-1.1370	1.0114	-1.1245	1.0421	-1.1323
APC	324	-1.0674	-1.4986	-1.2794	-1.0184	-1.1618
CSNK1A1	1452	-1.0028	-1.0073	-1.2442	-1.1706	-1.2162
CSNK1E	1454	1.8168	2.2686	-1.0147	1.9968	1.4481
CSNK1D	1453	-1.3106	-1.1585	-1.1473	-1.0886	-1.2703
CSNK2A1	1457	1.7151	1.4747	1.1542	1.4473	-1.0620
CSNK2A2	1459	1.3787	1.4801	1.1321	1.5653	1.1586
CSNK2B	1460	1.5749	1.5673	-1.1649	1.2529	1.0740
CTNNB1	1499	1.0325	1.3101	2.1273	-1.0417	1.1365
CTNNBIP1	56998	-1.2974	-1.2827	-1.4591	-1.3467	-1.0918
NDRG1	10397	1.2263	-1.0287	1.0248	2.3875	1.3126
NDRG2	57447	3.2720	-1.2540	-1.4075	1.2947	-1.3170
FRAT1	10023	-2.0934	-4.2753	-4.8864	-1.9421	-2.5590
FRAT2	23401	-1.0051	-1.8382	-2.4926	1.0518	-1.5536
PAK4	10298	-1.0559	-1.0419	1.0545	-1.0362	-1.0467
AKT1	207	1.0727	1.0076	-1.2579	-1.2273	1.0050
AKT2	208	-1.0234	-1.0023	1.2957	-1.0031	-1.0020
AKT3	10000	-1.0556	1.2061	2.7455	2.1395	1.7693
ILK	3611	-1.3309	-1.2260	1.1650	-1.4029	-1.0632
CXXC4	80319	-1.0795	-1.0460	-1.1647	-1.0098	-1.1332
SUMO1	7341	1.2422	1.0634	1.0334	-1.0801	1.0897
RANBP2	5903	1.1914	1.4217	-1.0105	1.0314	-1.0073
SENP2	59343	-1.2144	-1.3138	-1.0094	1.0007	-1.4116
BTRC	8945	1.5230	1.1182	1.0634	1.3534	1.0955
SKP1	6500	1.0463	-1.1129	-1.0360	1.0865	-1.1832
CUL1	8454	1.0682	1.1666	3.5811	1.2519	-1.2846
NKD1	85407	-1.0889	-1.0214	1.1297	-1.0088	-1.0119
ARRB1	408	-1.5309	-1.5627	-1.0906	-1.6392	-1.2186
ARRB2	409	-1.8236	-1.3505	-1.9410	-1.7086	-1.2804
MACF1	23499	1.0032	1.4368	3.1303	-1.4268	1.4177
PPP1CA	5499	-1.0971	-1.2032	-1.6766	-1.2980	-1.0472

PPP1CB	5500	-1.3857	-1.2836	-1.1046	-1.4058	-1.4033
PPP1CC	5501	1.0556	-1.0985	-1.5390	1.2284	-1.0003
PPP2R5B	5526	-1.4492	-1.5188	1.0017	-1.2962	-1.2832
PPP2CB	5516	1.1577	1.4632	1.9676	1.2064	1.3461
PPP2CA	5515	-1.3256	-1.1105	-1.1280	-1.3437	-1.3523
PPP3CB	5532	-1.1929	-1.1702	-1.2772	-1.0798	-1.0620
DAB2	1601	6.8342	8.9126	3.3473	8.9411	11.2741
TCF1	6927	1.0999	1.0152	-1.0610	-1.0259	1.0979
TCF3	6929	1.1808	1.2276	-1.3194	1.0366	1.0088
TCF4	6925	2.0252	2.7192	5.1342	-1.8166	2.1165
LEF1	51176	-1.1706	-1.2622	-1.1247	-1.0747	1.4940
TCF7L1	83439	-1.1656	-1.1750	1.2834	-1.0844	-1.1102
TCF7L2	6934	-5.6145	-5.3457	-4.0381	1.9644	-2.7601
TLE1	7088	4.2189	3.5446	1.3227	1.6946	1.2847
TLE2	7089	-1.1592	1.0052	-1.2013	1.0606	-1.0114
TLE3	7090	-1.7896	-1.2458	-5.6279	-1.4681	-1.0852
TLE4	7091	-1.9182	-1.7843	-1.8317	-1.7156	-2.0216
CDX1	1044	-1.2265	-1.1330	-1.2034	-1.1406	-1.0821
BCL9	607	1.2041	1.1923	-1.4637	-1.1155	-1.2702
PIAS4	51588	-1.1180	-1.1361	-1.1656	1.0687	-1.1316
FHL2	2274	-1.1385	-1.0177	-1.0116	-1.0242	-1.1351
TAX1BP3	30851	1.1900	1.1222	-1.1825	1.0423	1.0370
SALL1	6299	-1.0629	1.0353	-1.1064	-1.0805	-1.1476
SALL4	57167	-1.0078	-1.0791	-1.0304	-1.0509	-1.0910
MAP1B	4131	-1.0230	1.0534	1.0761	-1.0505	1.0295
PCP signalling						
ANKRD6	22881	1.3379	1.2828	1.1069	1.4564	1.6408
DAAM1	23002	2.0291	1.2277	-2.4222	-1.6253	-1.2703
DAAM2	23500	-1.1115	-1.1538	-1.0051	-1.0658	-1.0630
RHO A	387	-1.0749	-1.1261	-1.2114	-1.2304	-1.1508
RHO B	388	-1.9047	-2.0169	-2.8387	-1.5755	-1.4729
ROCK1	6093	-1.3520	-1.4745	-1.7087	-1.3189	-1.5281
ROCK2	9475	1.2736	1.0840	1.0213	1.0924	-1.1808
RAC1	5879	-1.0341	-1.1305	1.4357	1.1597	1.0920
RAC2	5880	1.1084	-1.4144	-6.7489	-1.0065	-1.3686
RAC3	5881	-1.0337	-1.0597	-1.0107	-1.0068	-1.1778
MAP2K7	5609	-1.3565	-1.1139	-1.0733	-1.0140	-1.3529
MAP2K4	6416	1.1980	1.0955	1.3847	1.0420	-1.0306
MAP3K4	4216	1.0504	-1.1367	-1.7921	-1.0399	-1.3015
MAPK8	5599	-1.5394	-1.1032	-1.2819	-1.2300	-1.1249
MAPK9	5601	1.4818	1.1390	-1.1602	1.0375	1.1043
MAPK10	5602	-1.1782	-1.0914	-1.0572	-1.1085	-1.0427
JUN	3725	1.0972	1.5890	1.3903	1.4314	-1.0270
ATF2	1386	1.0705	1.1227	1.2299	-1.0230	1.2329
CDC42	998	-1.6011	-1.4475	-1.2920	-1.3913	-1.4254
MARK2	2011	-1.5442	-1.7883	-1.7048	-1.7351	-1.8013
Ca-Signalling						
PLCB1	23236	-6.1276	-7.2183	-8.6383	-9.5319	-8.8037
PLCB2	5330	-1.3916	-1.7778	-15.9277	-2.8603	-1.7213
PLCB3	5331	-1.2168	1.0497	-1.1470	-1.2337	-1.1461
PLCB4	5332	-1.1066	-1.1022	1.0774	-1.0391	-1.0927
PLCG1	5335	1.4294	1.0326	1.0172	1.0453	1.2639
PLCG2	5336	-1.1341	-1.6673	-2.1837	-1.4115	-1.2078
PLCD1	5333	1.4100	1.1912	-1.0767	2.0738	1.3305
PLCD3	113026	-1.0531	-1.0058	-1.1065	-1.0824	-1.1213
PLCD4	84812	-1.2495	-1.0002	-1.0473	-1.0208	-1.0271
PLCE1	51196	1.1222	1.1445	1.0809	1.1054	1.1868
PRKCA	5578	3.3514	1.6840	-1.6743	1.3901	1.8637
PRKCB	5579	-3.2992	-4.1438	-6.1427	-3.6640	-1.9495
PRKCG	5582	-1.1439	-1.1418	-1.1841	-1.0150	-1.0262
CAMK1	8536	1.6321	1.0665	-3.3369	-1.3655	1.1039
CAMK1D	57118	1.6759	1.4681	-3.3233	-1.4166	1.3677
CAMK1G	57172	-1.0030	1.0487	3.4686	-1.0618	1.1956
CAMK2A	815	-1.2510	-1.3186	-1.0654	-1.2583	-1.2725
CAMK2B	816	-1.2008	-1.0613	1.0337	-1.0812	-1.0314
CAMK2G	818	-1.5428	-1.9162	-2.6514	-1.6674	-1.4086
CAMK2D	817	1.3780	-1.8171	-1.0562	-1.4306	-1.3717
CAMK4	814	1.1173	-1.0041	1.0244	1.0170	1.4807
PPP3CA	5530	-1.0679	-1.1391	-4.4206	-1.0901	-1.1414

NFkB1	4790	-1.8829	1.6466	1.8537	-1.3429	-1.1220
NFkB2	4791	-1.9227	1.1474	3.0284	-1.3349	-1.4022
RELA	5970	1.0161	1.3137	3.5154	1.4552	-1.0315
RELB	5971	-1.4547	1.3258	2.4936	1.0235	-1.0003
REL	5966	-1.0572	1.2662	-1.3225	1.0080	1.0842
NFATC1	4772	1.0171	2.2826	1.1181	1.0658	1.3799
NFATC2	4773	2.2980	1.9122	-1.0952	-1.2216	1.4803
NFATC3	4775	1.4524	1.1518	-1.5166	1.2830	1.2650
NFATC4	4776	-1.1882	-1.1059	-1.2274	-1.2375	-1.1479
CREB1	1385	-1.5866	-1.7637	-1.2734	-1.3750	-1.4478
MAPK1	5594	1.1860	1.0449	-1.4963	-1.2695	-1.4842
MAP3K7	6885	1.0506	1.0291	-1.0495	1.2353	1.0365
NLK	51701	2.2148	1.0336	1.1425	1.7717	1.0901
HIPK2	28996	1.8257	-1.0352	-1.7297	1.3915	1.1315
MYB	4602	-1.9721	-1.7544	-1.7517	1.2062	-1.0282

9.2 Supplementary table 2: Microarray data of ex vivo derived myeloid cells

Supplementary table 2 displays the microarray data of the ex vivo obtained myeloid cells. It displays calculated Fold changes (FC) of cD1c$^+$DC, slan_DC and MΦ _RCC compared to ercDC_RCC for the canonical and non-canonical Wnt-pathways. Additionally, it also displays the FC of in vitro generated cDC compared to ercDC. Genes are represented by gene-IDs and official gene-symbols. The green colour indicates an up regulation compared to ercDC_RCC with an FC of >1.5. The red colour a down regulation with a FC of <-1.5.

Gene:	Entrez-ID:	FC: cD1c$^+$DC/ercDC_RCC	FC: slanDC/ercDC_RCC	FC: MΦ_RCC/ercDC_RCC	FC: cDC/ercDC in vitro
Wnt-ligands					
Wnt 1	7471	1.0097	-1.1544	-1.1480	1.0021
Wnt 2	7472	-1.0224	-1.0892	-1.0734	-1.0600
Wnt 2b	7482	-1.0438	-1.3770	-1.2097	-1.3406
Wnt3	7473	-1.0000	-1.0751	-1.0061	-1.0227
Wnt 3a	89780	1.0786	1.1578	-1.0093	-1.0189
Wnt 4	54361	-1.0034	1.0307	-1.0648	-1.0823
Wnt 5a	7474	-1.0080	-1.0503	1.2209	6.2926
Wnt 5b	81029	-1.0824	-1.1094	-1.0041	1.1526
Wnt 6	7475	-1.1454	-1.2974	-1.2274	-1.1001
Wnt 7a	7476	-1.0903	1.0194	-1.0115	1.0568
Wnt 7b	7477	-1.0664	1.1921	1.0045	1.2180
Wnt 8a	7478	1.1079	1.0210	1.1149	1.0452
Wnt 8b	7479	1.0430	-1.0117	1.0118	1.0170
Wnt 9a	7483	1.0289	-1.2044	-1.0915	-1.0406
Wnt 9b	7484	-1.0428	-1.1106	-1.0676	1.0624
Wnt 10a	80326	-1.3670	-1.1560	-1.3498	-1.3330
Wnt 10b	7480	-1.2812	-1.1624	-1.2105	-1.1946
Wnt 11	7481	-1.1320	-1.1984	-1.0435	1.0661
Receptors					
Fzd1	8321	-1.0349	-1.0299	-1.0823	-1.0394
Fzd2	2535	-1.1635	-1.4565	-1.1449	1.3873
Fzd3	7976	1.3665	1.0812	-1.0461	1.7617
Fzd4	8322	-1.0897	-1.1428	1.0094	-1.1865
Fzd5	7855	-1.2693	-1.4711	-1.1802	1.0222
fzd6	8323	1.0141	1.0409	-1.0227	-1.1573
Fzd7	8324	-1.0589	-1.0328	-1.0418	1.1079
Fzd8	8325	-1.3583	-1.2150	-1.1282	-1.0574
Fzd9	8326	-1.0458	-1.2537	-1.0551	1.0256
Fzd10	11211	1.0678	-1.3507	-1.0507	-1.1383
Co-receptors					
LRP5	4041	1.0912	1.0100	-1.0408	1.1721
LRP6	4040	-1.0158	-1.0174	-1.0934	1.3216
LRP1	4035	-2.4504	-1.6889	-1.1696	-1.0803
Kremen 1	83999	1.0218	1.0004	-1.0258	1.0948
Kremen 2	79412	-1.0196	-1.1387	-1.0224	-1.1078
RYK	6259	-1.4538	1.5468	1.1389	1.5257
ROR1	4919	-1.0267	-1.1371	-1.0253	1.0990
ROR2	4920	-1.0104	-1.0176	1.0526	-1.2039

VANGL1	81839	1.0120	-1.1749	-1.0265	-1.0991
VANGL2	57216	-1.0823	-1.0346	1.0867	-1.0855
CELSR1	9620	-1.2823	1.0675	-1.0670	-1.1313
CELSR2	1952	-1.0539	-1.1833	-1.1143	1.1074
CELSR3	1951	-1.0653	-1.1039	-1.0586	-1.0636
PTK7	5754	-1.0413	-1.2401	-1.0548	1.0258
SDC1	6382	-1.1586	-1.2876	-1.1446	-1.1348
SDC2	6383	-2.0238	-3.0293	1.1840	2.4422
SDC3	9672	-13.9840	-17.7616	-2.2844	-1.2611
SDC4	6385	-3.3641	-5.2096	-1.1604	-1.2838
GPC2	221914	1.0280	-1.1169	1.0218	-1.0776
GPC3	2719	1.0086	1.0355	-1.0112	-1.0938
GPC4	2239	-1.0581	-1.0137	1.0073	-1.2177
GPC5	2262	1.0165	1.0211	-1.0607	-1.0976
GPC6	10082	-1.0489	1.0607	1.0356	1.1023
GPC1	2817	-1.2736	-1.1863	-1.1308	1.0234
CD44	960	1.7607	2.3867	1.6069	1.3199
Inhibitors					
Dkk1	22943	-1.1640	1.0137	-1.0596	1.0133
Dkk2	27123	1.0489	-1.0804	1.0889	1.0432
Dkk3	27122	-1.1317	-1.1360	-1.0182	-1.1449
Dkk4	27121	-1.1292	-1.0598	-1.1939	1.1142
WIF1	11197	-1.0493	1.0038	1.0410	-1.2619
sFRP1	6422	-1.1710	1.0444	-1.1043	1.0285
sFRP2	6423	-1.1927	-1.2204	-1.2165	-1.0340
sFRP3	2487	-1.1185	-1.0538	-1.0984	-1.0177
sFRP4	6424	-1.0741	-1.0741	-1.1922	-1.0948
sFRP5	6425	-1.0412	-1.1051	1.0468	-1.0391
Shisa2	387914	1.0506	-1.0021	1.0746	1.0431
Shisa3	152573	-1.0619	-1.1272	-1.1695	-1.1468
CTHRC1	115908	-1.2800	-1.2979	-1.1785	-1.0866
IGFBP1	3484	-1.0606	-1.0005	-1.1331	-1.0923
IGFBP2	3485	-1.0713	-1.1487	-1.0785	1.5769
IGFBP4	3487	-2.1345	-2.3517	-1.7152	-1.2767
IGFBP6	3489	-1.1611	1.7273	-1.0471	1.2318
CER1	9350	1.0559	-1.1610	1.0868	-1.1534
SOST	50964	-1.0677	-1.0641	-1.0556	1.0414
SOSTDC1	25928	-1.1579	1.0825	-1.0490	-1.0792
TPBG	7162	-1.0855	-1.1817	-1.0269	-1.1761
APCDD1	147495	-1.1348	-1.2389	-1.1245	1.1224
TRABD2A	129293	1.3821	-1.1138	-1.0627	3.5819
agonists/ positive modulators					
NDP	4693	-1.0369	1.0240	-1.0718	2.0848
RSPO1	284654	1.0478	-1.1746	-1.0174	-1.0283
RSPO2	340419	1.0370	-1.0039	-1.0317	-1.0654
RSPO3	84870	-1.2302	-1.0685	-1.1931	-1.0999
RSPO4	343637	1.0945	-1.0467	1.0296	1.0660
ß-Catenin dependent signalling					
Dvl1	1855	-1.1003	-1.1709	-1.0041	1.0043
Dvl2	1856	1.0455	-1.1767	-1.0992	-1.0679
Dvl3	1857	-1.2685	-1.3125	1.1232	1.0129
GSK3ß	2932	1.2338	1.8717	-1.0518	-1.0684
Axin 1	8312	1.2076	1.1760	1.0062	1.1292
Axin 2	8313	1.0350	-1.0332	1.0269	1.0315
APC	324	1.0375	2.2416	-1.0043	1.0717
CSNK1A1	1452	1.8013	1.5521	1.3138	1.1535
CSNK1E	1454	1.6840	-2.0421	1.3688	1.2844
CSNK1D	1453	1.0470	1.1399	1.0297	-1.0389
CSNK2A1	1457	2.6044	1.8369	1.4823	2.0097
CSNK2A2	1459	1.1685	1.1476	1.2627	1.0946
CSNK2B	1460	1.0833	1.1026	1.0244	1.5215
CTNNB1	1499	-1.3528	-1.8149	1.0964	-1.1370
CTNNBIP1	56998	1.0367	-1.1387	1.0184	-1.1564
NDRG1	10397	1.3675	-1.2411	1.1185	-1.0052
NDRG2	57447	13.6004	-3.6222	2.6683	5.0442
FRAT1	10023	1.4554	2.5653	-1.1292	1.1066
FRAT2	23401	1.7967	1.9805	1.1342	1.5524
PAK4	10298	1.0538	1.0361	-1.0052	-1.0163
AKT1	207	-1.5811	-1.3680	-1.1693	1.1469

AKT2	208	1.7915	1.8000	1.1900	-1.0811
AKT3	10000	1.0042	1.7683	1.0245	-1.9218
ILK	3611	1.3884	1.1856	1.0791	-1.2412
CXXC4	80319	-1.0787	-1.1329	-1.0647	1.0324
SUMO1	7341	1.4611	-1.2652	1.1000	-1.0351
RANBP2	5903	-1.8099	-2.2638	-1.2854	1.1359
SENP2	59343	1.2568	1.3686	1.2128	1.1050
BTRC	8945	-1.5329	1.0744	1.0409	1.3042
SKP1	6500	-1.0166	-1.0535	-1.0877	1.3078
CUL1	8454	1.2999	-1.2547	1.4976	1.3651
NKD1	85407	1.0227	-1.0490	-1.0427	-1.0767
ARRB1	408	1.5494	2.9757	-1.0999	-1.2502
ARRB2	409	1.1524	1.5570	-1.0507	-1.4050
MACF1	23499	-1.0623	1.5709	-1.1375	-1.3735
PPP1CA	5499	2.1597	2.5729	1.4084	-1.0946
PPP1CB	5500	1.2699	1.3017	1.0037	1.0019
PPP1CC	5501	1.4864	1.8177	1.1833	1.0558
PPP2R5B	5526	-1.0427	1.1492	1.0507	-1.0998
PPP2CB	5516	-1.2115	-1.1894	-1.1775	-1.1469
PPP2CA	5515	1.3410	1.4718	1.1537	-1.0081
PPP3CB	5532	1.4256	1.7219	1.1706	-1.1373
DAB2	1601	-8.9419	-41.7488	-2.0490	-1.6478
TCF1	6927	-1.1087	-1.0798	-1.0857	1.0309
TCF3	6929	1.4746	1.1788	-1.0796	1.1391
TCF4	6925	-2.3677	-5.3755	-1.6344	1.0000
LEF1	51176	-1.0256	1.0626	-1.0399	-1.9252
TCF7L1	83439	-1.1257	-1.0008	-1.0836	-1.0007
TCF7L2	6934	-7.2930	10.9486	-1.5495	-1.7468
TLE1	7088	-1.1562	-1.1055	-1.1633	4.4839
TLE2	7089	-1.1277	-1.1117	-1.0439	-1.1298
TLE3	7090	-1.2666	-1.4523	1.3582	-1.6283
TLE4	7091	1.7511	5.0735	1.4129	-1.0544
CDX1	1044	-1.0217	-1.1464	-1.0495	-1.1573
BCL9	607	-1.1029	-1.1549	1.0165	1.5439
PIAS4	51588	1.1418	1.5378	1.1064	-1.0070
FHL2	2274	-1.0335	-1.1472	-1.1182	1.0811
TAX1BP3	30851	1.0130	-1.3228	1.0601	1.1446
SALL1	6299	-1.0840	-1.0511	-1.1329	1.0422
SALL4	57167	1.0180	-1.2479	-1.0865	1.1593
MAP1B	4131	-1.1177	-1.0840	1.0195	-1.0332
PCP signalling					
ANKRD6	22881	-1.1921	-1.0092	-1.0709	-1.2642
DAAM1	23002	1.3875	1.2873	1.0657	2.5715
DAAM2	23500	1.0333	-1.0028	-1.0796	-1.0499
RHO A	387	1.3881	1.4257	1.2972	1.0488
RHO B	388	-2.7277	-1.2100	-1.2101	-1.3863
ROCK1	6093	1.3576	1.3783	1.1282	1.0642
ROCK2	9475	1.3726	1.6438	1.0249	1.4028
RAC1	5879	1.6136	-1.2333	1.3042	-1.1747
RAC2	5880	3.8572	6.4737	1.4315	1.5024
RAC3	5881	1.2227	1.3297	1.0410	1.0900
MAP2K7	5609	1.1772	1.2152	1.0743	1.0392
MAP2K4	6416	1.6228	1.7046	1.2000	1.2608
MAP3K4	4216	1.8839	1.4221	1.0294	1.3378
MAPK8	5599	1.4700	1.5345	1.3773	-1.4576
MAPK9	5601	1.2817	1.3061	1.2371	1.3208
MAPK10	5602	-1.0157	1.1798	1.0655	-1.2491
JUN	3725	-4.5396	-8.5569	-1.0195	1.0658
ATF2	1386	1.0757	-1.1054	1.1084	-1.1124
CDC42	998	1.2107	-1.0321	1.0517	1.0262
MARK2	2011	1.9981	2.3728	1.5145	1.1750
Ca-Signalling					
PLCB1	23236	-1.0711	-1.0142	1.0832	1.4089
PLCB2	5330	1.5102	1.7951	-1.0470	1.2400
PLCB3	5331	1.1409	-1.1602	-1.0389	-1.1196
PLCB4	5332	-1.1018	-1.0804	-1.1142	-1.0168
PLCG1	5335	-1.3671	-1.2939	-1.0268	1.0632
PLCG2	5336	1.1676	1.6333	-1.0479	1.0387
PLCD1	5333	-1.0294	-1.0821	1.0977	1.1187

PLCD3	113026	-1.0137	-1.0446	-1.0161	1.0868
PLCD4	84812	-1.0273	-1.0314	-1.1525	-1.1341
PLCE1	51196	1.0021	1.0926	-1.0255	-1.0663
PRKCA	5578	1.3714	-1.4873	1.0023	1.6590
PRKCB	5579	3.9927	7.5222	1.7442	-1.6910
PRKCG	5582	1.0591	-1.0952	1.0456	-1.0857
CAMK1	8536	1.0037	2.3223	1.0299	1.4221
CAMK1D	57118	1.8969	1.4238	1.4937	1.1630
CAMK1G	57172	-1.1636	-1.0564	-1.0457	-1.1238
CAMK2A	815	-1.2072	-1.0568	1.0183	1.0790
CAMK2B	816	1.0781	-1.0263	-1.0593	-1.1159
CAMK2G	818	1.5570	-1.1664	1.0419	-1.0961
CAMK2D	817	-1.5758	-2.5413	1.2151	1.7960
CAMK4	814	-1.0485	-1.1461	-1.0883	-1.4048
PPP3CA	5530	2.0980	1.8450	1.5470	1.0562
NFkB1	4790	1.6854	-1.0498	1.6017	-1.7144
NFkB2	4791	1.0364	-1.7759	1.1308	-1.3089
RELA	5970	1.0204	1.1109	1.0592	1.0439
RELB	5971	-1.0420	-1.3304	-1.0693	-1.3590
REL	5966	1.0393	-1.0561	1.1015	-1.1801
NFATC1	4772	-1.5256	2.5389	-1.1689	-1.4578
NFATC2	4773	1.3582	-6.7436	-1.2706	1.4631
NFATC3	4775	1.4056	1.6297	1.0922	1.1901
NFATC4	4776	1.0049	-1.0797	-1.0440	1.0244
CREB1	1385	1.1763	1.8634	-1.0683	-1.1082
MAPK1	5594	1.9619	3.0605	1.1845	1.8177
MAP3K7	6885	1.2715	2.0198	-1.0133	-1.0448
NLK	51701	-1.1397	1.1441	-1.0498	1.9392
HIPK2	28996	-1.0261	1.2703	1.0243	1.5712
MYB	4602	-1.1398	-1.0786	1.0075	-1.8152

9.3 Supplementary table 3: Microarray data of RCC tissue samples

Supplementary table 3 displays the microarray data of RCC tissue samples with WHO G1 and G3. It displays calculated Fold changes (FC) of RCC tissue samples with WHO grading G1 and G3 compared to control healthy renal tissue for the canonical and non-canonical Wnt-pathways. Genes are represented by gene-IDs and official gene-symbols. The green colour indicates an up regulation with a FC of >1.5. The red colour a down regulation with a FC of <-1.5. #N/A indicates that this gene was not present on the microarray chip.

Gene:	Entrez-ID:	FC: G1 /Control	FC: G3/Control	FC: G3/G1
Wnt-ligands				
Wnt 1	7471	-1.133980143	-1.115985825	-1.029608124
Wnt 2	7472	-1.324275188	-1.245568656	1.000790296
Wnt 2b	7482	-1.383356436	1.195510709	1.388362855
Wnt3	7473	-1.303414366	-1.18008834	1.164342384
Wnt 3a	89780	#N/A	#N/A	#N/A
Wnt 4	54361	-1.168875127	-1.170559825	-1.005386424
Wnt 5a	7474	2.967342144	6.876444758	2.299245364
Wnt 5b	81029	1.066702146	1.403380922	1.249449144
Wnt 6	7475	1.057031097	-1.07443072	-1.248936964
Wnt 7a	7476	-1.208725642	-1.112176136	-1.02900337
Wnt 7b	7477	-1.455952281	-1.445384083	-1.004953069
Wnt 8a	7478	1.122277964	1.073397815	1.093807796
Wnt 8b	7479	-1.555566312	-1.427779097	1.047735221
Wnt 9a	7483	#N/A	#N/A	#N/A
Wnt 9b	7484	-1.336612456	-1.290677636	1.012397217
Wnt 10a	80326	-1.026980859	1.013708925	1.110479976
Wnt 10b	7480	-1.761407872	-1.581129476	1.066790244
Wnt 11	7481	-1.373157757	-1.390156425	-1.015667923
Receptors				
Fzd1	8321	3.584257605	1.849677915	-2.010417659

Fzd2	2535	1.382497028	2.303297739	1.800645271
Fzd3	7976	-1.277587363	-1.87702466	-1.533562287
Fzd4	8322	1.423966297	-1.308237859	-2.083311916
Fzd5	7855	-1.634196906	-1.947267112	-1.258913966
fzd6	8323	-1.294774616	1.060103946	1.515763069
Fzd7	8324	-1.115610105	-1.369425415	-1.251774174
Fzd8	8325	1.270067557	-1.071674828	-1.336411161
Fzd9	8326	-1.044390052	-1.1607386	-1.055789619
Fzd10	11211	1.012074109	1.025773762	1.034965364
Co-receptors				
LRP5	4041	1.452710066	1.102076251	-1.395097147
LRP6	4040	1.466950006	-1.138501484	-1.877185505
LRP1	4035	1.380646437	2.375572422	1.640301972
Kremen 1	83999	-1.365676664	-1.253400595	1.046379683
Kremen 2	79412	-1.22663849	-1.062784499	1.168823393
RYK	6259	1.004126323	1.073230925	1.046274711
ROR1	4919	1.107936489	1.120996208	1.003997867
ROR2	4920	1.246196506	1.446230373	1.431407663
VANGL1	81839	1.365706487	1.180956609	-1.152042507
VANGL2	57216	-1.291596448	1.016583275	1.355722227
CELSR1	9620	-1.4027793	-1.261592842	1.036283093
CELSR2	1952	1.461351444	1.036603234	-1.374416876
CELSR3	1951	-1.203939888	1.021429824	1.123296299
PTK7	5754	1.314843236	1.125148787	1.013381741
SDC1	6382	-2.653625065	-1.312103094	1.841708379
SDC2	6383	1.675387267	1.424077117	-1.350628384
SDC3	9672	1.205074266	1.511596329	1.334483728
SDC4	6385	-1.318786785	-1.259788369	1.120200438
GPC2	221914	-1.252343651	-1.111942655	1.029825539
GPC3	2719	-10.34923525	-7.298622465	1.816855872
GPC4	2239	-1.713973771	1.140729316	1.399841684
GPC5	2262	-21.44636268	-14.44903445	-1.001580361
GPC6	10082	1.32757433	1.113963397	-1.406348327
GPC1	2817	1.125962321	1.476452189	1.306008657
CD44	960	3.635172769	15.32325927	4.476799056
Antagonists				
Dkk1	22943	1.398918147	1.98636612	12.46478436
Dkk2	27123	-1.152840138	-1.233538254	-1.226955505
Dkk3	27122	8.778332478	9.220783697	1.08650795
Dkk4	27121	-1.347272405	-1.206882165	1.174759914
WIF1	11197	-2.769029059	-2.673839412	1.101479509
sFRP1	6422	-5.763880963	-7.132151556	1.070088766
sFRP2	6423	10.89794626	6.780467736	-1.727027119
sFRP3	2487	6.70220794	3.640778043	-1.719907159
sFRP4	6424	3.48080581	3.389897133	1.117281517
sFRP5	6425	-1.230444446	-1.189231739	1.016892915
Shisa2	387914	-6.127026881	-6.633182403	1.13942511
Shisa3	152573	-4.264092225	-6.062618983	-1.407634887
CTHRC1	115908	34.38466931	99.39512642	3.202101901
IGFBP1	3484	-2.458884854	18.98350353	40.41981721
IGFBP2	3485	1.202135667	-1.171464323	-1.017927391
IGFBP4	3487	1.417368018	1.14861181	-1.149470495
IGFBP6	3489	1.924971692	3.518554816	1.534162127
CER1	9350	-1.622301362	-1.622993816	1.016844264
SOST	50964	-5.385682106	-6.543979511	-1.144876174
SOSTDC1	25928	-6.795064991	-12.72653298	-1.950021998
TPBG	7162	2.312788181	3.474359865	1.621467976
APCDD1	147495	6.103822689	5.190308729	-1.157545143
TRABD2A	129293	-1.332610907	-1.038193912	1.187153844
agonists/ positive modulators				

NDP	4693	-1.096484654	1.107123335	1.526145594
RSPO1	284654	-1.3649201	-1.293597928	1.060267233
RSPO2	340419	-1.059399167	-1.021525136	1.056231263
RSPO3	84870	-1.051008475	1.769600894	1.316544231
RSPO4	343637	-1.431480644	-1.203809198	1.21129907
ß-Catenin dependent signalling				
Dvl1	1855	1.289714447	1.246211774	1.107754455
Dvl2	1856	1.028367491	1.085761675	1.005707339
Dvl3	1857	1.491242996	2.134870565	1.500093647
GSK3ß	2932	1.328278241	1.323190456	1.089648881
Axin 1	8312	-1.196247428	-1.14847243	1.060728434
Axin 2	8313	-1.258074717	-1.200803178	1.021873822
APC	324	1.465982822	1.23273068	-1.277144188
CSNK1A1	1452	1.311053249	1.295546305	1.009418706
CSNK1E	1454	1.911017554	1.748559183	-1.079365007
CSNK1D	1453	1.69226951	2.129454545	1.154614177
CSNK2A1	1457	1.401391878	1.753027332	1.255121631
CSNK2A2	1459	1.248237741	1.64423934	1.171093671
CSNK2B	1460	1.269759514	1.134931547	-1.088843294
CTNNB1	1499	-2.66095652	-3.898603411	-1.262693819
CTNNBIP1	56998	-1.358448567	-1.361630174	-1.014461705
NDRG1	10397	2.290167694	2.003738116	-1.16936675
NDRG2	57447	1.16828069	-2.038885469	-2.832898978
FRAT1	10023	1.259220336	1.256125631	-1.025011507
FRAT2	23401	1.550701092	1.825562063	1.08886623
PAK4	10298	-1.240240289	-1.323829306	-1.046531636
AKT1	207	2.390895553	2.151040028	-1.107751563
AKT2	208	-1.335050618	-1.198904989	1.145284987
AKT3	10000	2.37748746	1.411176519	-1.536053311
ILK	3611	2.245027334	2.013829177	-1.22528232
CXXC4	80319	-1.257415191	-1.536550648	-1.325931229
SUMO1	7341	-1.121368304	-1.251783678	-1.043864812
RANBP2	5903	-1.109158462	-1.169324841	-1.043454544
SENP2	59343	-1.066203629	1.053395277	1.099180338
BTRC	8945	-1.018086309	-1.043770138	-1.021840072
SKP1	6500	1.063203059	-1.152498308	-1.221901265
CUL1	8454	1.704737398	2.095852631	1.179458761
NKD1	85407	-1.373908261	-1.268853517	1.040940034
ARRB1	408	1.809813068	1.452289174	-1.267615895
ARRB2	409	2.029399769	3.434748787	1.580898944
MACF1	23499	1.786425641	1.506029338	-1.22782369
PPP1CA	5499	1.477688468	1.71407989	1.17414777
PPP1CB	5500	-1.238201441	-1.195191299	1.108768723
PPP1CC	5501	1.260405787	1.250892278	1.035899142
PPP2R5B	5526	1.061451675	1.025841853	1.025026972
PPP2CB	5516	-1.436446446	-1.33886331	-1.102953743
PPP2CA	5515	-1.004758838	1.072804763	1.051081344
PPP3CB	5532	1.080063556	1.356917165	1.236252359
DAB2	1601	1.164301469	-1.158955809	-1.380338409
TCF1	6927	-1.530051115	-1.972436498	-1.280701909
TCF3	6929	1.084544628	1.294155363	1.180643626
TCF4	6925	10.22102336	5.189265059	-1.922066902
LEF1	51176	1.138632599	1.657525087	1.65601457
TCF7L1	83439	2.248597044	1.259975702	-2.038217267
TCF7L2	6934	1.462326866	-1.162132728	-1.601614088
TLE1	7088	2.429193731	2.155936325	-1.193833056
TLE2	7089	1.280791965	-1.127047458	-1.374994321
TLE3	7090	1.496525347	1.494982502	1.074806545
TLE4	7091	-1.183244107	-1.091672674	1.12347155
CDX1	1044	-1.085536361	-1.011578062	1.150406159

BCL9	607	-1.362178286	-1.741934664	-1.091691886
PIAS4	51588	-1.111491921	-1.1980189	1.038515881
FHL2	2274	3.329528166	8.329019353	2.198952864
TAX1BP3	30851	#N/A	#N/A	#N/A
SALL1	6299	1.004734576	-2.477178189	-2.415650485
SALL4	57167	-1.436634307	-1.431046897	-1.051475876
MAP1B	4131	6.074013744	5.238552109	-1.069927648
PCP signalling				
ANKRD6	22881	1.742713169	1.359020888	-1.042948328
DAAM1	23002	1.009453656	-1.262825447	-1.315831589
DAAM2	23500	1.732905748	1.207742125	-1.31315434
RHO A	387	1.846909082	2.110809094	1.042177498
RHO B	388	1.520962404	-1.716785354	-2.500086048
ROCK1	6093	1.584387054	1.425687306	-1.108313198
ROCK2	9475	1.339074617	1.247466827	1.00111951
RAC1	5879	1.328458805	1.433274369	1.060350703
RAC2	5880	4.08874283	10.07493166	2.263784778
RAC3	5881	-1.542901535	-1.51462049	1.137959544
MAP2K7	5609	-1.027864834	-1.005100529	-1.014774998
MAP2K4	6416	-1.099965766	1.068826953	1.052906644
MAP3K4	4216	1.483073738	1.194525514	-1.262007554
MAPK8	5599	-2.25872637	-2.63432144	-1.243079946
MAPK9	5601	1.29004651	1.355271919	1.038577125
MAPK10	5602	-2.524020898	-3.432548437	-1.454735636
JUN	3725	1.988653599	1.7417627	-1.350791103
ATF2	1386	1.234215251	1.082645845	-1.027613523
CDC42	998	-1.139600981	-1.018081185	1.101781963
MARK2	2011	2.126391661	2.214945365	1.031941706
Ca-Signalling				
PLCB1	23236	2.777261538	1.623132108	-1.724282305
PLCB2	5330	-1.321955152	-1.141593069	1.201913509
PLCB3	5331	-1.244635264	-1.067696636	1.04100577
PLCB4	5332	2.029270852	8.627119408	3.535088233
PLCG1	5335	1.009942854	1.016920234	-1.044699153
PLCG2	5336	-1.722484548	-1.356941956	1.116611218
PLCD1	5333	-1.345298093	-1.441158673	-1.181675697
PLCD3	113026	-1.100471874	-1.008918092	1.19476375
PLCD4	84812	-4.312582026	-2.698849939	1.424287042
PLCE1	51196	-1.393012619	1.136634573	1.355819519
PRKCA	5578	-1.699574687	-1.246047358	1.405377313
PRKCB	5579	1.197818149	1.595511116	1.349703551
PRKCG	5582	-1.311002605	-1.310415823	1.062479787
CAMK1	8536	1.828809625	1.891619375	-1.007996616
CAMK1D	57118	2.026101077	1.923216022	-1.031548829
CAMK1G	57172	-1.12031656	-1.139301845	1.009346511
CAMK2A	815	-2.141586935	-2.140552189	1.031997465
CAMK2B	816	-1.285865389	-1.226629584	1.092573587
CAMK2G	818	-1.743880887	-1.568126553	1.132000332
CAMK2D	817	-1.016006978	-1.191151311	-1.219818519
CAMK4	814	-1.231335085	-1.213443951	-1.015567417
PPP3CA	5530	1.073327679	1.014770572	-1.018062525
NFkB1	4790	2.620207883	2.512596401	-1.150557457
NFkB2	4791	1.712433148	1.869465336	1.392446338
RELA	5970	1.355806855	1.420662784	1.020914462
RELB	5971	1.64304941	2.037120771	1.279179867
REL	5966	1.941812493	2.411602709	1.240428454
NFATC1	4772	1.209499021	1.161418352	-1.080612511
NFATC2	4773	1.579927484	1.715789398	1.133516808
NFATC3	4775	1.241450506	1.33321685	1.001947506
NFATC4	4776	-1.048379179	-1.167421008	-1.144693204

CREB1	1385	1.966645631	1.845680333	-1.127479107
MAPK1	5594	1.941009924	2.049992218	1.088210692
MAP3K7	6885	1.537663421	1.7339144	1.146743566
NLK	51701	1.341225471	1.207841684	-1.191006666
HIPK2	28996	2.757924464	1.727160185	-1.590288812
MYB	4602	-1.13805442	1.066585629	1.34276616

10 Acknowledgements

First of all, I would like to thank my thesis adviser, Prof. Dr. Peter J. Nelson, for making this work possible and guiding me through this period. During my time in your laboratory, I have learnt a great deal about scientific work, but also about myself. Working in your laboratory for almost half my medical studies, I have learnt endurance, not to give up even during difficult times and to appreciate even the smallest achievements. You have been a great inspiration, motivation and support. Thank you for giving me the opportunity to work in your group and for all your time and advice all way through.

I also want to thank Prof. Dr. Elfriede Nößner, for allowing me to perform a large part of my experiments in your laboratory. Thank you for your support and advice and I am grateful for all the skills I was able to learn under your supervision. You have an exceptional working group, with an incredibly inspiring and stimulating atmosphere. I truly enjoyed working in your group and am excited to see the future work your group will publish.
A special thank you also goes to Dorothee Brech, for the close collaboration and the many things I learnt from you. Thank you for allowing me to use the array data for further analysis and teaching me how to raise and care for all the small dendritic cells.

None of this work would have been possible without the help and great support of everyone else in the laboratories of AG Nelson as well as AG Nößner. I thank every single one of you and I am deeply grateful for the warm welcome into your working groups. Thank you, Alex for all the support regarding the migration assays. Thank you, Anke for truly introducing me to cell culture. Thank you Carsten, for guiding me through the array data and supporting me through all the “Excel-crashes”. Thank you Sylke, for teaching me how to properly perform qPCRs. Thank you, Moni for teaching me western blot. And thank you everyone for the great conversations, dreaming about mountains and journeys, and all the relaxing lunch- and coffee times.

Thank you also to Prof. Dr. Hermann-Josef Gröne at the DKFZ Heidelberg for providing the kidney section samples for immunohistochemistry and to PD Dr. Matthias Maruschke from the Department of Urology of the University of Rostock for the microarray expression data of RCC samples.

I also do not want to forget my family and great friends, who supported me all time through. You have been great and such support. Thank you for cheering me up, for discussing problems and being there, whenever I needed you. You have been there through my ups and downs and helped me with your inspiration to finish this work. Thank you Mum, Dad, Til, Caro, Viola, Ava and the many more.
A special thanks to Philipp, who has been outstanding in supporting me. I am so grateful for having you during this turbulent times.

EIDESSTATTLICHE VERSICHERUNG

Diepenbruck, Sabine Daphne

Ich erkläre hiermit an Eides statt, dass ich die vorliegende Dissertation mit dem Thema:

The potential impact of Wnt5a on differentiation and phenotype of dendritic cells found in renal cell carcinoma.

selbstständig angefertigt habe, mich außer der angegebenen keiner weiteren Hilfsmittel bedient und alle Erkenntnisse, die aus dem Schrifttum ganz oder annähernd übernommen sind, als solche kenntlich gemacht und nach ihrer Herkunft unter Bezeichnung der Fundstelle einzeln nachgewiesen habe.

Ich erkläre des Weiteren, dass die hier vorgelegte Dissertation nicht in gleicher oder in ähnlicher Form bei einer anderen Stelle zur Erlangung eines akademischen Grades eingereicht wurde.

München, den ....

(Unterschrift)